Synthetic studies toward 4*S*,5*S*-dihydroxy docosapentaenoic acid

Åsmund Haatveit

Thesis submitted for the degree of
Master of Pharmacy
45 credits

Section for Pharmaceutical Chemistry
Department of Pharmacy
Faculty of Mathematics and Natural Sciences

UNIVERSITY OF OSLO

Spring 2023

Synthetic studies toward 4*S*,5*S*-dihydroxy docosapentaenoic acid

Åsmund Haatveit

Synthetic studies toward 4*S*,5*S*-dihydroxy docosapentaenoic acid

http://www.duo.uio.no/

Printed: Reprosentralen, University of Oslo

Acknowledgements

The work for this master's thesis was performed at the Section for Pharmaceutical Chemistry, Department of Pharmacy, University of Oslo, from September 2022 to May 2023. My supervisors during this period have been Professor Trond Vidar Hansen, Associate Professor Anders Vik, and Doctoral Research Fellow Mina Bathen.

I would like to express my sincere gratitude to Professor Trond Vidar Hansen and Associate Professor Anders Vik for providing me with the opportunity to take part in the LIPCHEM group and to work on an engaging project. They have repeatedly inspired me by encouraging me to pursue my ideas, and by sharing their vast knowledge of organic chemistry with rousing enthusiasm. Their kindness and excellent guidance has made working on this project a pleasure.

I would also like to thank my co-supervisor Mina Bathen for having been an ideal mentor to me. I have been privileged to have worked beside such a skilful and virtuous colleague. She has always answered my queries, whether practical or theoretical, taught me a great deal about laboratory work, and done a great deal for my sake. I thank her for all the aid and support, for creating a positive working environment, and of course, for always tolerating my choice of music in the lab, even when that included the postwar avant-garde.

I also thank the rest of the LIPCHEM group for providing a hospitable and stimulating milieu, as well as generously sharing chemicals and equipment. Special thanks to Mathias Ryslett Lepsøe for supplying me with various apparatus and helping with spectroscopy. My thanks also go to Åsmund Kaupang for giving me practical advice and a model for my LaTeX document.

I thank BASF for providing a generous gift of DHA-ethyl ester.

Finally, I thank my friends and family for their continuous support, without which I would not have come this far.

Abstract

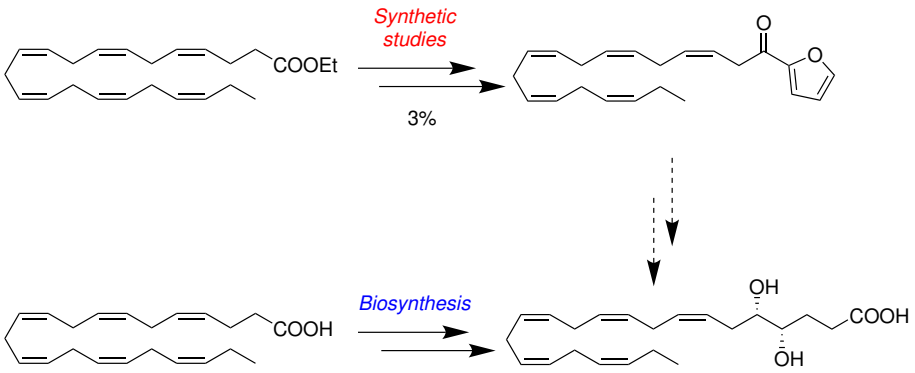

Polyunsaturated fatty acids are metabolically converted into lipid mediators which play an important role in the regulation of several biological processes, including inflammation, resolution, and homeostasis. The anti-inflammatory epoxy fatty acids are degraded *in vivo* by the enzyme soluble epoxide hydrolase to give the corresponding 1,2-dihydroxy fatty acids (DiHFAs). One endogenous DiHFA which demands further biological evaluation is 4*S*,5*S*-dihydroxy docosopentaenoic acid (DPA).

This master's thesis aimed to develop a synthesis of 4*S*,5*S*-dihydroxy DPA using the ethyl ester of docosahexaenoic acid (DHA) as a convenient starting material. The retrosynthetic analysis of the target molecule involved the conversion of the ethyl ester of DHA into an 18C aldehyde, followed by the synthesis of the *S*,*S*-diol via a furanyl ketone intermediate. The ethyl ester of DHA was converted into an epoxy ester using a three-step procedure. However, the protocol used to prepare the 18C aldehyde from the epoxy ester gave impure product and poor reproducibility. Preparation of the furanyl ketone by Stille coupling failed. The synthesis of the ketone was finally achieved by the use of 2-lithiofuran and Dess-Martin oxidation, albeit in low yield. Because of these challenges, the full synthesis was not accomplished.

Sammendrag

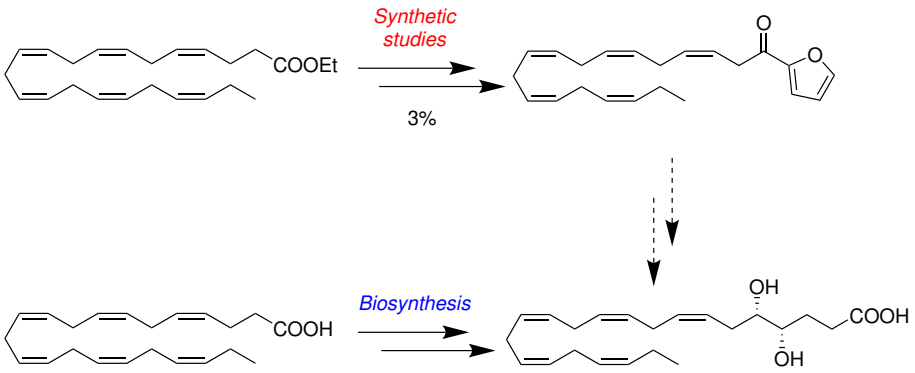

Flerumettede fettsyrer konverteres metabolsk til lipidmediatorer som spiller en viktig rolle i reguleringen av flere biologiske prosesser, inkludert inflammasjon, oppløsning og homeostase. De antiinflammatoriske epoksy-fettsyrene omdannes *in vivo* av enzymet løselig epoksidhydrolase til tilsvarende 1,2-dihydroksy-fettsyrer. En endogen dihydroksyfettsyre som behøver videre biologisk evaluering er 4*S*,5*S*-dihydroksydokosopentaensyre (DPA).

Denne masteroppgaven hadde som formål å utarbeide en syntese av 4*S*,5*S*-dihydroksy-DPA ved å bruke etylesteren av dokosaheksaensyre (DHA) som et praktisk utgangsstoff. Den retrosyntetiske analysen av målmolekylet involverte omdannelsen av etylesteren av DHA til et 18C-aldehyd, etterfulgt av syntesen av *S*,*S*-diolen via et furanylketonintermediat. Etylesteren av DHA ble omdannet til en epoksyester ved hjelp av en tretrinns prosedyre. Protokollen anvendt for å lage 18C-aldehydet fra epoksyesteren ga imidlertid urent produkt og dårlig reproduserbarhet. Syntese av furanylketonet ved hjelp av Stille-kobling mislyktes. Ketonet ble til slutt syntetisert ved bruk av 2-litiumfuran og Dess-Martin-oksidasjon, riktignok med lavt utbytte. På grunn av disse utfordringene kunne ikke hele syntesen fullføres.

List of abbreviations

2-Me-THF	2-methyltetrahydrofuran
AA	arachidonic acid
ADP	adenosine diphosphate
aq.	aqueous
BLT	leukotriene B_4 receptor
calc.	calculated
cAMP	cyclic adenosine monophosphate
CBS	Corey-Bakshi-Shibata
COSY	correlation spectroscopy
COX	cyclooxygenase
CYP	cytochrome P
d	doublet
DBU	1,8-diazabicyclo(5.4.0)undec-7-ene
DEPT	distortionless enhancement by polarisation transfer
DHA	docosahexaenoic acid
DHET	dihydroxyeicosatrienoic acid
DIBAL-H	diisobutylaluminium hydride
DiHFA	dihydroxy fatty acid
DMF	dimethylformamide
DMP	Dess-Martin periodinane
DMSO	dimethyl sulfoxide
DPA	docosapentaenoic acid
EDTA	ethylenediaminetetraacetic acid
EPA	eicosapentaenoic acid
EpFA	epoxy fatty acid
eq.	equivalent(s)
ESI	electrospray ionisation
ETA	eicosatetraenoic acid
et al.	and others

EET	epoxyeicosatrienoic acid
FN	furan
h	hour(s)
HEPE	hydroxyeicosapentaenoic acid
HETE	hydroxyeicosatetraenoic acid
HMBC	hereonuclear multiple bond correlation
HMPA	hexamethylphosphoramide
HPETE	hydroperoxyeicosatetraenoic acid
HSQC	heteronuclear single quantum coherence
IR	infrared
LOX	lipoxygenase
LT	leukotriene
LX	lipoxin
m	multiplet
MS	mass spectroscopy
NaHMDS	sodium hexamethyldisilazide
NMR	nuclear magnetic resonance
p	quintet
PCC	pyridinium chlorochromate
PG	prostaglandin
ppm	part(s) per million
PUFA	polyunsaturated fatty acid
r.t.	room temperature
R_f	retention factor
s	singlet
sat.	saturated
sEH	soluble epoxide hydrolase
SPM	specialised pro-resolving mediator
t	triplet
temp.	temperature
THF	tetrahydrofuran
TLC	thin layer chromatography
TX	thromboxane
UV-Vis	ultraviolet-visible

Numbered compounds

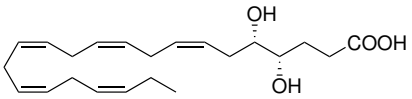

1

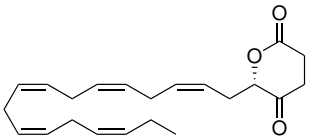

2

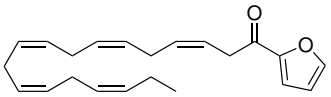

3

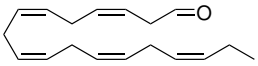

4

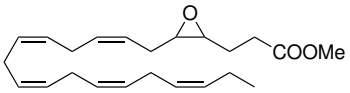

5

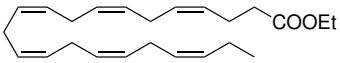

6

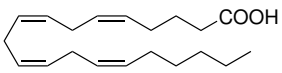

7

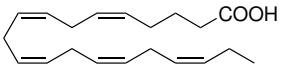

8

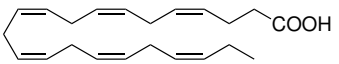

9

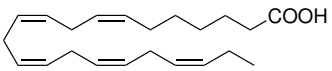

10

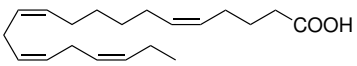

11

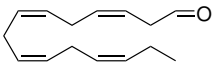

12

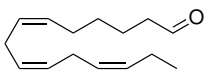

13

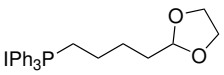

14

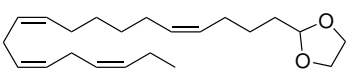

15

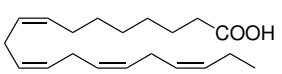

16

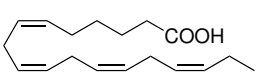

17

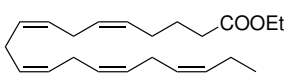

18

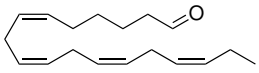

19

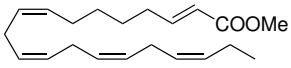

20

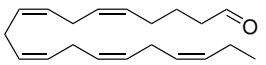

21

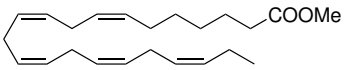

22

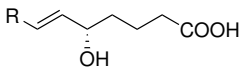

23: R=a
24: R=b

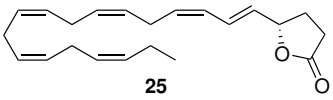

25

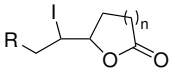

26a: R=a, n=2
26b: R=b, n=2
26c: R=c, n=1

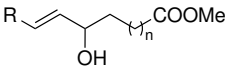

27a: R=a, n=2
27b: R=b, n=2
27c: R=c, n=1

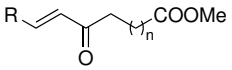

28a: R=a, n=2
28b: R=b, n=2
28c: R=c, n=1

a:

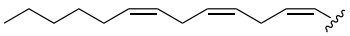

b:

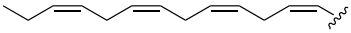

c:

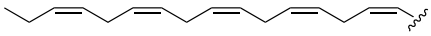

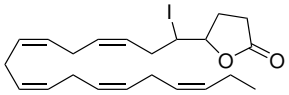

29

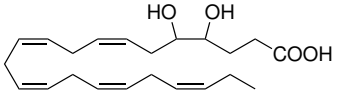

30

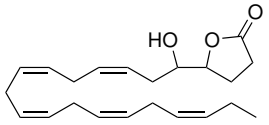

31

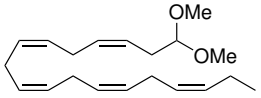

32

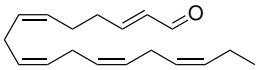

33

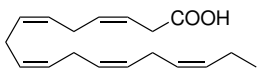

34

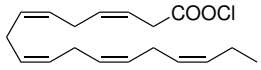

35

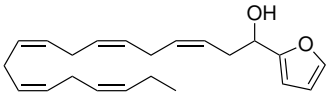

36

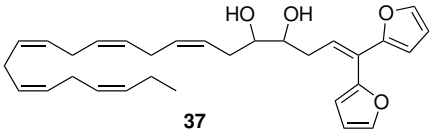

37

Contents

1 Introduction

1.1 Aim of study

The aim of this master's thesis was to synthesise 4*S*,5*S*-dihydroxy DPA (**1**), depicted in Fig. 1.1, in a stereoselective manner. 4,5-dihydroxy DPA is a dihydroxylated metabolite of DHA reported from human serum samples in 2013 by Lundstrøm *et al.*[1] However, the literature on the biological activity of this fatty acid is deficient as of yet.

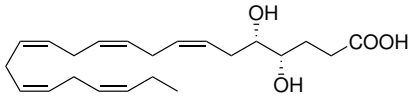

4*S*,5*S*-dihydroxy DPA (**1**)

Fig. 1.1 Chemical structure of 4*S*,5*S*-dihydroxy DPA (**1**).

Polyunsaturated fatty acids (PUFAs) are endogenously converted into lipid mediators which play an important role in the regulation of inflammation, resolution, and homeostasis. Among these are the epoxy fatty acids (EpFAs), which are produced by the cytochrome P450 oxidase system and hold special scientific interest due to their anti-inflammatory, analgesic, and cardiovasculoprotective effects.[2] The major pathway by which EpFAs are degraded is epoxide hydration by the enzyme soluble epoxide hydrolase, giving the corresponding 1,2-dihydroxy fatty acids.[3] Currently, it is of interest to study the effects of PUFAs and their metabolites against pain and itch. The synthesis of 4*S*,5*S*-dihydroxy DPA is thus of interest in order to investigate the compound's biological actions, as well as to perform exact configurational assignment. When available, 4*S*,5*S*-dihydroxy DPA (**1**) will be subjected to *in vitro* biological assays via collaborations in Oslo, Boston, and Durham.

Fig. 1.2 presents the retrosynthetic analysis upon which the synthesis for this project was based. This strategy is built on a semisynthetic

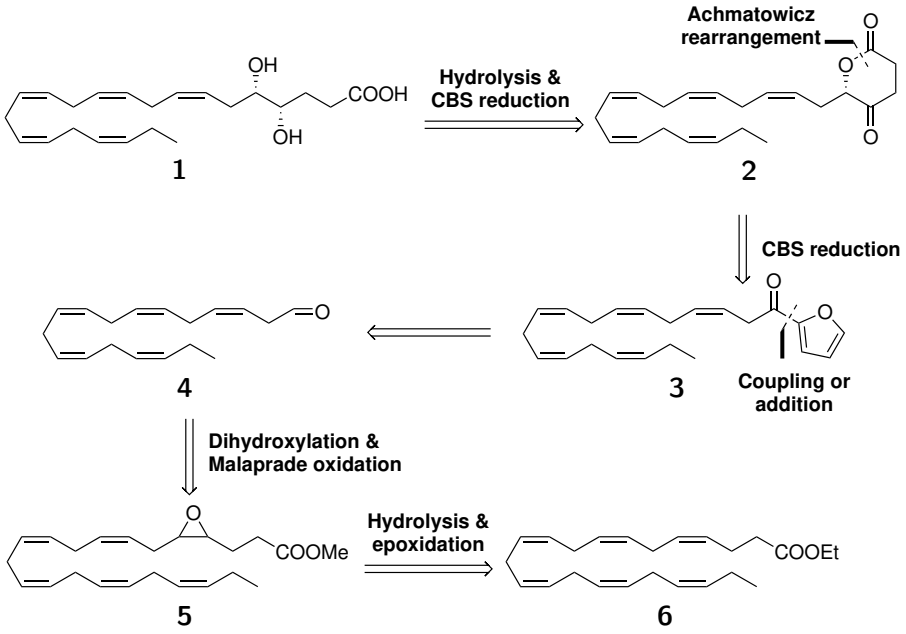

Fig. 1.2 Retrosynthetic analysis of 4*S*,5*S*-dihydroxy DPA (**1**).

approach using the ethyl ester of docosahexaenoic acid (**6**) as a starting material, informed by previous experience in the LIPCHEM group.[4] The first part of the synthetic strategy involves the cleavage of the double bond between C_4 and C_5 to generate the 18C aldehyde **4**, using a previously described procedure.[5] This is followed by the regeneration of the carboxylic end of the fatty acid by way of a coupling or addition reaction, with formation of the *S*,*S*-diol through stereoselective reduction. Conveniently, this strategy preserves five of the six *Z*-configured double bonds present in the starting material.

1.2 Inflammation and resolution of inflammation

Inflammation is a protective response of biological tissue to extraneous threats such as injury or infection. Generally, inflammation is *acute*, and restoration of normal tissue function is indeed the outcome.[6] However, if the pathogen should persist, the acute inflammatory response may turn into *chronic* inflammation. In contrast to acute inflammation, this is a prolonged destructive response, characterised by the presence of mononuclear and macrophage-derived cells in tissues, which leads to tissue damage and local cell proliferation.[7]

The nonspecific (innate) inflammatory response occurs immediately

as a series of cellular and humoural responses following tissue damage.[7] Pattern recognition receptors expressed on innate immune cells bind pathogen-associated macromolecules and promote the production of pro-inflammatory mediators, such as cytokines and chemokines.[8] Aided by paracrine mediators, including leukotriene and prostaglandin lipids,[9,10] they induce vasodilation, exudation, platelet aggregation, expression of adhesives on arterial endothelium, and increased vascular permeability.[7] Through these mechanisms, leukocytes are recruited to the tissue. Additionally, they give rise to some of the cardinal symptoms of inflammation: increased blood flow to the local area produces redness and raised temperature, as well as oedema due to increased transfer of fluids into the tissue, and pain is caused by increased hydrostatic pressure and increased concentration of histamine and bradykinin.[7]

Once the invading pathogen has been eliminated or the damaged tissue repaired, the inflammatory response needs to be terminated. The resolution of inflammation was previously largely thought to be a passive process, consisting of the dissipation of leukocyte chemoattractants.[6] However, during the 20th century, the discovery of potent resolvents which return inflamed tissues to homeostasis gave rise to an emerging understanding of resolution as an active biochemical process. During resolution, the synthesis of pro-inflammatory mediators ceases, and their catabolism begins. This leads to the clearance phase, where polymorphonuclear leukocytes diminish, as they are removed by monocyte-derived phagocytes.[7] The phagocytes subsequently leave the site of inflammation via lymphatic drainage or apoptosis. The mediators of resolution are chiefly polyunsaturated fatty acid derivatives which are generated locally. During the resolution phase, lipid mediators undergo *class switching*, whereby leukocytes are reprogrammed by eicosanoids to synthesise pro-resolving lipid mediators.[10] The specific roles of polyunsaturated fatty acids in inflammation and resolution shall be covered in greater detail in Section 1.3.

Failure of resolution results in the development of chronic inflammation, resulting in secondary necrosis, scarring, and tissue damage. This mechanism is likely the cause of most immune-mediated inflammatory diseases, including rheumatoid arthritis, asthma, psoriasis, and inflammatory bowel disease.[11]

1.3 Polyunsaturated fatty acids

Polyunsaturated fatty acids (PUFAs) such as arachidonic acid (AA) (**7**), eicosapentaenoic acid (EPA) (**8**), and docosahexaenoic acid (DHA) (**9**) are crucial in the regulation of a range of physiological processes. In addition to their roles in cell membrane structure[12] and cell signalling,[13] these compounds are converted into manifold oxygenated lipid mediators which modulate inflammation and immune function by three main metabolic pathways: the cyclooxygenase (COX), lipoxygenase (LOX), and cytochrome P450 (CYP450) pathways.[3,14]

1.3.1 Arachidonic acid

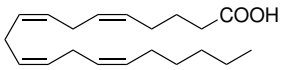

AA (**7**)

Fig. 1.3 Chemical structure of arachidonic acid.

Arachidonic acid (AA, **7**) is an ω-6 PUFA synthesised from linoleic acid, an essential fatty acid.[15] It is one of the most abundant fatty acids in the brain,[13] as well as a major fatty acid in skeletal muscle.[16] AA (**7**) acts as precursor to the eicosanoids, a diverse class of paracrine signalling molecules which modulate inflammation and cardiovascular physiology.[7] The eicosanoids derived from AA (**7**) are generally pro-inflammatory,[15] comprising the prostanoids (prostaglandins, prostacyclin, thromboxanes), and the leukotrienes. AA (**7**) is usually stored in esterified form in the phospholipid pool, and is released by phospholipase A_2, which may be activated by a diversity of pathological stimuli.[17] The free AA (**7**) is metabolised by the COX pathway to generate prostanoids, the LOX pathway to generate leukotrienes and lipoxins, and the CYP450 pathway to generate epoxyeicosatrienoic acids.

1.3.2 ω-3 PUFAs

The ω-3 PUFAs are characterised by the presence of a double bond at the third position counting away from the terminal methyl group. This class of PUFAs includes eicosapentaenoic acid (EPA, **8**), docosahexaenoic acid (DHA, **9**), and n-3 docosapentaenoic acid (n-3 DPA, **10**). ω-3 PUFAs are

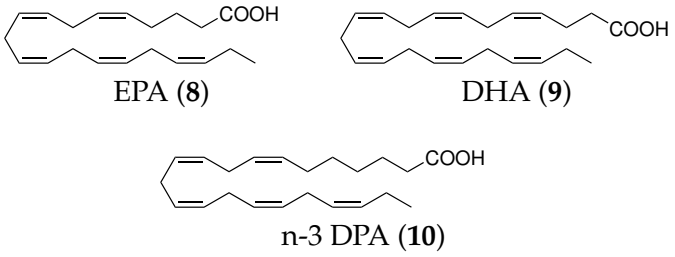

EPA (**8**) DHA (**9**)

n-3 DPA (**10**)

Fig. 1.4 Chemical structures of eicosapentaenoic acid, docosahexaenoic acid, and n-3 docosapentaenoic acid.

essential fatty acids that must be obtained through diet. EPA (**8**), DHA (**9**), and n-3 DPA (**10**) may be biosynthesised from dietary α-linolenic acid,[15] but are acquired much more efficiently from oils of fish[18,19] and algae.[20]

ω-3 PUFAs serve several critical functions in human physiology. DHA (**9**) is a structural component of the central nervous system. It is one of the most abundant fatty acids in the brain together with AA (**7**),[13] and also occurs in high concentration in the retina of the eye.[21] In these tissues, DHA (**9**) is a key factor in maintaining cognitive and neurological function.[15] ω-3 PUFAs are also converted into a variety of lipid mediators distinct from those synthesised from AA (**7**).

Notably, EPA (**8**), DHA (**9**), and n-3 DPA (**10**) are precursors to the non-lipoxin specialised pro-resolving mediators (SPMs) and the ω-3 epoxy fatty acids (EpFAs), which promote the resolution of inflammation.[18] EPA (**8**) gives rise to the E-series resolvins, DHA (**9**) the D-series resolvins, protectins, and maresins, and n-3 DPA (**10**) is precursor to the n-3 DPA resolvins, protections, and maresins. The positive health effects of ω-3 PUFAs have been attributed in part to the production of these lipid mediators. The protective effects of ω-3 PUFAs, SPMs, and EpFAs will be discussed further in Sections 1.3.4 and 1.4.

1.3.3 Inflammatory eicosanoids

1.3.3.1 Prostanoids

Free intracellular AA (**7**) is rapidly metabolised to prostanoids by COX-1 and COX-2 (Scheme 1.1), two membrane-bound enzyme isoforms which are ubiquitous in human cells.[7] While COX-1 is a constitutive, ubiquitously distributed enzyme, COX-2 is inducible, accompanying inflammatory response.[22] The first step involves the cyclisation of AA (**7**)

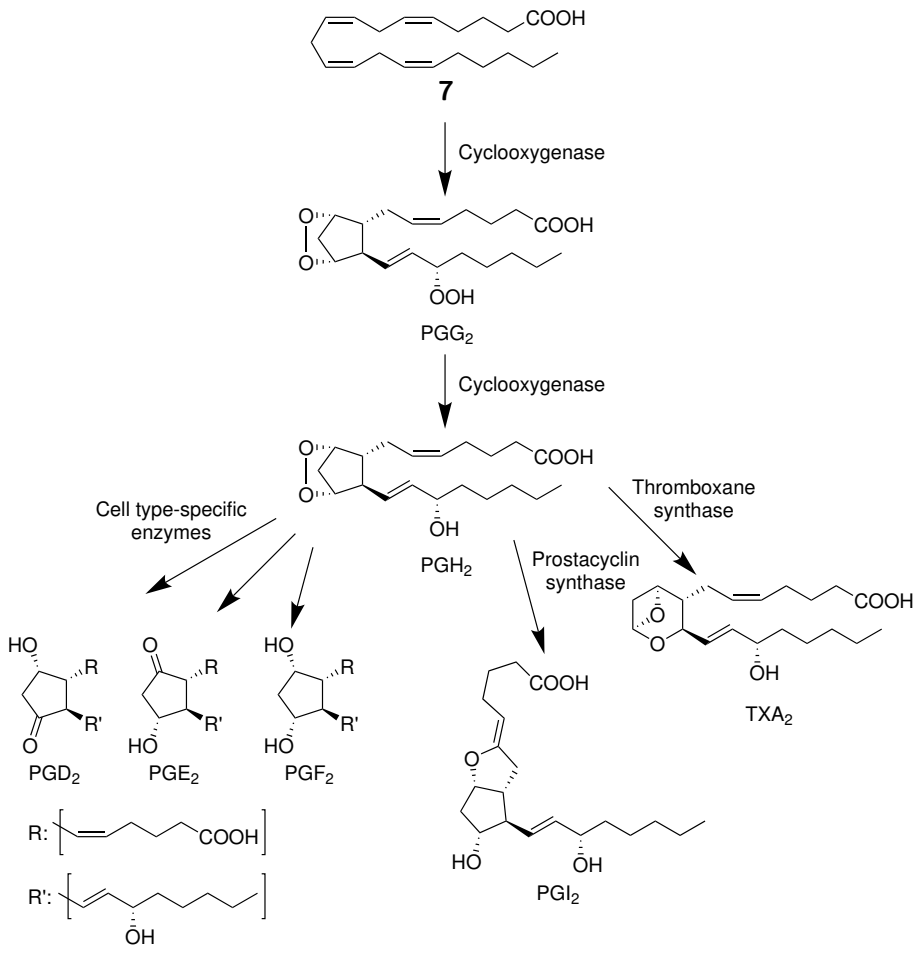

Scheme 1.1 Biosynthesis of prostanoids from arachidonic acid (**7**).[7]

into prostaglandin (PG)G_2, quickly followed by reduction to PGH_2.

PGH_2 is further converted to various prostaglandins by cell type-dependent synthases.[22] The prostaglandins exert a variety of important effects in homeostasis. PGE_2 is found in various tissues, and plays a housekeeping role, modulating gastrointestinal mucosal protection, secretion, and motility,[23] vasodilation and blood flow, as well as inflammation and bronchoconstriction.[7]

Thromboxane and prostacyclin are critical mediators of vascular physiology. Thromboxane synthase is expressed in platelets, and synthesises thromboxane A_2 from PGH_2.[7] Thromboxane induces vasoconstriction and platelet aggregation. It binds to thromboxane receptors and stimulate ADP release, thus making the platelet surface more adhesive. Vascular endothelium, on the other hand, expresses prostacyclin synthase, which produces PGI_2. Prostacyclin functions as an antagnoist to thromboxane, acting

as a vasodilator and inhibitor of platelet aggregation.

1.3.3.2 Leukotrienes

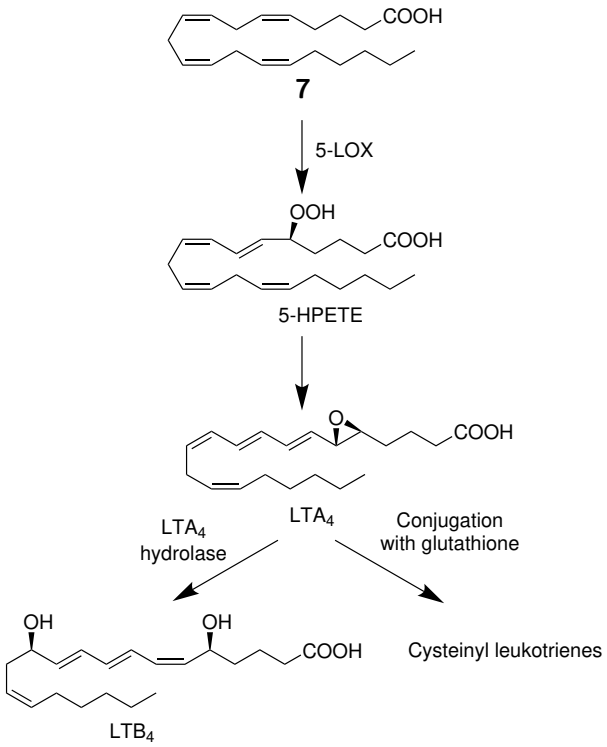

Scheme 1.2 Biosynthesis of leukotrienes from arachidonic acid (**7**).[7]

The leukotrienes are synthesised from AA (**7**) by LOX enzymes (Scheme 1.2) found in lung tissue, platelets, mast cells and leukocytes.[24] 5-lipoxygenase (LOX) catalyses the incorporation of a hydroperoxy group at C_5 in AA (**7**), thereby converting it to 5-hydroperoxyeicosatetraenoic acid (HPETE).[7] 5-LOX is further responsible the transformation of 5-HPETE to the epoxide leukotriene A_4 (LTA_4). This intermediate is converted enzymatically by leukotriene A_4 hydrolase to LTB_4, or by conjugation with glutathione to cysteinyl leukotrienes (LTC_4, LTD_4, and LTE_4), in a cell type-dependent manner. LTB_4 is mainly produced by neutrophils, while the cysteinyl leukotrienes are produced chiefly by eosinophils, mast cells, basophils, and macrophages.

LTB_4 binds to BLT receptors to exert several pro-inflammatory effects. It causes neutrophil chemotaxis and adherence, production of toxic oxygen metabolites, and release of granular enzymes.[25,26] It also stimulates proliferation of and release of cytokines from macrophages and lymphocytes.

LTB_4 is part of the pathophysiological profile of many inflammatory conditions, such as rheumatoid arthritis, psoriasis, and inflammatory bowel disease.[25]

The cysteinyl leukotrienes exert major inflammatory actions on the respiratory and cardiovascular systems.[27,28] In the respiratory system, they act as spasmogens, in addition to enhancing mucus secretion. In the cardiovascular system, LTC_4 and LTD_4 induce coronary vasoconstriction, but vasodilation in other vessels, and increase vascular permeability locally. The cysteinyl leukotrienes are among the most important inflammatory mediators in the pathogenesis of asthma.

1.3.4 Pro-resolving fatty acids

1.3.4.1 Specialised pro-resolving mediators

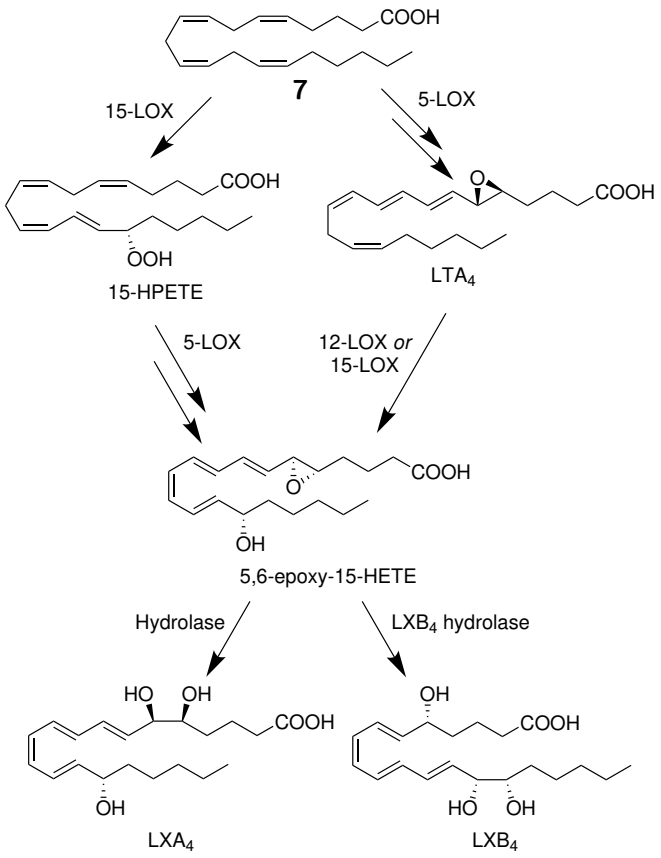

Scheme 1.3 Biosynthesis of lipoxins from arachidonic acid (**7**).[7,29]

In 1984, Serhan *et al.*[30,31] reported the formation of lipoxins from AA (**7**) by 5- and 12- or 15-LOX in leukocytes. This discovery represented

the advent of our understanding of the anti-inflammatory lipid mediators known as specialised pro-resolving mediators (SPMs), as more findings were made of the potent pro-resolving actions of the lipoxins.[32] Since then, the amount of recognised SPMs has expanded dramatically to include numerous resolvins, maresins, and protectins. These compounds fulfil a similar function to the lipoxins, but are distinguished by their biosynthetic origin, being derived from the ω-3 fatty acids EPA (**8**), DHA (**9**), and n-3 DPA through the COX and LOX pathways.[18]

Lipoxins and resolvins oppose pro-inflammatory stimuli chiefly by acting on a system of G protein-coupled receptors expressed in leukocytes.[18,29] Among other actions, these mediators inhibit leukocyte trafficking[33–35] and inflammatory cytokine production,[36] reduce pain,[29,37] and activate non-phlogistic phagocytes.[38–40]

1.3.4.2 Epoxy fatty acids

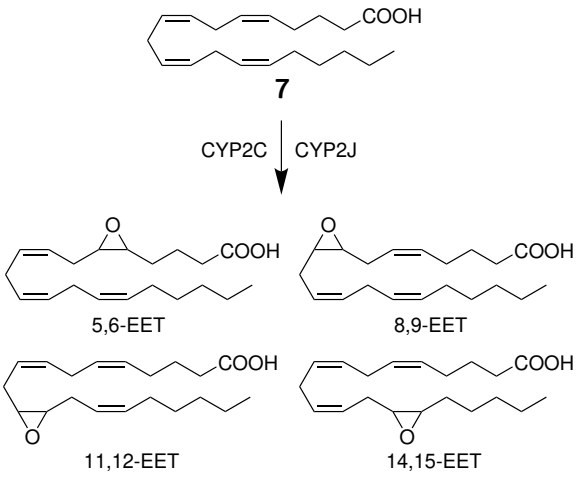

Scheme 1.4 Biosynthesis of epoxyeicosatrienoic acids from arachidonic acid (**7**).[41]

The epoxy fatty acids (EpFAs) are a broad class of anti-inflammatory PUFA derivatives synthesised by *cis*-epoxidation via the CYP450 pathway.[3] One of the double bonds present in the fatty acid is enzymatically epoxygenated, with each CYP epoxygenase producing several regioisomers.[41] CYP450 is also able to produce the pro-inflammatory hydroxylated fatty acid 20-hydroxy eicosatetraenoic acid;[42] there seems to exist an equilibrium between the synthesis of hydroxylated and epoxygenated products.[43]

EpFAs act as both autocrine and paracrine mediators, and have sev-

eral biochemical targets.[41] Like the SPMs, EpFAs exhibit pro-resolving actions, generally promoting a return from inflammation to homeostatic conditions, but also importantly participate in the regulation of cardiovascular and renal function. EpFAs relax vascular smooth muscle,[44] promote angiogenesis,[45] inhibit leukocyte adhesion,[46] thromboxane synthesis and, independently, platelet aggregation,[47] and might enhance lipid metabolism and regulate insulin sensitivity.[48]

ω-3 EpFAs have shown many similar actions to the EpFAs derived from AA (**7**) on the cardiovascular system, including vasorelaxant,[49,50] anti-thrombotic,[51] and vasculoprotective[52,53] effects. EpFAs derived from EPA (**8**) and DHA (**9**) inhibit platelet aggregation, but only weakly inhibit thromboxane synthesis.[51] DHA (**9**)-derived EpFAs have shown the most potent activation of calcium-activated potassium channels[50] and inhibition of platelet aggregation.[51] Furthermore, epoxygenated derivatives of EPA (**8**) and DHA (**9**) exert antihyperalgesic effects peripherally, and epoxygenated DHA (**9**) also centrally.[54]

1.3.5 Dihydroxy fatty acids

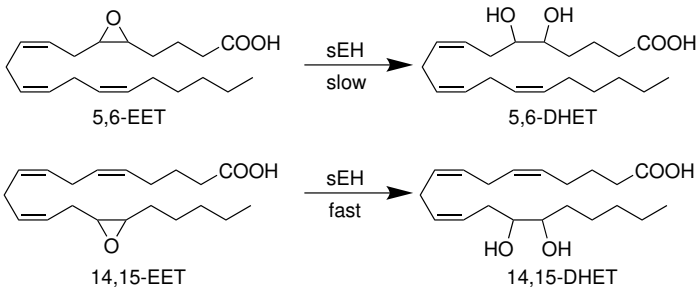

Scheme 1.5 Biosynthesis of dihydroxyepoxyeicosatrienoic acids from epoxyeicosatrienoic acids.[55]

EpFAs are rapidly metabolised by multiple pathways, of which the most important is hydration by soluble epoxide hydrolase (sEH), giving the corresponding 1,2-dihydroxy fatty acids (DiHFAs).[41,45] The sEH is broadly distributed in mammalian tissue, with highest activity in the liver, followed by the kidney, and lower levels in extra-hepatic tissues.[56] In many tissues, sEH co-localises with CYP2C9.[57] Several EpFAs are excellent substrates for sEH, although there seems to be a preference toward epoxides distal to the carboxylic end, as substrates such as 5,6-EET show poor conversion rates.[3,55]

The activity of DiHFAs is generally attenuated compared to their parent EpFAs, and so this was initially viewed as a pathway of inactivation by reducing the pool of EpFAs.[3] However, diols derived from ω-6 fatty acids appear to have distinct, generally pro-inflammatory effects.[58] High levels of DiHFAs appear to be associated with respiratory distress, retinopathy, and coronary artery disease.[48,59,60] However, seemingly opposite actions have been described. Low concentrations of dihydroxyoctadecenoic acid might also suppress neutrophil respiratory burst, thus hindering destructive actions of reactive oxygen species.[61] Decreased sEH activity has been correlated with atherosclerosis,[62] perhaps indicating a vasculoprotective effect of DiHFAs.[63] Dihydroxyeicosatrienoic acids also appear to modulate fatty acid metabolism by promoting β-oxidation.[48]

Relatively little is known of the actions of ω-3 DiHFAs. Recent studies have, however, demonstrated that DiHFAs derived from DHA exhibit concentration-dependent protective or toxic effects on the oculovascular system.[60,64] 19,20-dihydroxy DPA has been shown to be able to participate in physiological retinal angiogenesis, and prevent retinopathy of prematurity at low concentrations through inhibition of astrocyte apoptosis.[65] However, supra-physiological concentrations of 19,20-dihydroxy DPA have been implicated in the pathophysiology of diabetic retinopathy by disrupting vascular endothelial function.[66]

It is becoming apparent that DiHFAs are not just inactivated metabolites of EpFAs, but have distinct biological actions. As DiHFAs, particularly those derived from ω-3 PUFAs, have not yet been exhaustively examined, they may fulfil a physiological role that has yet to be described.

1.4 Marine ω-3 PUFAs as pharmaceuticals

ω-3 PUFAs such as EPA (**8**) and DHA (**9**) are amply found in fish oils,[18] and are widely used as dietary supplements due to their association with a variety of health benefits.[67] These positive effects include reduced expression of pro-inflammatory factors,[68,69] reduction of serum triglycerides,[70] neuroprotection,[71,72] and consequent preventive effects against rheumatoid arthritis,[73], cardiovascular disease,[74] Alzheimer's disease,[72] type 2 diabetes,[75,76] and cancer.[77] The health benefits associated with ω-3 PUFAs have made them attractive to the pharmaceutical industry.

In 1994, Omacor®, an orally administered drug containing the ethyl

esters of DHA (**9**) and EPA (**8**), was approved for marketing by the Norwegian Medicines Agency.[78] Developed by Pronova BioPharma, a company with its roots in the Norwegian cod liver oil industry and Norsk Hydro, it was the first patented drug developed in Norway. Omacor® is indicated for the treatment of endogenous hypertriglyceridaemia. Its mechanism of action is complex and not fully understood, involving multiple processes.[78] DHA (**9**) and EPA (**8**) are poor substrates for enzymes involved in the hepatic synthesis of triglycerides, and inhibit esterification of other fatty acids. They inhibit acyl CoA:diacylglycerol acyltransferase, which catalyses the final step in the acyl-CoA-dependent biosynthesis of triglycerides, and increase peroxisomal β-oxidation of fatty acids in the liver. Hepatic triglyceride secretion is also reduced, while degradation is enhanced. Additionally, cholesterol levels are attenuated.[79] These actions lead to a decrease in triglycerides and very-low-density lipoprotein. Omacor® was also authorised for secondary preventive treatment after myocardial infarction in several EU countries in 2000, but a 2019 reassessment by the European Medicines Agency's committee for human medicines concluded that this use should be terminated due to a lack of evidence.[80]

Since the approval of Omacor®, other pharmaceutical companies have followed suit. In 2014, AstraZeneca won FDA approval for Epanova®, a free fatty acid formulation of DHA (**9**) and EPA (**8**) for use in patients with severe hypertriglyceridaemia.[81] In 2021, the Irish-American company Amarin Pharmaceuticals' Vazkepa® was authorised for European markets.[79] Vazkepa® is a formulation of EPA-only esters indicated to reduce the risk of cardiovascular events as an adjunct to statin therapy in patients with elevated serum triglyceride levels.

It is only recently that the pharmacodynamics of ω-3 fatty acids have been understood to be connected to their specialised pro-resolving lipid mediator derivatives.[18] As our understanding of the properties and biological actions of PUFAs grows more sophisticated, the future is likely to see more therapeutics based around these compounds.

1.5 Previous work by the LIPCHEM group

Our research group has previously worked with a wide range of endogenously formed oxygenated PUFA derivatives, including protectins[82] and

maresins,[83] E-series resolvins,[84,85] n-3 DPA resolvins,[86,87] protectins[88] and maresins,[89] and various other epoxy fatty acids[90] and hydroxylated fatty acids.[91–93] While these syntheses have mainly been performed as convergent syntheses, some have instead been based on semisynthesis from fatty acid starting materials.

A review by Vik and Hansen[4] discusses the benefits of synthesising PUFA derivatives from commercially available PUFAs. Derivatives of fatty acids such as AA (**7**), EPA (**8**), and DHA (**9**) contain multiple *Z*-skipped double bonds which render the preparation of these compounds challenging, and syntheses have typically relied on methods such as reduction of internal alkynes and *Z*-selective Wittig or modified Horner-Wadsworth-Emmons reactions, which often suffer from issues in terms of selectivity. By employing fatty acids like AA (**7**), EPA (**8**), and DHA (**9**) as starting materials, it is possible to preserve the *Z*-configured double bonds already present in these molecules while incorporating the desired functionalities synthetically.

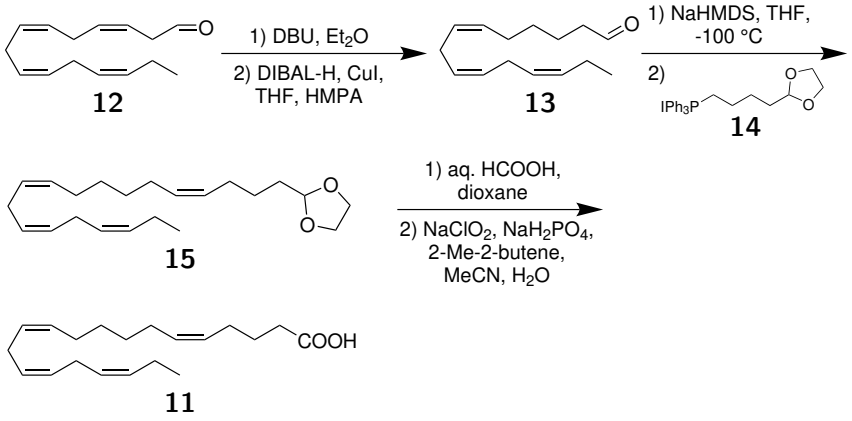

12 **13** **14** **15** **11**

Scheme 1.6 Synthesis of juniperonic acid (**11**).[94]

This strategy has proven its utility in a number of syntheses. In 2010, Vik *et al.*[94] synthesised juniperonic acid (**11**) starting from EPA (**8**) (Scheme 1.6). Aldehyde **12** was prepared using a three-step iodolactonisation-epoxidation-oxidative cleavage procedure. Subsequent rearrangement to an α,β-unsaturated aldehyde using DBU, followed by reduction of the conjugated double bond with DIBAL-H/CuI, afforded the stable aldehyde **13**. A Wittig reaction with phosphonium iodide **14** using NaHMDS as a base provided acetal **15**. Hydrolysis of compound **15** followed by Pinnick-Lindgren oxidation yielded juniperonic acid (**11**).

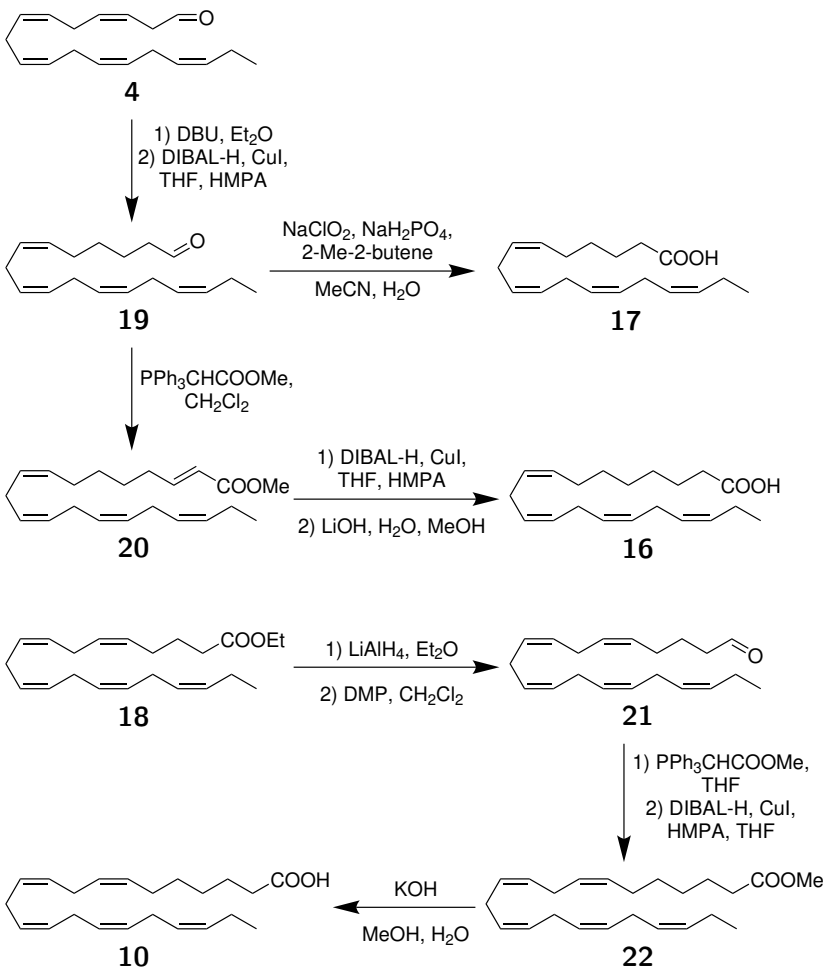

Scheme 1.7 Synthesis of stearidonic acid (**17**), ETA (**16**), and n-3 DPA (**10**).[5]

In 2012, Hansen and co-workers[5] synthesised three ω-3 PUFAs, ETA (**16**), n-3 DPA (**10**), and stearidonic acid (**17**), using DHA (**9**) or the ethyl ester of EPA (**18**) as starting materials (Scheme 1.7). ETA (**16**) and stearidonic acid (**17**) were prepared via an 18C aldehyde (**4**) derived from DHA (**9**). The aldehyde was rearranged with DBU into its corresponding α,β-unsaturated aldehyde, and the conjugated double bond selectively reduced using DIBAL-H/CuI in the presence of HMPA. Pinnick-Lindgren oxidation of the aldehyde (**19**) so formed gave stearidonic acid (**17**). An *E*-selective Wittig reaction of aldehyde **19** gave an α,β-unsaturated ester (**20**), which after reduction of the conjugated double bond and hydrolysis, gave ETA (**16**). n-3 DPA (**10**) was prepared from a C20 aldehyde (**21**) derived from the ethyl ester of EPA (**18**). An *E*-selective Wittig reaction followed by reduction gave a C22 ester (**22**), which after hydrolysis provided the

desired PUFA (**10**).

In 2016, Primdahl *et al.*[92] published stereoselective syntheses of 5-(*S*)-HETE (**23**), 5-(*S*)-HEPE (**24**), and (+)-zooxanthellactone (**25**) using AA (**7**), EPA (**8**), and DHA (**9**), respectively, as starting materials (Scheme 1.8). The free fatty acids were converted into their corresponding iodolactones **26a–c**, which were subsequently esterified under alkaline conditions to hydroxy esters **27a–c**. Oxidation of the alcohols by Dess-Martin or Swern protocol afforded ketones **28a–c** which could then be asymmetrically reduced by CBS reduction before a final hydrolysis or cyclisation to the desired compounds **23**, **24**, and **25**.

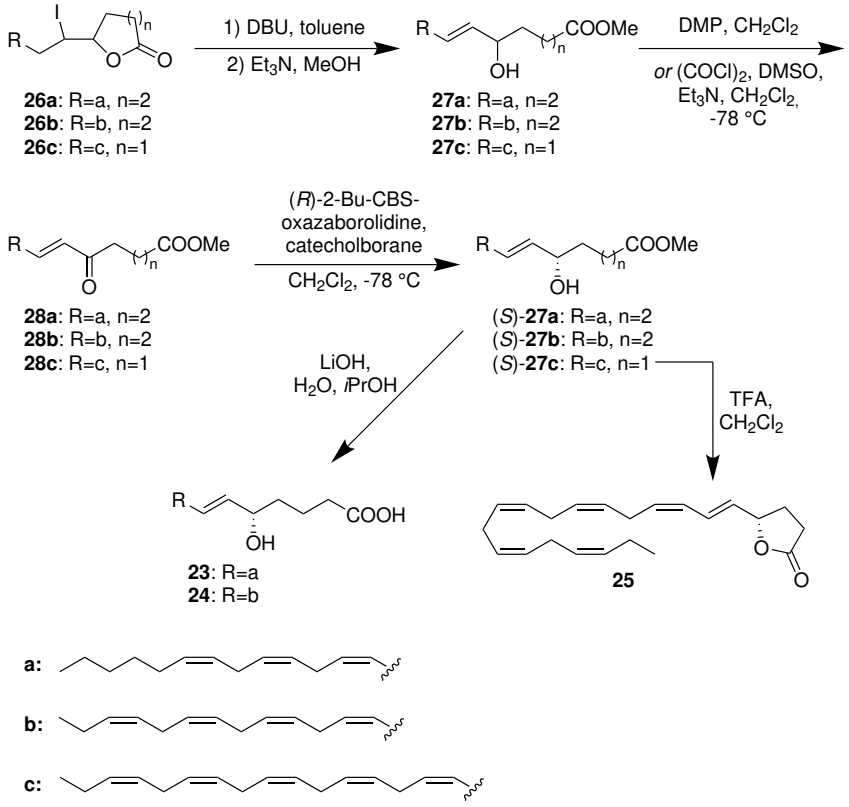

Scheme 1.8 Synthesis of 5-(*S*)-HETE (**23**), 5-(*S*)-HEPE (**24**), and (+)-zooxanthellactone (**25**).[92]

The syntheses described above have served as an important foundation for the synthetic approach employed in this project.

1.6 Synthetic methods

In the synthesis of derivatives from PUFA starting materials, a number of methods have become conventional. Regioselective iodolactonisation and epoxidation reactions are prevalent. As is oxidative cleavage of the resulting epoxides to aldehydes. These procedures afford useful building blocks which are found ubiquitously in the syntheses PUFA-derived natural products and analogues. For examples of their applications, refer to Section 1.5.

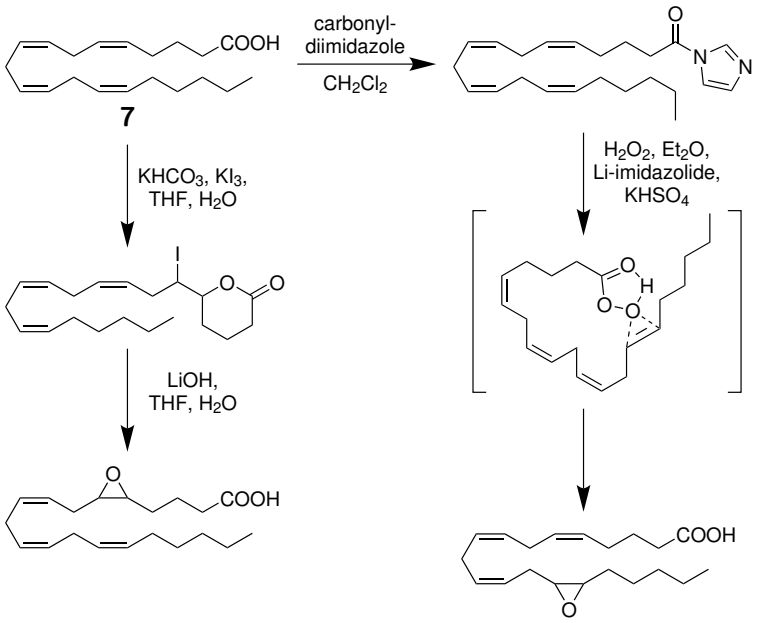

Scheme 1.9 Regioselective epoxidations of AA (**7**) by Corey and co-workers.[95]

An early protocol for regioselective epoxidations of AA (**7**) was developed by Corey and co-workers (Scheme 1.9).[95] Selective epoxidation of the 14,15 double bond was achieved by the preparation of arachidonylimidazole followed by treatment with hydrogen peroxide in the presence of catalytic lithium imidazolide. The selectivity of this reaction was explained by the formation of an energetically favourable 15-membered cyclic intermediate. Selective epoxidation of the 4,5 double bond was also performed via iodolactonisation of AA (**7**), followed by basic hydrolysis. When iodolactonisation occurs under basic conditions, the carboxylate anion attacks the carbon of the cyclic iodonium ion through an S_N2 mechanism.[96] Only the double bond closest to the carboxylate participates, thus giving the

δ- and γ-lactones for Δ^5- and Δ^4-PUFAs, respectively, in accordance with Baldwin's rules.[97]

The iodolactonisation reaction has later been developed considerably and used for other PUFAs such as EPA (**8**) and DHA (**9**). Later iterations have improved many aspects of the Corey protocol by utilising I_2 and collidine bases in MeCN or CH_2Cl_2.[4] These conditions give shorter reaction times, more reproducible yields, and avoid the use of large excesses of reagents. Stenstrøm and co-workers[98] have reported a one-pot procedure for the conversion of the ethyl ester of EPA into its corresponding δ-iodolactone. Said synthesis was achieved by hydrolysis of the ester with LiOH, followed by addition of HI to neutral pH, and finally addition of I_2.

The above procedures were used in the preparation of aldehyde **4**. In addition to these more PUFA chemistry-based reactions, organometal chemistry was utilised in the synthesis of ketone **3**. These methods will be discussed following sections.

1.6.1 Stille coupling

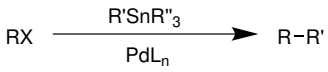

Scheme 1.10 General outline of the Stille reaction.[99]

The Stille reaction[99] is a versatile carbon-carbon bond forming, palladium-catalysed coupling reaction between a stannane and an electrophilic coupling partner. It was named after the American chemist John K. Stille, who developed the reaction in the late seventies.[100] The Stille coupling is remarkable due to its impressive scope. The reaction accepts organotin compounds containing a variety of functional groups, including carbonyls, alkenes, alkynes, and aryls.[99] Moreover, stannanes are quite stable and tolerate oxygen and moisture well. Various substrates may be used. Typically, the electrophile is a halide or pseudohalide, but allylic acetates may also be reactive.[101]

The catalytic cycle begins with oxidative addition of the halide to the palladium, generating a 16 e^- Pd(II) intermediate. The *trans* complex is energetically favoured, and is formed by isomerisation.[102] Next, the organostannane forms an 18 e^- cyclic transition state with the palladium and the halide, exchanging L for the R group of the stannane. The R

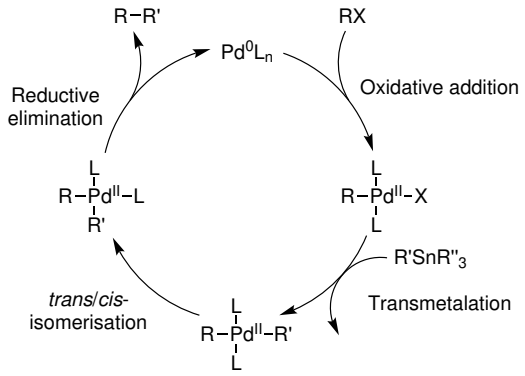

Scheme 1.11 Catalytic cycle of direct Stille coupling. Adapted from Stille.[99]

group is then transferred to the palladium, and the tin halide dissociates. With a stoichiometric amount of stannane, only one group is transferred.[99] Different groups transfer from tin selectively, with simple alkyl groups having the poorest transfer rates. The transmetalation step is slower than both subsequent steps, and is thus rate-determining. Before the final elimination step, the *trans* R groups must isomerise back to a *cis* intermediate for the coordination of their bonding. Finally, the complex undergoes a concerted reductive elimination, whereby the R groups of the stannane and substrate form a σ bond and dissociate from the palladium, which returns to its 14 e^- Pd(0) state.

Stille coupling of acid chlorides, even when sterically hindered or proximal to various other functionalities, typically gives high yields with hardly any byproduct formation under mild, neutral conditions.[99]

1.6.2 Organolithium reagents

Organolithium reagents were first prepared by Schlenk in 1917, and later elaborated by Ziegler, Gilman, and Wittig.[103] This class of compounds contains strongly polar carbon-lithium bonds. As such, organolithium compounds are a useful source of nucleophilic carbon. As nucleophiles, organolithium reagents can add to carbonyl electrophiles to form carbon-carbon bonds. Compared to Grignard reagents, organolithium compounds are less prone to reduce sterically hindered ketones. They are also very strong bases, reacting irreversibly with water to form hydrocarbons.

Organolithium reagents exist as aggregates.[103] Generally, lower aggregates are more reactive. The structure of the aggregate is determined by

solvent effects and steric effects between the ligands on lithium. Lewis bases such as THF and HMPA may coordinate organolithium complexes and deaggregate them, thereby increasing the reagent's solubility and reactivity.[104] However, reactions with organolithium compounds in THF should be performed at low temperature. At temperatures above 0 °C, THF is susceptible to deprotonation by organolithium bases, followed by cycloreversion to ethylene and the lithium enolate of acetaldehyde.[105]

2 Results and discussion

2.1 Synthesis of epoxide 5

Epoxide **5** was prepared from the ethyl ester of DHA (**6**) over three steps, as shown in Scheme 2.1, using a literature procedure.[5] First, the ethyl ester of DHA (**6**) was hydrolysed to DHA (**9**). Compound **9** was subsequently subjected to an iodolactonisation reaction to afford iodolactone **29**. Finally, basic solvolysis of the lactone and epoxidation yielded epoxide **5**. The outline of this synthesis is given in Scheme 2.1. The synthesis was performed multiple times, first using 2 g of the starting material, then later at a 6 g scale. The total yield over the three steps ranged from 52% to 76%.

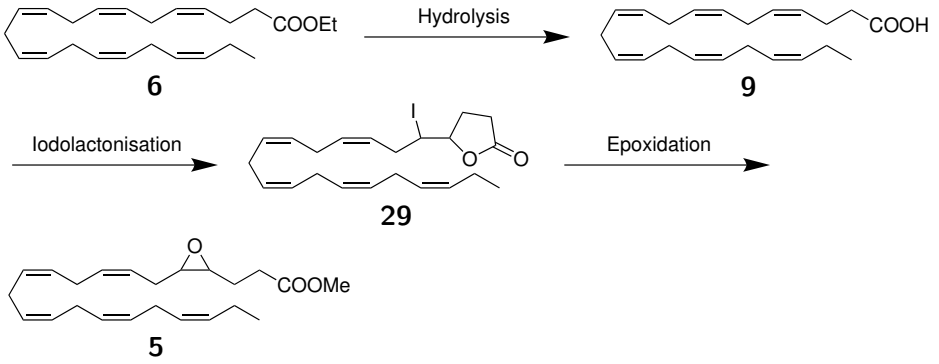

Scheme 2.1 Outline of the preparation of epoxide **5** from DHA ethyl ester (**6**).

2.1.1 Preparation of DHA (9)

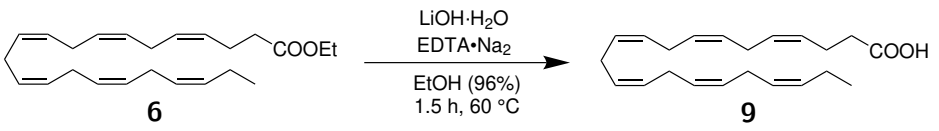

Scheme 2.2 Conditions for the preparation of DHA (**9**).

DHA (**9**) was prepared from its ethyl ester (**6**) by basic hydrolysis with LiOH. EDTA·Na_2 was employed as a radical scavenger.

The recorded ^{1}H spectrum of DHA (**9**) is shown in Fig. 7.1, and the corresponding ^{13}C spectrum in Fig. 7.2. The spectral data were in agreement with those previously reported for this compound.[106]

2.1.2 Preparation of iodolactone 29

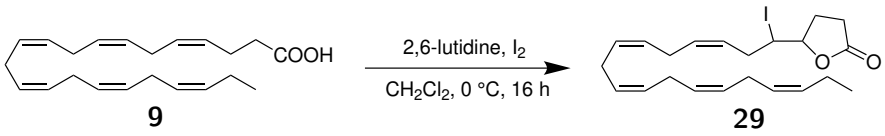

9 **29**

Scheme 2.3 Conditions for the preparation of iodolactone **29**.

DHA (**9**) was deprotonated using 2,6-lutidine and treated with I_2 to produce a cyclic iodonium, which could in turn react with the carboxylate to selectively give a Baldwin-favoured[97] *5-exo-tet* ring closure, affording iodolactone **29**.

The recorded ^{1}H and ^{13}C spectra of the crude mixture containing compound **29** are shown in Fig. 7.3 and Fig. 7.4, respectively. The spectra show that 2,6-lutidine was retained even after the workup. The signals at 7.49 and 6.98 ppm in the ^{1}H NMR spectrum correspond to 2,6-lutidine, and its presence additionally accounts for the signal at 2.61 - 2.50 integrating for five protons, rather than one.[107] The signals at 157.6, 137.1, 120.5, and 24.4 ppm in the ^{13}C spectrum also belong to 2,6-lutidine.[107] Otherwise, the spectral data were in agreement with those reported in the literature.[92]

2.1.3 Preparation of epoxide 5

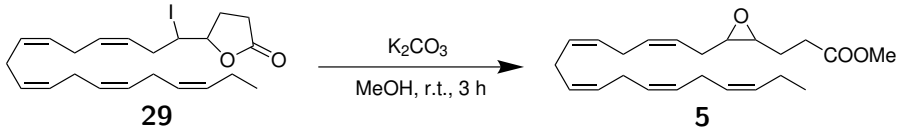

29 **5**

Scheme 2.4 Conditions for the preparation of epoxide **5**.

Solvolysis of iodolactone **29** in MeOH using K_2CO_3 as a base enabled an intramolecular epoxidation, expelling iodide, which finally afforded epoxide **5**. The obtained ^{1}H and ^{13}C spectra are found in the appendix

(Fig. 7.5 and Fig. 7.6). The spectral data were in agreement with those reported previously for this compound.[5]

2.2 Synthesis of aldehyde 4

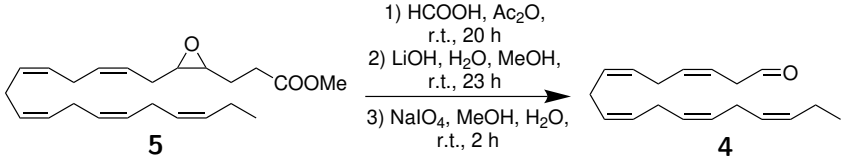

Scheme 2.5 Conditions for the preparation of compound **4**.

The preparation of aldehyde **4** from epoxide **5** was performed over three steps, initially based on a procedure performed in the LIPCHEM group previously by Jakobsen *et al.*[5] The synthesis of compound **4** presented more of a challenge compared that of compound **5** due to a problematic workup in the second step. It was attempted several times, with varying success in terms of both yield and purity. Thus the literature procedure by Holmeide and Skattebøl[108] referenced in Jakobsen *et al.*'s paper was investigated, and it was observed that the former achieved quite satisfactory results. A comparison between the two procedures revealed a couple of key differences.

Firstly, Holmeide and Skattebøl's procedure used a 10:1 mixture of formic acid and acetic anhydride in the first step, which is consistent with Corey and co-workers' analogous treatment of methyl 5,6-epoxyarachidonate.[109] The mixture of excess formic acid and acetic anhydride contains acetic formic anhydride, which functions as a formylating agent.[110] According to Corey *et al.*,[109] two products are formed: a diformate, as well as a formate lactone, resulting from an intramolecular reaction between a hydroxy group and the activated carbonyl of the methyl ester.

The second reaction step consisted of basic hydrolysis of the esters formed during the first step to produce a diol **30**. Jakobsen *et al.* acidified the mixture to pH < 3 during the workup, while Holmeide and Skattebøl describe the mixture as "neutralised". The choice of pH during the workup proved to be crucial. An acidic pH value favours the formation of a stable hydroxy lactone **31** from diol **30** (Scheme 2.6). Indeed, the hydroxy γ-lactone was the major byproduct when following the initial protocol.

However, the carboxylic acid is deprotonated at neutral pH, elevating the compound's solubility in aqueous solvent. The optimal pH value for the workup was determined as being slightly below 4. Yet even this gave a mixture of aldehyde and lactone, and to achieve consistent results would require very sensitive control of the pH value. Thus, the synthesis of aldehyde **4** through diol **30** seems unsuitable as it does not afford reproducible results. The implications of the poor stability of diol **30** must also be taken into account when its stereoisomer 4*S*,5*S*-dihydroxy DPA is finally prepared, as lactonisation may pose an issue in the final hydrolysis step. This could render preparing a pure sample for characterisation difficult.

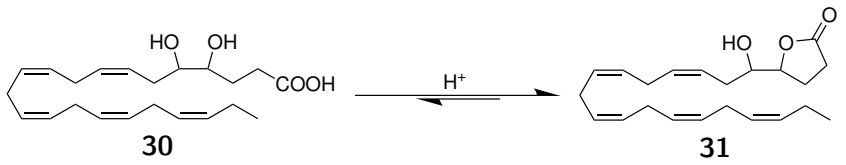

Scheme 2.6 Formation of hydroxy lactone **31** from diol **30** in acidic environment.

A precedent strategy for the synthesis of compound **4** was described by Flock *et al.*[111] Applying this approach, epoxide **5** would be cleaved directly with periodic acid in dry methanol to give an acetal **32**. This intermediate may in turn be converted to aldehyde **4** by acidic hydrolysis (Scheme 2.7). Byproduct formation was noted as a challenge with the periodic acid cleavage, and the yields reported are moderate, leading to the development of Holmeide and Skattebøl's revised approach.[108] The acetal strategy does, however, provide a significant advantage over the later three-step procedure used in this project. Unlike aldehyde **4**, acetal **32** is quite stable and may be purified by flash column chromatography. Thus, using the acetal strategy allows for the preparation of chemically pure aldehyde **4**.[112]

During the final attempt at the synthesis, compound **4** was separated from the corresponding lactones by flash column chromatography. The lactone mixture was hydrolysed again, extracted at pH 4, and oxidised to give the aldehyde in a ^{1}H NMR-estimated 39% yield. The crude product was used in the following reactions as purification by flash column chromatography would lead to isomerisation of the aldehyde into a stable α,β-unsaturated aldehyde **33**.[111]

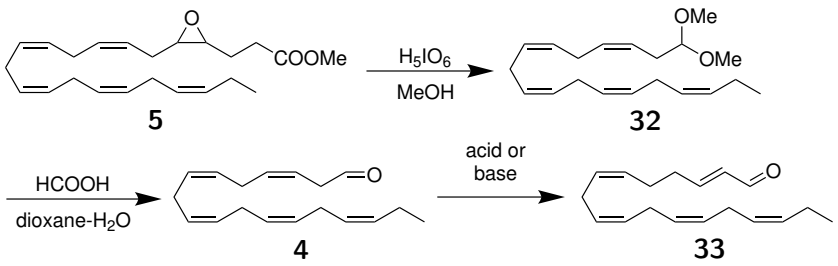

Scheme 2.7 Conditions for the preparation of aldehyde **4** and its isomerisation to aldehyde **33** described by Flock *et al.*[111]

The ^{1}H NMR spectrum of the crude mixture containing aldehyde **4** is shown in Fig. 7.7. The signal at 3.22 ppm integrates for one proton less than expected. This is due to the presence of the hydroxy γ-lactone byproduct discussed previously, which increases the intensity of all signals except for those at 9.67 and 3.22 ppm, which are unique to the aldehyde. This also contributes to the low integral for the aldehydic proton. It should also be noted that all derivatives synthesised from aldehyde **4** showed the expected number of protons in their corresponding peaks. Otherwise, the signals were in agreement with those reported for this compound previously.[113] The corresponding ^{13}C NMR spectrum is shown in Fig. 7.8. The signals were in agreement with those reported in the literature.[112]

2.3 Synthesis of ketone 3 - Stille coupling route

It is said that all roads lead to Rome; however, the same was not the case for ketone **3**. The original retrosynthetic analysis for this project envisioned the preparation of **3** by Stille coupling of acid **34** and 2-(tributylstannyl)furan, which would avoid the oxidation step necessary when going the organolithium route via alcohol **36**. On paper, the Stille reaction should be perfectly suited for this compound, as it should give high yields under mild reaction conditions, with no side reactions.[99] Yet in practice, the Stille protocol failed to give the desired product.

2.3.1 Preparation of acid 34

The synthesis of a fatty acid similar to compound **34** had previously been performed in the LIPCHEM group by Vik *et al.* in high yield.[94] The same Pinnick-Lindgren protocol was therefore used for the synthesis of acid **34**.

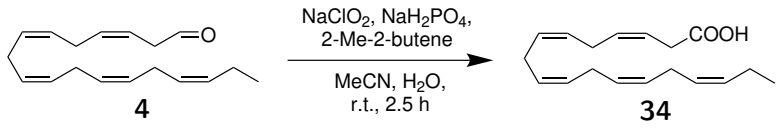

Scheme 2.8 Conditions for the preparation of compound **34**.

Aldehyde **4** was reacted with $NaClO_2$ in a phosphate buffer over 2.5 h to afford acid **34** in a ^{1}H NMR-estimated 63% yield. 2-Me-2-butene was used as an HOCl scavenger.

The crude product was used in the following reaction as testing the Stille reaction was prioritised at the time, and significant tailing and thus loss of acid **34** was anticipated in case of column chromatography. The product of the synthesis of acid **34**'s purity was comparable to that of the synthesis of aldehyde **4**. The major expected impurities apart from possibly 3-chloro-2-methylbutan-2-ol should not react competitively in a Stille coupling.

The ^{1}H NMR spectrum of the crude mixture containing acid **34** is shown in Fig. 7.9. The signals were in agreement with those previously described for this compound.[113]

2.3.2 Attempted Stille couplings

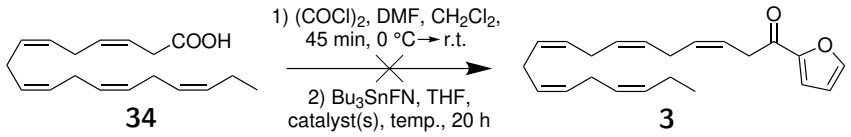

Scheme 2.9 General conditions for the attempted preparation of compound **3** by Stille coupling.

Stille coupling of acid chloride **35** derived from compound **34** and 2-(tributylstannyl)furan was attempted multiple times. The chlorination step was based on a literature procedure[114] using DMF as a catalyst. Unfortunately, the Stille reaction refused to afford a product under various conditions (Table 2.1).

The reaction was first attempted at r.t. TLC of the reaction mixture showed a UV-active spot with R_f 0.6 (EtOAc:heptane 1:2) for which ketone **3** was initially thought to be a candidate, but ^{1}H NMR of the product showed that the desired compound had not been formed. Instead, additional signals had appeared in the alkanic-allylic area of the spectrum, indicating

Table 2.1 Conditions used in the attempted Stille couplings of **34** and 2-(tributylstannyl)furan.

Entry	Catalyst	Co-catalyst	Temperature
1	10 mol% $PdCl_2(PPh_3)_2$		r.t.
2	10 mol% $PdCl_2(PPh_3)_2$		reflux
3	10 mol% $PdCl_2(PPh_3)_2$	3 eq. LiCl	reflux
4	10 mol% $Pd(PPh_3)_4$		reflux

that perhaps some competing addition to the acyl chloride had occurred. It was concluded that the Stille reaction was not proceeding quickly enough, so the reaction temperature was increased to reflux for all subsequent attempts. Additionally, the chlorination reaction and the Stille coupling were consolidated into a sequential one-pot synthesis, in order to lessen the acid chloride's exposure to the environment.

Despite the increased reaction temperature, the lack of a coupling product and decomposition or loss of the acid chloride was still observed. It was thus decided to attempt the use of LiCl as an additive in order to enhance the rate-determining transmetalation step.[99] When this did not produce the desired reaction either, a final attempt was made changing the type of catalyst from a Pd(II) catalyst to the 18 e^- Pd(0) catalyst palladium tetrakis. Ultimately, also this failed to yield ketone **3**. The Stille reaction was thus abandoned.

2.4 Synthesis of ketone 3 - Organolithium route

As the Stille coupling reaction failed to give a product, an alternative route employing an organolithium reaction was pursued.

2.4.1 Preparation of alcohol 36

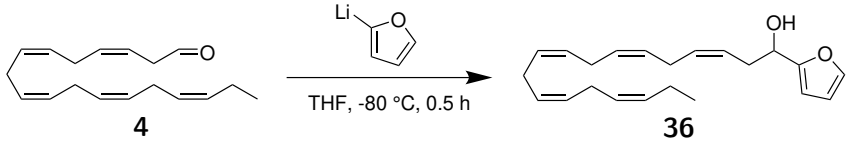

Scheme 2.10 Conditions for the preparation of alcohol **36**.

Alcohol **36** was synthesised by a reaction between aldehyde **4** and

2-lithiofuran according to a literature procedure.[115] The organolithium reagent was generated in situ over the course of 2 h, then reacted with the aldehyde over 0.5 h at -80 °C to give compound **36**.

While the reaction was reliable and easy to perform, a few vexatious issues were still present. Firstly, the obtained yields were generally poor, the yield obtained initially being only 11% (over the four steps from epoxide **5**). One potential cause for the loss of product was determined to be the workup, which had followed the procedure of Tang *et al.*[115] The reaction mixture was quenched with water, extracted with Et_2O, and washed with sat. aq. NH_4Cl and brine. However, using this procedure, formation of emulsions was observed during extraction. Therefore, a different workup described by Yang and Zhou[116] was introduced: the mixture was quenched with sat. aq. NH_4Cl rather than water, and extracted with EtOAc. This increased the yield to 25%. Quenching the reaction mixture with NH_4Cl after the mixture had warmed to r.t. led to the formation of a salt precipitate which could be dissolved by the addition of water. Quenching the mixture after about 10 min of warming gave two layers with a clean border.

In order to further improve the yield, it was attempted to increase the amount of BuLi and furan from 1.2 and 1.6 equivalents, respectively, to 1.5 and 1.9 equivalents. This measure gave a slightly though not significantly higher range of yields of 26% to 34%, but ultimately had more drawbacks than intended. The increased amount of organolithium species seemed to promote byproduct formation, which relates to the other major issue, namely purity.

Due to the synthesis of aldehyde **4** employing a protocol not allowing for purification by column chromatography, any byproducts generated, including hydroxy lactone **31**, were inexorably brought to the organolithium reaction. This is doubly unfortunate, because these impurities both consumed 2-lithiofuran and rendered isolation of alcohol **36** unattainable. In the MS spectrum of the product mixture containing alcohol **36** (Fig. 7.17), three major impurities with *m/z* values of 441.2975, 485.2662, and 797.5834 are shown. Unfortunately, the impurities have not been isolated so as to identify them, but it is possible to suggest structural characteristics for some of them.

During Dess-Martin oxidation of alcohol **36** to ketone **3**, it was observed that the R_f value of one of these impurities in EtOAc-heptane increased,

which would indicate the oxidation of an alcohol. The mass of 485.2662 could correspond to a diol **37** formed from the reaction between hydroxy lactone **31** and 2-lithiofuran, involving dehydration of the resultant tertiary alcohol to form a conjugated double bond (Scheme 2.11). The formation of this compound would be enhanced by the presence of excess 2-lithiofuran when using the larger equivalents of BuLi and furan. The impurity with a mass of 797.5834 is possibly the product of lithiated furan reacting with both aldehyde **4** and a decomposition product of hydroxy lactone **31**. The impurity with a mass of 441.2975, however, was not oxidised by DMP, and thus should not contain an alcohol group which would react in a Dess-Martin oxidation. It is therefore likely not a decomposition product of hydroxy lactone **31**.

The described impurities were seemingly not separable from alcohol **36** by column chromatographic purification. Repeated column chromatography reduced the yield of the product without any increase in purity.

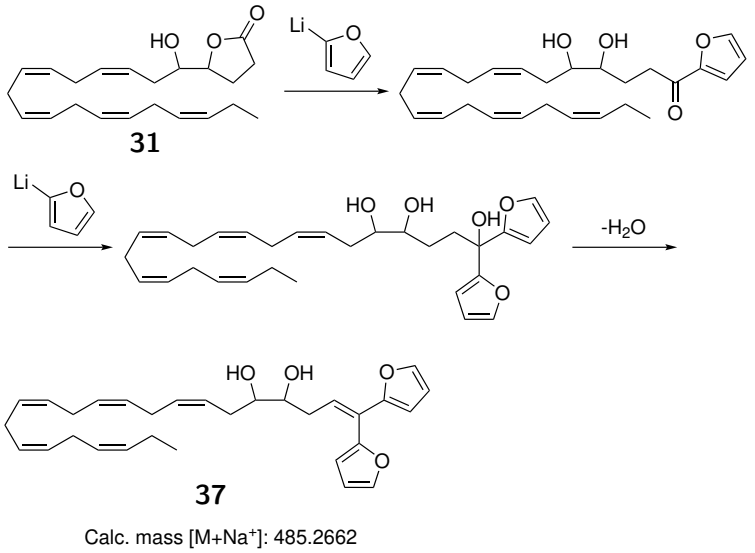

Scheme 2.11 Proposed formation of possible byproduct **37**.

2.4.2 Characterisation of alcohol 36

2.4.2.1 NMR assignments

The assigned shifts for compound **36** are listed in Table 2.2.

The recorded ^{1}H NMR spectrum of alcohol **36** (Fig. 7.11) contains ten signals integrating for thirty protons. The most upfield triplet signal at

Table 2.2 ^{1}H NMR (400 MHz) and ^{13}C NMR (101 MHz) shifts for compound **36** in $CDCl_3$.

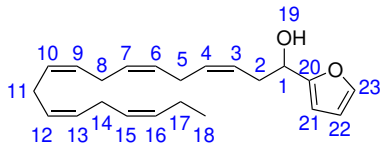

36

Pos.	δ_H [ppm]	Mult.	Int.	δ_C [ppm]	COSY	HMBC
1	4.73	q	1	67.5	2, 19	20
2	2.72 – 2.57	m	2	33.8	1, 3, 4	1, 3, 4, 20
3	5.60 – 5.48	m	1	131.6	2, 4, 5	1, 2, 4, 5
4	5.47 – 5.25	m	9	124.7	2, 3, 5	-
5	2.93 – 2.75	m	8	25.9	-	-
6	5.47 – 5.25	m	9	-	-	-
7	5.47 – 5.25	m	9	-	-	-
8	2.93 – 2.75	m	8	-	-	-
9	5.47 – 5.25	m	9	-	-	-
10	5.47 – 5.25	m	9	-	-	-
11	2.93 – 2.75	m	8	-	-	-
12	5.47 – 5.25	m	9	-	-	-
13	5.47 – 5.25	m	9	-	-	-
14	2.93 – 2.75	m	8	-	-	-
15	5.47 – 5.25	m	9	127.1	14, 16	-
16	5.47 – 5.25	m	9	132.2	15, 17	-
17	2.15 – 2.02	m	3	20.7	16, 18	15, 16, 18
18	0.98	t	3	14.4	17	16, 17
19	2.15 – 2.02	m	3	-	1	1, 2, 20
20	-	-	-	156.2	-	-
21	6.28 - 6.21	m	1	106.2	22	22, 23, 20
22	6.37 – 6.29	m	1	110.3	21, 23	20, 21, 23
23	7.42 – 7.35	m	1	142.1	22	21, 20

0.98 ppm corresponds to the terminal methyl group. The signal at 2.15 – 2.02 ppm corresponds with both the allylic protons adjacent to the terminal methyl, and the OH proton. The signal integrated for either two or three protons, depending on the water content of the solvent, and when integrating for three protons had a slightly asymmetric shape. The COSY spectrum of alcohol **36** (Fig. 7.15) showed correlations with the protons of positions 1, 17, and 18, indicating both the OH and the methylene. The signal at 2.72 – 2.57 ppm thus corresponds to the allylic protons at position 2, while the eight doubly allylic protons give rise to the multiplet at 2.93 – 2.75 ppm. The quartet at 4.73 ppm corresponds to the deshielded proton adjacent to the hydroxy group. The ten vinylic protons give rise to the multiplets at 5.47 – 5.25 ppm and 5.60 – 5.48 ppm, the latter belonging to the proton closest to the alcohol group. In the COSY spectrum of alcohol **36**, the signal at 5.60 – 5.48 ppm correlated with the protons at position 2. The final three signals at 6.28 - 6.21 ppm, 6.37 – 6.29 ppm, and 7.42 – 7.35 ppm correspond to the furan moiety. Their respective positions of 21, 22, and 23 were determined by COSY and HMBC (Fig. 7.16).

For the proton signals only belonging to a single position, HSQC (Fig. 7.14) was used to determine their corresponding carbons in the ^{13}C NMR spectrum (Fig. 7.12). The signals at 14.4 ppm, 20.7 ppm, and 33.8 ppm correspond to the sp^3 carbons at positions 18, 17, and 2, respectively. The sp^2 carbon at position 3 produces the signal at 131.6 ppm. The carbons of the furanyl group give rise to the signals at 106.2 ppm, 110.3 ppm, and 142.1 ppm. The signal at 156.2 ppm did not correlate with any protons and thus belongs to position 20. COSY and HMBC was used to determine the signals corresponding to positions 4, 15, and 16. The signal at 124.7 ppm corresponds to position 4, the signal at 127.1 to position 15, and the signal at 132.2 to position 16. Finally, the signal at 25.9 ppm was assigned based on comparison with data from compound **3**. The remaining nine signals could not be assigned, as they could not be distinguished by means of COSY or HMBC. The remaining carbons at the double allylic positions give shifts in the area 25.8 - 25.66 ppm. The vinylic carbons give shifts in the area 128.7 - 127.97 ppm.

2.4.2.2 Mass spectrometry

HRMS of alcohol **36** (Fig. 7.17) gave *m/z* 349.2137 for $[M+Na]^+$. The molecular formula $C_{22}H_{30}NaO_2$ with a calculated mass of 349.2138 was confirmed with an accuracy of 0.3 ppm.

The spectrum also showed signals for impurities at *m/z* 441.2975, 485.2662, 797.5834, and 947.5414. For the signal at *m/z* 485.2662, the molecular formula $C_{30}H_{38}NaO_4$ with a calculated mass of of 485.2662 was confirmed with an accuracy of 0.2 ppm.

2.4.2.3 UV-Vis spectroscopy

The UV-Vis spectrum of alcohol **36** (Fig. 7.18) contained no detected peaks in the area of 200 - 400 nm. However, the decline observed between 200 nm and 240 nm should almost certainly be taken to correspond to a peak around 200 - 210 nm, in agreement with the furan moiety.[117] Cf. the UV-Vis spectrum of ketone **3** (Fig. 7.27). Compound **36** was weakly active when visualised with UV light, requiring a relatively high concentration to be clearly visible.

2.4.2.4 IR spectroscopy

The IR spectrum of alcohol **36** (Fig. 7.19) showed the O-H bond as a weak broad band at 3383 cm^{-1}. At 3014 cm^{-1}, a signal corresponding with aromatic C-H stretching was observed.

2.4.3 Preparation of ketone 3

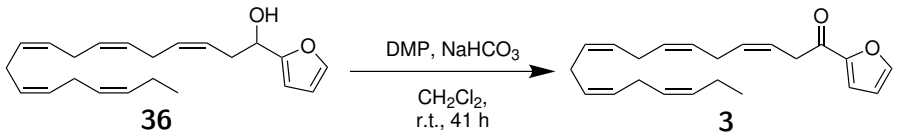

Scheme 2.12 Conditions for the preparation of ketone **3**.

The oxidation of alcohol **36** to ketone **3** proved to be yet another challenging step. Compound **36** unfortunately seemed to be a poor substrate for oxidation, requiring long reaction times. In addition to this, the impurities which were carried over from the previous reactions gave very complex product mixtures, making monitoring reactions more difficult.

It was initially thought that the oxidation could be performed using MnO_2 as the oxidising agent, yet when this was attempted, no conversion of the starting material was observed. In order to ascertain the activity of the MnO_2 used, the method was tested using 4-methoxybenzyl alcohol as a simpler substrate. ^{1}H NMR of the reaction mixture after 2.5 h confirmed the conversion to 4-anisaldehyde. The ineffectiveness of MnO_2 may be due to a lack of contact between the hydroxy moiety and the oxidant. While we would expect an unsaturated fatty acid derivative to have a large surface area, one possible explanation might be that the compound may adopt a conformation where the carbon chain is coiled such that its methyl end encumbers the hydroxy group. This would potentially be a larger issue for MnO_2 than for other oxidants, because MnO_2 is not dissolved and contact requires adsorption of the substrate.

Oxidation using DMP was first performed as a test reaction at a 25 mg scale. The reaction ran overnight for 20.5 h, after which the product was extracted. However, the reaction gave only 15 mg of crude material, and ^{1}H NMR of the product showed only an estimated 80% conversion to ketone **3**. Thus purification would leave a negligible yield. It was decided to investigate other methods of oxidation to see if they would give more satisfactory results.

Swern oxidation was attempted next. TLC of the reaction mixture showed consumption of alcohol **36**; however, ^{1}H NMR of the crude product revealed that the desired product had not been formed. Due to doubts about the integrity of the oxalyl chloride used, the reaction was attempted again using a different package, yet the same result was obtained. Had more time been available, it might have been possible to test variations such as the Pfitzner-Moffatt or Parikh-Doering reactions, but for the time being, reactions with activated DMSO were considered a dead end.

Oxidation with PCC was subsequently attempted, and initially seemed promising as TLC indicated some formation of ketone **3**. Yet after stirring overnight for 19 h, TLC of the reaction mixture showed no apparent increase in conversion. It also indicated a complex mixture of at least six compounds. Another equivalent of PCC was added to the reaction, but after 2 h, there was still no sign of further consumption of alcohol **36**. The ^{1}H NMR spectrum of the crude product gave the impression of significant impurities, and determining conversion was difficult, but a rough estimate gave approximately 45% conversion. PCC thus gave

inferior results compared to DMP. This, in addition to the issues of toxicity and griminess associated with PCC, made DMP seem like the preferable option.

It was thus decided to revisit the Dess-Martin reaction. At the larger scale used, however, conversion was significantly slower. After 18 h, TLC still showed preservation of a large amount alcohol **36**. In order to further the conversion, another 0.5 eq. of DMP was added, and the mixture was stirred for an additional 23 h. When even this did not advance the consumption of alcohol **36**, the reaction was considered to have reached a stasis. Despite the increase in both eq. DMP and reaction time, a conversion of only 63% was estimated. The product was extracted and purified to give ketone **3** in a modest yield of 17%. Also, an impurity with *m/z* 441.2975, which was also observed in the synthesis of alcohol **36**, was found to still be present in the product after column chromatography.

The reaction was attempted one more time with a different package of DMP, as batch-to-batch variation and age may affect the reagent's performance.[118,119] Yet the same issue of slow conversion as last time was observed. It was thus decided to attempt an alternative method adapted from Meyer and Schreiber.[119] After a reaction time of 23 h, 1 eq. of water was added dropwise to the reaction mixture in order to increase the rate of conversion. According to Meyer and Schreiber, partial hydrolysis of DMP enhances the reaction rate by providing an acetoxy periodinane hydroxide intermediate where the increased electron-donating effect of the hydroxide accelerates the dissociation of the remaining acetate ligand (Scheme 2.13). Their work suggests the addition of water over 0.5 h, after which the reaction should be complete.

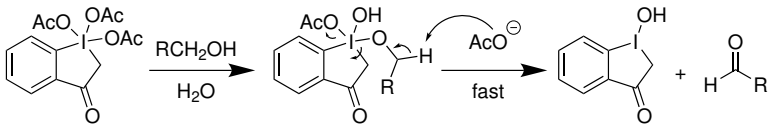

Scheme 2.13 Partial hydrolysis of DMP, as outlined by Meyer and Schreiber.[119]

Unfortunately, the addition of water did not lead to any noticeable improvement in terms of conversion. TLC after the addition of water showed no further consumption of alcohol **36**, nor after another 40 min. After a cumulative reaction time of 25.5 h, the product was extracted.

The crude mixture showed a similar conversion to the last attempt of approximately 57%, albeit with an even higher degree of impurity. The product was purified by flash column chromatography to give a trivial yield of 8%.

One possible obstacle to the Dess-Martin reaction, apart from the poor reactivity of alcohol **36**, is competitive oxidation of impurities present in the reaction mixture. As previously discussed, the product mixture containing compound **36** also contained a compound which underwent oxidation by DMP. If this compound were the product of hydroxy lactone **31** being opened by 2-lithiofuran, it would be a diol, which would be readily oxidised by DMP.[120] Thus increasing the amount of DMP would likely have been beneficial in this case, and the use of pure alcohol **36** even more advantageous.

A comparison of the oxidation reactions tested is given in Table 2.3. In summary, MnO_2 and activated DMSO were not suitable oxidants for compound **36**, and between DMP and PCC, DMP gave the best results.

Table 2.3 Conditions and conversion estimated by ^{1}H NMR for the various oxidation reactions tested to synthesise compound **3**.

Entry	Oxidant	Scale [mg]	Time [h]	Conversion [%]
1	13 eq. MnO_2	75	22.5	0
2	2.0 eq. DMSO + 1.2 eq. $(COCl)_2$	100	1.3	-
3	2.5 eq. PCC	150	21	45
4	1.2 eq. DMP	25	20.5	80
5	1.7 eq. DMP	100	41	63
6	1.2 eq. DMP + 1 eq. H_2O	100	25.5	57

2.4.4 Characterisation of ketone 3

2.4.4.1 NMR assignments

The assigned shifts for ketone **3** are given in Table 2.4. Due to their structural similarities, several of compound **3**'s ^{1}H and ^{13}C shifts were straightforwardly assigned based on comparison with alcohol **36**; refer to Section 2.4.2.1.

Table 2.4 ^{1}H NMR (400 MHz) and ^{13}C NMR (101 MHz) shifts for compound **3** in $CDCl_3$.

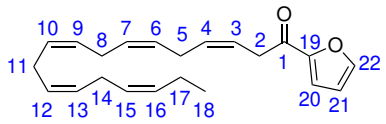

3

Pos.	δ_H [ppm]	Mult.	Int.	δ_C [ppm]	COSY	HMBC
1	-	-	-	187.1	-	-
2	3.64	d	2	37.5	3, 4, 5	1, 3, 4
3	5.76 – 5.57	m	2	131.8	2, 4, 5	2, 5
4	5.76 – 5.57	m	2	121.3	3, 5	5
5	2.94 – 2.77	m	8	26.1	2, 3, 4, 6	3, 4, 6
6	5.47 – 5.25	m	8	-	-	-
7	5.47 – 5.25	m	8	-	-	-
8	2.94 – 2.77	m	8	-	-	-
9	5.47 – 5.25	m	8	-	-	-
10	5.47 – 5.25	m	8	-	-	-
11	2.94 – 2.77	m	8	-	-	-
12	5.47 – 5.25	m	8	-	-	-
13	5.47 – 5.25	m	8	-	-	-
14	2.94 – 2.77	m	8	-	-	-
15	5.47 – 5.25	m	8	127.1	14, 16	-
16	5.47 – 5.25	m	8	132.2	15, 17	-
17	2.13 – 2.01	m	2	20.7	16, 18	15, 16, 18
18	0.97	t	3	14.4	17	16, 17
19	-	-	-	152.6	-	-
20	7.21	d	1	117.3	21	19, 21, 22
21	6.57 – 6.51	m	1	112.4	20, 22	19, 20, 22
22	7.59	d	1	146.5	21	19, 20, 21

The shifts for positions 17 and 18 were unchanged compared to the alcohol. The ^{13}C signal at 187.1 ppm corresponds to the carbonyl. HSQC (Fig. 7.23) confirmed the ^{13}C shifts of 37.5 ppm and 152.6 ppm for positions 2 and 19, respectively. COSY (Fig. 7.24) confirmed the aromatic ^{1}H shifts of 7.21 ppm, 6.57 – 6.51 ppm, and 7.59 ppm, and the corresponding ^{13}C shifts of 117.3 ppm, 112.4 ppm, and 146.5 ppm for their respective positions 20, 21, and 22. Finally, HMBC (Fig. 7.25) was used to assign the ^{13}C shifts of 131.8 ppm, 121.3 ppm, 26.1 ppm, 127.1 ppm, and 132.2 ppm to positions 3, 4, 5, 15, and 16.

2.4.4.2 Mass spectrometry

HRMS of ketone **3** (Fig. 7.26) gave *m/z* 347.1981 for $[M+Na]^+$. The molecular formula $C_{22}H_{28}NaO_2$ with a calculated mass of 347.1982 was confirmed with an accuracy of 0.2 ppm.

The spectrum also showed signals for impurities at *m/z* 441.2975 and 553.4591.

2.4.4.3 UV-Vis spectroscopy

The UV-Vis spectrum of ketone **3** (Fig. 7.27) showed, in the area of 190 - 400 nm, two peaks at 205 nm and 273 nm.

2.4.4.4 IR spectroscopy

The IR spectrum of ketone **3** (Fig. 7.28) showed a strong signal corresponding to the conjugated C=O bond at 1679 cm^{-1}. At 3014 cm^{-1}, the same signal corresponding with aromatic C-H stretching as in the spectrum of alcohol **36** was observed.

3 Conclusions

The synthetic studies toward 4*S*,5*S*-dihydroxy DPA (**1**) reported in this master's thesis have produced the key intermediate **3** in eight steps, starting from the ethyl ester of DHA (**6**), with an overall yield of 3%. Novel compounds **36** and **3** have been characterised by various spectroscopic methods. Certain challenges with the synthetic strategy have been identified.

The synthesis of epoxy ester **5** proceeded without much issue, giving pure product in high yield (76%). The protocol employed to prepare aldehyde **4**, however, was determined to be sub-optimal, as it inevitably led to the formation of the troublesome byproduct **31**. An older procedure, involving the preparation of an acetal (**32**), would likely produce superior results.

The Stille coupling protocol attempted in the synthesis of ketone **3** was seemingly ineffective. Both the organolithium reaction and subsequent oxidation used to synthesise ketone **3** gave poor yields (25% and 17%, respectively). These reactions thus pose somewhat of a bottleneck to the overall yield. The yields of both reactions were likely negatively impacted by the impurities present from the synthesis of aldehyde **4**. Neither oxidation with MnO_2 nor Swern oxidation of compound **36** afforded ketone **3**. Both PCC and DMP did, however, with DMP giving the better results.

Unfortunately, the synthesis could not be completed within the given time frame. Hopefully the work reported in this thesis will provide useful information for future studies, and perhaps even the development of new synthetic strategies.

4 Future work

The aim of this project was to develop a stereoselective synthesis of 4*S*,5*S*-dihydroxy DPA (**1**) from the ethyl ester of DHA (**6**). To that end, the intermediate furanyl ketone **3** was synthesised and characterised. Multiple steps still remain, however. Once the synthesis of 4*S*,5*S*-dihydroxy DPA (**1**) has been achieved, biological testing of the compound may be performed.

If the same synthetic route is to be pursued in the future, the protocol reported by Flock *et al.*[111] should be used to synthesise pure aldehyde **4**, thus hopefully allowing for higher yields of alcohol **36** and ketone **3**.

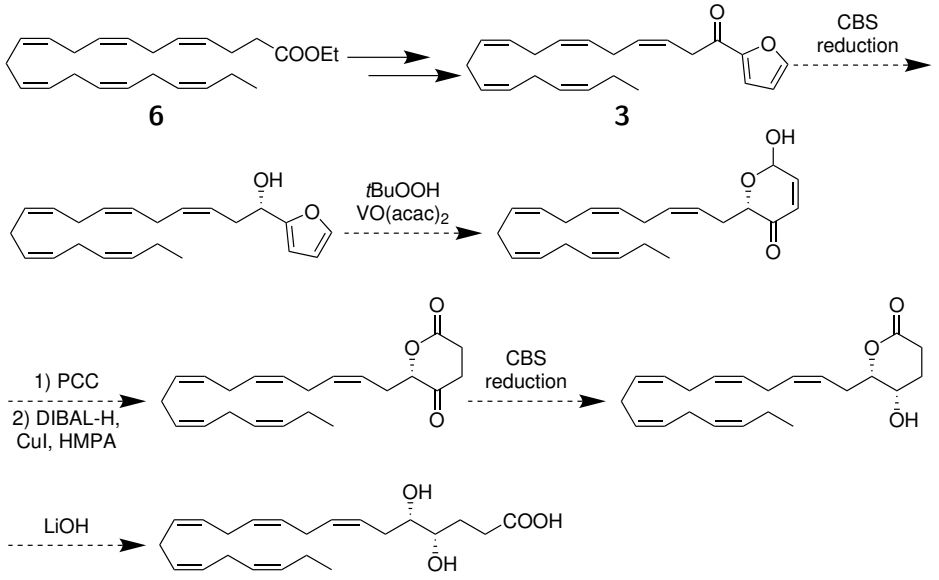

Scheme 4.1 Remaining steps in the planned synthesis of 4*S*,5*S*-dihydroxy DPA (**1**).

If the obtained yields are satisfactory, the remaining steps of the synthesis (Scheme 4.1) may be attempted. The next step involves asymmetric reduction of the ketone to the corresponding *S*-configured alcohol. The CBS reaction[121] was utilised by Primdahl *et al.*[92] in

the synthesis of 5-(*S*)-HETE (**23**) and 5-(*S*)-HEPE (**24**) with improved reproducibility over a Noyori protocol. When performed in CH_2Cl_2 with catecholborane as the reducing agent, the product was obtained in 85% yield and 79 % enantiomeric excess (ee). However, Noyori hydrogenation should not be ruled out, as it has been applied to an acylfuran by Ma and O'Doherty[122] for an 89% yield and 96% ee.

Next, the furanyl alcohol is to be converted into a hydroxy dihydropyranone using a vanadium-catalysed Achmatowicz rearrangement.[123] The use of *t*-butylhydroperoxide as an oxidant and $VO(acac)_2$ as a catalyst has previously proven to be an effective approach giving high yields on a comparable substrate.[124] Afterwards, all that remains is a simple oxidation and hydrogenation procedure, another CBS reduction, and finally hydrolysis of the lactone to yield the desired 4*S*,5*S*-dihydroxy DPA (**1**).

However, if this synthetic route should prove to be challenging, an alternative approach to the synthesis of the carboxylic end is possible. Namely, preparing the hydroxy δ-lactone moiety as a separate fragment and connecting it to an EPA (**8**)-derived C15 aldehyde (**12**) by a *Z*-selective Wittig reaction (Fig. 4.1). This fragment could be prepared in eight steps from commercially available 3-bromopropanoyl chloride and 2-(tributylstannyl)furan. While this approach increases the number of steps, the simpler substrates used in the Stille and Achmatowicz reactions would potentially render them more compliant.

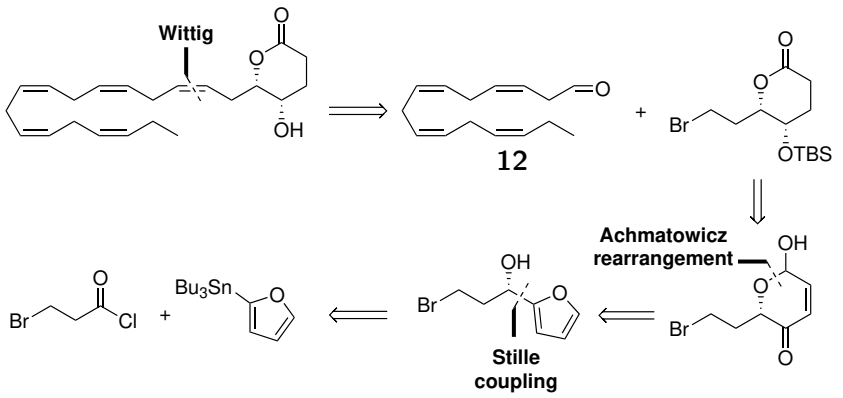

Fig. 4.1 Alternative retrosynthetic analysis using aldehyde **12** derived from EPA (**8**).

5 Experimental

5.1 Materials & general information

Unless otherwise indicated, all reactions were performed under argon atmosphere, with aluminium foil wrapped around the reaction flask in order to minimise exposure to light. Unless otherwise indicated, all commercially available reagents and solvents were used in their supplied form without further purification. All weights reported at the milligram level were recorded on a Sartorius QUINTIX313-1S, while weights reported at the 0.1 milligram level were measured on a VWR LAG 414i-C. Dried solvents were dried over molecular sieves (3 Å) for at least 24 hours.

Thin layer chromatography was performed on silica gel 60 F_{254} aluminium-backed plates manufactured by Merck (Darmstadt, Germany). Visualising agents used include UV light and potassium permanganate ($KMnO_4$).

Flash column chromatography was performed on silica gel 60 (0.040 - 0.063 mm) manufactured by Merck (Darmstadt, Germany).

NMR spectra were recorded on either a Bruker AVII 400 or Bruker AV 400 Neo spectrometer at 400 MHz for ^{1}H NMR, and at 101 MHz for ^{13}C NMR. Coupling constants (J) are reported in Hz, while chemical shift values (δ) are reported in parts per million relative to the residual central solvent resonance ($CDCl_3$ δ_H = 7.26, δ_C = 77.16).

Mass spectra were recorded at the Department of Chemistry, University of Oslo, on a maXis II ETD instrument, using ESI as the method of ionisation.

UV-Vis spectroscopy was performed on an Agilent Cary 8454 UV-Vis spectroscopy system. The Agilent OpenLab ChemStation software was used to process the spectra.

IR spectra were recorded on an Agilent 5500 Series FTIR spectrometer. The spectra were recorded in the range of 4000 - 650 cm^{-1}. The Agilent

MicroLab software was used to process the spectra.

5.2 Experimental procedures

5.2.1 Synthesis of DHA (9)

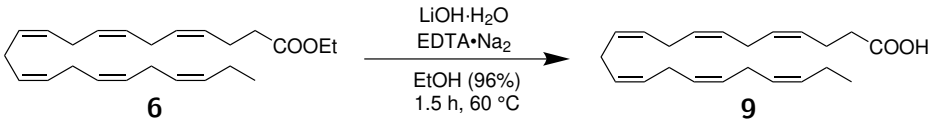

Scheme 5.1 Synthesis of DHA (**9**).

DHA ethyl ester (**6**) (6.01 g, 16.9 mmol, 1.00 eq.) was dissolved in ethanol (50 mL, 96%) and added to a mixture of $LiOH{\cdot}H_2O$ (4.95 g, 118 mmol, 7.00 eq.) and $EDTA{\cdot}Na_2$ (29.9 mg) in water (50 mL) under argon atmosphere before stirring for 1.5 h (60 °C). The mixture was cooled and quenched with HCl (40 mL, 10%) before it was extracted with 2:1 EtOAc:hexane (5×25 mL). The combined organic layers were washed with water (20 mL) and brine (20 mL), then dried over $MgSO_4$. The solvent was removed at reduced pressure, affording a yellow oil (5.19 g). The product was used in the following step without further purification. **^{1}H NMR** (400 MHz, $CDCl_3$) δ_H 5.48 – 5.26 (m, 12H), 2.92 – 2.75 (m, 10H), 2.47 – 2.35 (m, 4H), 2.08 (p, J = 1.4 Hz, 2H), 0.97 (t, J = 7.5 Hz, 3H). The acidic proton was not detected in the spectrum. **^{13}C NMR** (101 MHz, $CDCl_3$) δ_C 179.2, 132.1, 129.6, 128.6, 128.3, 128.3, 128.3, 128.1 (2C), 128.0, 127.9, 127.6, 127.0, 34.0, 25.6 (3C), 25.6, 25.6, 22.5, 20.6, 14.3. The data were in agreement with those described in the literature.[106]

5.2.2 Synthesis of iodolactone 29

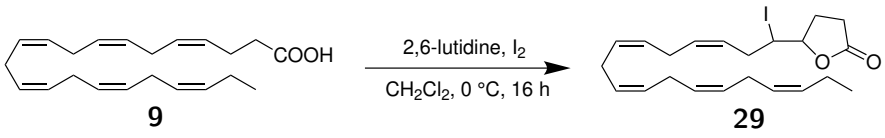

Scheme 5.2 Synthesis of compound **29**.

Compound **29** was prepared according to a protocol reported by Ulven and co-workers.[125] DHA (**9**) (5.17 g, 15.7 mmol, 1.00 eq.) was dissolved in CH_2Cl_2 (50 mL), and a solution of 2,6-lutidine (3.67 mL, 31.5 mmol, 2.00

eq.) in CH_2Cl_2 (61 mL) was added dropwise to the acid under stirring. The flask was subsequently immersed in an ice bath, and an ice cold mixture of I_2 (7.99 g, 31.5 mmol, 2.00 eq.) in CH_2Cl_2 (157 mL) was added to the flask. The system was purged with argon and stirred for 16 h overnight at 0 °C.

The mixture was quenched with $Na_2S_2O_3$ (260 mL, 10%), transitioning from claret to orange, before it was extracted with CH_2Cl_2 (2×50 mL). The organic layer was washed with NaH_2PO_4 (2×50 mL) and brine (2×50 mL), then dried over $MgSO_4$. The solvent was removed at reduced pressure, affording a dark amber liquid. The product was used immediately in the following step. **^{1}H NMR** (400 MHz, $CDCl_3$) δ_H 5.62 – 5.51 (m, 1H), 5.44 – 5.26 (m, 9H), 4.26 (td, *J* = 7.2, 3.0 Hz, 1H), 4.12 (td, *J* = 7.4, 3.0 Hz, 1H), 2.90 – 2.66 (m, 11H), 2.61 – 2.50 (m, 1H), 2.47 – 2.33 (m, 1H), 2.15 – 1.98 (m, 3H), 0.97 (t, *J* = 7.5 Hz, 3H); **^{13}C NMR** (101 MHz, $CDCl_3$) δ_C 176.3, 132.2, 131.7, 128.9, 128.7, 128.6, 128.1, 128.0, 127.5, 127.1, 126.9, 80.8, 37.9, 34.7, 28.6, 27.4, 26.0, 25.82, 25.79, 25.7, 20.7, 14.4.

5.2.3 Synthesis of epoxide 5

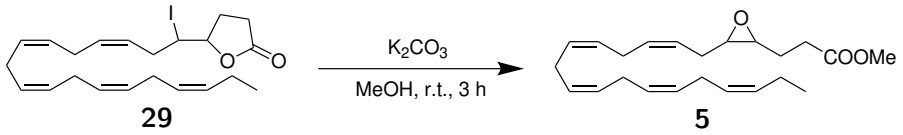

29 **5**

Scheme 5.3 Synthesis of compound **5**.

Compound **29** was dissolved in MeOH (100 mL), K_2CO_3 (6.96 g, 50.4 mmol, 3.20 eq.) was added, and the mixture was stirred for 3 h at r.t. Upon completion of the reaction, the mixture was filtered through celite and washed with Et_2O. Water (100 mL) and brine (100 mL) were added to the filtrate, which was then extracted with Et_2O (3×100 mL). The combined organic layers were washed with water (2×30 mL) and brine (30 mL) and dried over $MgSO_4$. The solvent was removed at reduced pressure, leaving a brown oily residue (4.91 g). The crude product was purified by flash column chromatography on silica gel (EtOAc:hexane 1:5) to afford epoxide **5** as a pale yellow oil. **Yield:** 4.61 g (76% over three steps); **^{1}H NMR** (400 MHz, $CDCl_3$) δ_H 5.58 – 5.25 (m, 10H), 3.69 (s, 3H), 3.03 – 2.93 (m, 2H), 2.90 – 2.77 (m, *J* = 6.1, 5.6 Hz, 9H), 2.59 – 2.46 (m, 2H), 2.44 – 2.31 (m, 1H), 2.30 – 2.18 (m, 1H), 2.12 – 2.02 (m, 2H), 2.01 – 1.87 (m, 1H), 1.87 – 1.73 (m, 1H), 0.97 (t, *J* = 7.5 Hz, 3H); **^{13}C NMR** (101 MHz, $CDCl_3$) δ_C 173.3, 132.1, 130.8,

128.7, 128.6, 128.5, 128.1, 127.9, 127.8, 127.1, 124.3, 56.7, 56.1, 51.8, 31.1, 26.3, 25.9, 25.8, 25.74, 25.65, 23.5, 20.7, 14.4. The NMR data were in agreement with those reported in the literature.[5] **MS** (ESI): exact mass calculated for $C_{23}H_{34}O_3Na$ [M+Na]$^+$: 381.2400, found 381.2399.

5.2.4 Synthesis of aldehyde 4

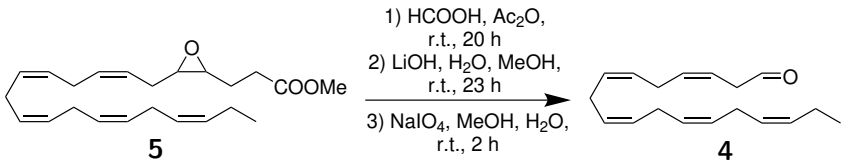

Scheme 5.4 Synthesis of compound **4**.

Aldehyde **4** was prepared based on protocols reported by Jakobsen *et al.*[5] and Holmeide and Skattebøl.[108] A solution of compound **5** (1.00 g, 2.79 mmol, 1.00 eq.) in HCOOH (2.9 mL, 77 mmol, 28 eq.) and Ac_2O (2.9 mL, 31 mmol, 11 eq.) was stirred under argon at r.t. for 20 h. The mixture was concentrated at reduced pressure, affording a ruddy oil, which subsequently was dissolved in MeOH (25 mL) and immersed in an ice bath. A solution of $LiOH{\cdot}H_2O$ (884 mg, 21.1 mmol, 7.56 eq.) in water (25 mL) was added, and the pH was confirmed to be $\geq$10. The mixture was stirred under argon at r.t. for 23 h, then acidified to pH 2 using 0.5 M HCl (70 mL). The mixture was extracted with Et_2O (4$\times$45 mL). The combined organic layer was washed with brine (15 mL) and dried over $MgSO_4$. The solvent was removed at reduced pressure to afford a golden oil. The oil was subsequently dissolved in MeOH (23 mL) and submerged in an ice bath. A solution of $NaIO_4$ (898 mg, 4.20 mmol, 1.51 eq.) in water (17 mL) was added. The mixture was removed from the ice bath and allowed to stir under argon at r.t. for 2 h. The mixture was then diluted with 47 mL of water before it was extracted with Et_2O (4$\times$50 mL). The organic phase was washed with sat. aq. $NaHCO_3$ (2$\times$30 mL) and brine (30 mL), then dried over $MgSO_4$. The solvent was removed at reduced pressure to give a yellow oil (570 mg). **^{1}H NMR** (400 MHz, $CDCl_3$) δ_H 9.67 (t, J = 1.9 Hz, 1H), 5.74 – 5.65 (m, 1H), 5.63 – 5.54 (m, 1H), 5.52 – 5.25 (m, 8H), 3.22 (dt, J = 7.2, 1.7 Hz, 1H), 2.95 – 2.75 (m, 8H), 2.14 – 2.00 (m, 2H), 0.97 (t, J = 7.5 Hz, 3H). The ^{1}H NMR spectrum integrated for one proton less than expected, see section **2.2** for an account. **^{13}C NMR** (101 MHz, $CDCl_3$) δ_C 199.5, 133.3,

132.2, 129.0, 128.8, 128.6, 127.94, 127.91, 127.2, 127.1, 118.8, 42.6, 26.1, 25.79, 25.77, 25.7, 20.7, 14.4. The ^{13}C NMR shifts were in agreement with those reported previously.[112]

5.2.5 Synthesis of acid 34

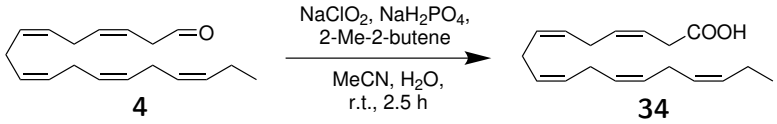

Scheme 5.5 Synthesis of compound **34**.

Acid **34** was prepared using a Pinnick-Lindgren oxidation.[126] Aldehyde **4** (250 mg) was dissolved in a solution of $NaH_2PO_4 \cdot H_2O$ (1.063 g) in MeCN (24 mL) and water (9.6 mL). 2-Me-2-butene (5.84 mL) and $NaClO_2$ (993 mg) were added to the flask, and the mixture was stirred under argon at r.t. for 2.5 h. The mixture was then diluted with 200 mL of water, acidified to pH 2 using 0.5 M HCl (35 mL), and extracted with hexane (4×25 mL). The combined organic layer was washed with water (20 mL) and dried over $MgSO_4$. The solvent was removed at reduced pressure to afford a yellow oil (137 mg). **^{1}H NMR** (400 MHz, $CDCl_3$) δ_H 5.65 – 5.54 (m, 2H), 5.50 – 5.24 (m, 8H), 3.18 (d, J = 5.3 Hz, 2H), 2.88 – 2.77 (m, 8H), 2.08 (p, J = 7.4 Hz, 2H), 0.97 (t, J = 7.5 Hz, 3H). The acidic proton was not detected in the spectrum. The chemical shifts were in agreement with those described in the literature.[113] **^{13}C NMR** (101 MHz, $CDCl_3$) δ_C 177.7, 132.2, 132.0, 128.9, 128.8, 128.6, 128.0, 127.9, 127.3, 127.1, 120.7, 32.7, 25.9, 25.8 (2C), 25.7, 20.7, 14.4.

5.2.6 Attempted synthesis of ketone 3 by Stille coupling

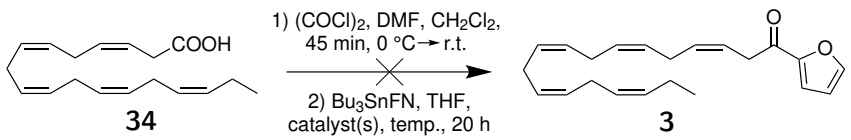

Scheme 5.6 General conditions for the attempted preparation of compound **3** by Stille coupling.

The preparation of acid chloride **35** was based on a procedure reported by Hori *et al.*[114] Compound **34** (45 mg, 0.16 mmol, 1.0 eq.) was dissolved

in 2-Me-THF (1 mL), and the solvent was evaporated. The acid was subsequently dissolved in dry CH_2Cl_2 (1 mL) under argon atmosphere and immersed in an ice bath. 2 drops of dry DMF were added. $(COCl)_2$ (20 µL, 0.23 mmol, 1.4 eq.) was added dropwise to the flask, and the mixture was stirred at 0 °C for 15 min, then for another 30 min at r.t. to afford acid chloride **35**.

Compound **35** was used immediately in the following Stille coupling.[99] Representative procedure: $PdCl_2(PPh_3)_2$ (10 mg, 0.014 mmol, 0.088 eq.) and dry THF (9 mL) were added to the reaction flask, before the addition of 2-(tributylstannyl)furan (54 µL, 0.17 mmol, 1.1 eq.). The mixture was stirred at reflux for 20 h. The reaction mixture was subsequently diluted with water (50 mL), and extracted with Et_2O (3×40 mL). The combined organic layers were washed with brine (15 mL), dried over $MgSO_4$, and evaporated to give a brown oily residue. The desired product was not formed.

5.2.7 Synthesis of alcohol 36

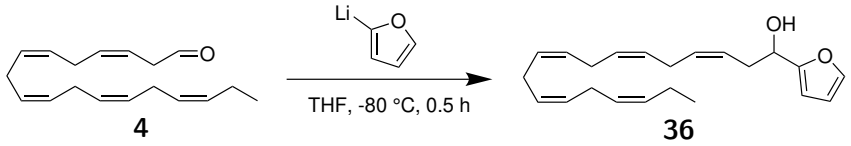

Scheme 5.7 Synthesis of alcohol **36**.

The preparation of alcohol **36** was based on a procedure reported by Tang *et al.*,[115] using a workup described by Yang and Zhou.[116] Furan (0.30 mL, 4.13 mmol, 1.61 eq.) was added to a flame-dried round-bottom flask and dissolved in anhydrous THF (6 mL). A 1.6 M solution of BuLi in hexanes (1.92 mL, 3.07 mmol, 1.20 eq.) was added dropwise to the flask, and the mixture was stirred for 2 h. Aldehyde **4** (662 mg, 2.56 mmol, 1.00 eq.) was dissolved in 2-Me-THF and evaporated, then dissolved in dry THF (6 mL). The reaction flask containing 2-lithiofuran was immersed in a dry ice/acetone bath, and the solution of **4** in THF was added dropwise to the flask. The reaction mixture was purged with argon and stirred for 0.5 h, without the flask being wrapped in aluminium foil. The mixture was allowed to warm, then quenched with sat. aq. NH_4Cl (12 mL). The organic layer was separated, and the aqueous layer was extracted with EtOAc (6×10 mL). The combined organic layers were washed with brine (10 mL), then dried over $MgSO_4$. The solvent was evaporated to afford

a yellow oil (594 mg). The crude product was purified by flash column chromatography on silica gel (EtOAc:heptane 1:10) to afford compound **36**. **Yield:** 208 mg (25% over four steps); **IR** (neat, cm^{-1}) 3383 (w, br), 3014, 2965, 2913, 2876; **^{1}H NMR** (400 MHz, $CDCl_3$) δ_H 7.42 – 7.35 (m, 1H), 6.37 – 6.29 (m, 1H), 6.28 – 6.21 (m, 1H), 5.60 – 5.48 (m, 1H), 5.47 – 5.25 (m, 9H), 4.73 (q, J = 4.9 Hz, 1H), 2.93 – 2.75 (m, 8H), 2.72 – 2.57 (m, 2H), 2.15 – 2.02 (m, 3H), 0.98 (t, J = 7.5 Hz, 3H). **^{13}C NMR** (101 MHz, $CDCl_3$) δ_C 156.2, 142.1, 132.2, 131.6, 128.7, 128.5, 128.4, 128.1, 127.99, 127.97, 127.1, 124.7, 110.3, 106.2, 67.5, 33.8, 25.9, 25.8, 25.75, 25.66, 20.7, 14.4; **MS** (ESI): exact mass calculated for $C_{22}H_{30}O_2Na$ $[M+Na]^+$: 349.2138, found 349.2137.

5.2.8 Attempted synthesis of ketone 3 by oxidation with MnO_2

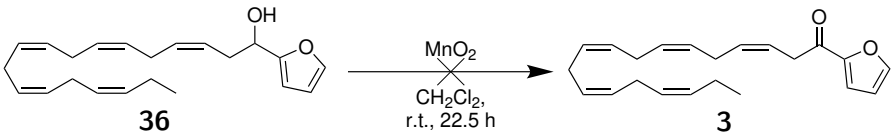

Scheme 5.8 Attempted synthesis of ketone **3** using MnO_2 as oxidant.

The attempted oxidation of alcohol **36** using MnO_2 was based on a procedure described by Sæther *et al.*[127] Compound **36** (85 mg, 0.26 mmol, 1.0 eq.) was added to a flame-dried flask, dissolved in dry CH_2Cl_2 (15 mL), and added celite (460 mg) and MnO_2 (85%, 230 mg, 2.25 mmol, 8.65 eq.). The system was purged with argon and stirred at r.t. for 22.5 h, where MnO_2 (85%, 115 mg, 1.12 mmol, 4.31 eq.) was added in portions over the first 4.5 h. TLC (EtOAc:heptane 1:4, UV/$KMnO_4$ stain) indicated no consumption of alcohol **36**. The mixture was filtered through a plug of celite and washed with EtOAc. The solvent was evaporated to recover the starting compound in quantitative yield.

5.2.9 Attempted synthesis of ketone 3 by Swern oxidation

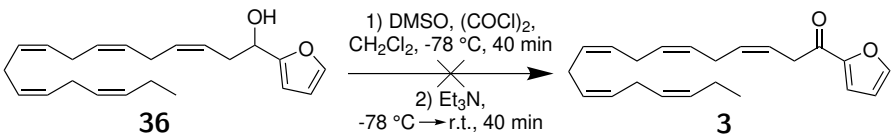

Scheme 5.9 Attempted synthesis of ketone **3** by Swern oxidation.

The attempted oxidation of alcohol **36** using activated DMSO followed

a Swern protocol.[128] $(COCl)_2$ (31 µL) was added to a flame-dried flask and dissolved in dry CH_2Cl_2 (3 mL). The flask was immersed in a dry ice/acetone bath. DMSO (43 µL) was added dropwise under stirring. Alcohol **36** (102 mg) was dissolved in dry CH_2Cl_2 (0.3 mL) and added dropwise to the reaction flask. The mixture was stirred for 40 min, added Et_3N and removed from the cooling bath, then stirred for 40 min while warming to r.t. The mixture was diluted with CH_2Cl_2 (3 mL), washed with NH_4Cl (3×4 mL) and brine (3 mL), and dried over $MgSO_4$. The solvent was evaporated at reduced pressure to give a brown oil (87 mg). The desired product was not formed.

5.2.10 Synthesis of ketone 3 by oxidation with PCC

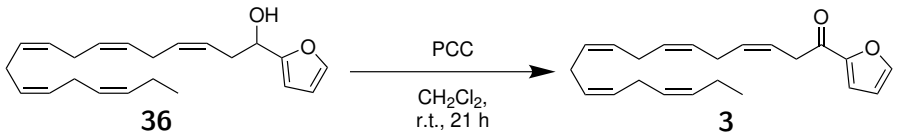

Scheme 5.10 Synthesis of ketone **3** by oxidation with PCC.

The oxidation of alcohol **36** using PCC was based on a procedure reported by Aurrecoechea *et al.*[129] PCC (247 mg) and celite (529 mg) were added to a flame-dried flask and mixed with CH_2Cl_2 (3 mL). Alcohol **36** was dissolved in CH_2Cl_2 (1 mL) and added to the flask. After stirring at r.t. for 20 h, TLC analysis (EtOAc:heptane 1:4, UV/$KMnO_4$ stain) showed incomplete conversion. PCC (99 mg) was added, and the mixture was allowed to stir for an additional 2.5 h. Et_2O (6 mL) was added dropwise to the mixture before it was filtered through celite and washed with Et_2O (6+6+2 mL). The solvent was evaporated to give a mixture of yellow oily and particulate residue (77 mg). The crude product was not purified or used further.

5.2.11 Synthesis of ketone 3 by Dess-Martin oxidation

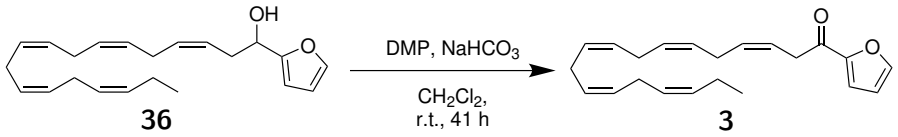

Scheme 5.11 Synthesis of ketone **3**.

Ketone **3** was prepared using a Dess-Martin oxidation.[130] Compound **36** (103 mg, 0.316 mmol, 1.00 eq.) was dissolved in dry CH_2Cl_2 (10 mL) and added to a flame-dried round-bottom flask. $NaHCO_3$ (152 mg, 1.81 mmol, 5.73 eq.) and DMP (161 mg, 0.380 mmol, 1.20 eq.) were added to the flask. The reaction mixture was stirred at r.t. for 18 h. After analysis by TLC (EtOAc:heptane 1:4, UV/$KMnO_4$ stain), $NaHCO_3$ (27 mg, 0.32 mmol, 1.0 eq.) and DMP (67 mg, 0.16 mmol, 0.50 eq.) were added, and the mixture was stirred for another 23 h. The reaction mixture was then quenched with sat. aq. $Na_2S_2O_3$ (4 mL), and the aqueous layer was extracted with CH_2Cl_2 (5×5 mL). The combined organic layers were washed with $NaHCO_3$ (5 mL), and dried ($MgSO_4$). The solvent was evaporated at reduced pressure to afford a yellow oily residue (127 mg). After purification by flash column chromatography (EtOAc:heptane 1:20), ketone **3** was obtained as a clear oil. **Yield:** 18 mg (17%); **UV-Vis** (MeOH) λ_{max} 205 nm (ε = 2602 $M^{-1}cm^{-1}$); **IR** (neat, cm^{-1}) 3014, 2965, 2932, 1679, 1569, 1468; **^{1}H NMR** (400 MHz, $CDCl_3$) δ_H 7.59 (d, *J* = 1.6 Hz, 1H), 7.21 (d, *J* = 3.6 Hz, 1H), 6.57 – 6.51 (m, 1H), 5.76 – 5.57 (m, 2H), 5.47 – 5.25 (m, 8H), 3.64 (d, *J* = 1.4 Hz, 2H), 2.94 – 2.77 (m, 8H), 2.13 – 2.01 (m, 2H), 0.97 (t, *J* = 0.9 Hz, 3H); **^{13}C NMR** (101 MHz, $CDCl_3$) δ_C 187.1, 152.6, 146.5, 132.2, 131.8, 128.79, 128.75, 128.5, 128.1, 128.0, 127.6, 127.1, 121.3, 117.3, 112.4, 37.5, 26.1, 25.81, 25.78, 25.7, 20.7, 14.4; **MS** (ESI): exact mass calculated for $C_{22}H_{28}O_2Na$ $[M+Na]^+$: 347.1982, found 347.1981.

6 Bibliography

[1] S. L. Lundström, J. Yang, J. D. Brannan, J. Z. Haeggström, B. D. Hammock, P. Nair, P. O'Byrne, S.-E. Dahlén and C. E. Wheelock, *Mol. Nutr. Food Res.*, 2013, **57**, 1378–1389.

[2] A. A. Spector and H.-Y. Kim, *Biochim. Biophys. Acta*, 2015, **1851**, 356.

[3] C. Morisseau and B. D. Hammock, *Annu. Rev. Pharmacol. Toxicol.*, 2013, **53**, 37–58.

[4] A. Vik and T. V. Hansen, *Org. Biomol. Chem.*, 2018, **16**, 9319–9333.

[5] M. G. Jakobsen, A. Vik and T. V. Hansen, *Tetrahedron Lett.*, 2012, **53**, 5837–5839.

[6] C. N. Serhan, *FASEB J.*, 2011, **25**, 1441–1448.

[7] *Fundamentals of Inflammation*, ed. C. N. Serhan, P. A. Ward and D. W. Gilroy, Cambridge University Press, Cambridge, 2010.

[8] H. Kumar, T. Kawai and S. Akira, *Int. Rev. Immunol.*, 2011, **30**, 16–34.

[9] P. Borgeat and P. H. Naccache, *Clin. Biochem.*, 1990, **23**, 459–468.

[10] B. D. Levy, C. B. Clish, B. Schmidt, K. Gronert and C. N. Serhan, *Nat. Immunol.*, 2001, **2**, 612–620.

[11] C. N. Serhan, S. D. Brain, C. D. Buckley, D. W. Gilroy, C. Haslett, L. A. J. O'Neill, M. Perretti, A. G. Rossi and J. L. Wallace, *FASEB J.*, 2007, **21**, 325–332.

[12] J. Whelan and K. Fritsche, *Adv. Nutr.*, 2013, **4**, 311–312.

[13] S. M. Alashmali, K. E. Hopperton and R. P. Bazinet, *Curr. Opin. Lipidol.*, 2016, **27**, 54–66.

[14] A. C. Araújo, C. E. Wheelock and J. Z. Haeggström, *Antioxid. Redox Signal.*, 2018, **29**, 275–296.

[15] R. K. Saini and Y.-S. Keum, *Life Sci.*, 2018, **203**, 255–267.

[16] H. Tallima and R. El Ridi, *J. Adv. Res.*, 2017, **11**, 33–41.

[17] M. Murakami and I. Kudo, *J. Biochem.*, 2002, **131**, 285–292.

[18] C. N. Serhan and N. A. Petasis, *Chem. Rev.*, 2011, **111**, 5922–5943.

[19] G. Drouin, V. Rioux and P. Legrand, *Biochimie*, 2019, **159**, 36–48.

[20] G. Lenihan-Geels, K. S. Bishop and L. R. Ferguson, *Nutrients*, 2013, **5**, 1301–1315.

[21] AM. Stinson, RD. Wiegand and RE. Anderson, *J. Lipid Res.*, 1991, **32**, 2009–2017.

[22] H. R. Herschman, *Trends Cardiovasc. Med.*, 1998, **8**, 145–150.

[23] I. Dey, M. Lejeune and K. Chadee, *Br. J. Pharmacol.*, 2006, **149**, 611–623.

[24] R. Mashima and T. Okuyama, *Redox Biol.*, 2015, **6**, 297–310.

[25] A. Di Gennaro and J. Z. Haeggström, *Advances in Immunology*, Academic Press, 2012, vol. 116, pp. 51–92.

[26] M. Le Bel, A. Brunet and J. Gosselin, *J. Innate Immun.*, 2014, **6**, 159–168.

[27] K. Okunishi and M. Peters-Golden, *Biochim. Biophys. Acta - Gen. Subj.*, 2011, **1810**, 1096–1102.

[28] A. Wachsmann-Maga, M. Kaszuba, M. Maga, A. Włodarczyk, J. Krężel, P. Kaczmarczyk, K. Bogucka and P. Maga, *Acta Angiol.*, 2022, **28**, 147–153.

[29] A. Ryan and C. Godson, *Curr. Opin. Pharmacol.*, 2010, **10**, 166–172.

[30] C. N. Serhan, M. Hamberg and B. Samuelsson, *Biochem. Biophys. Res. Commun.*, 1984, **118**, 943–949.

[31] C. N. Serhan, M. Hamberg and B. Samuelsson, *Proc. Natl. Acad. Sci. U.S.A.*, 1984, **81**, 5335–5339.

[32] C. N. Serhan, *Prostaglandins Leukot. Essent. Fatty Acids*, 2005, **73**, 141–162.

[33] O. Soyombo, B. W. Spur and T. H. Lee, *Allergy*, 1994, **49**, 230–234.

[34] C. Bandeira-Melo, P. T. Bozza, B. L. Diaz, R. S. B. Cordeiro, P. J. Jose, M. A. Martins and C. N. Serhan, *J. Immun.*, 2000, **164**, 2267–2271.

[35] C. N. Serhan, J. F. Maddox, N. A. Petasis, I. Akritopoulou-Zanze, A. Papayianni, H. R. Brady, S. P. Colgan and J. L. Madara, *Biochemistry*, 1995, **34**, 14609–14615.

[36] A. T. Gewirtz, B. McCormick, A. S. Neish, N. A. Petasis, K. Gronert, C. N. Serhan and J. L. Madara, *J. Clin. Invest.*, 1998, **101**, 1860–1869.

[37] Z.-Z. Xu, L. Zhang, T. Liu, J. Y. Park, T. Berta, R. Yang, C. N. Serhan and R.-R. Ji, *Nat. Med.*, 2010, **16**, 592–599.

[38] J. F. Maddox and C. N. Serhan, *J. Exp. Med.*, 1996, **183**, 137–146.

[39] C. Godson, S. Mitchell, K. Harvey, N. A. Petasis, N. Hogg and H. R. Brady, *J. Immunol.*, 2000, **164**, 1663–1667.

[40] J. M. Schwab, N. Chiang, M. Arita and C. N. Serhan, *Nature*, 2007, **447**, 869.

[41] A. A. Spector, *J. Lipid. Res.*, 2009, **50**, S52–S56.

[42] J. M. Williams, S. Murphy, M. Burke and R. J. Roman, *J. Cardiovasc. Pharmacol.*, 2010, **56**, 336–344.

[43] A. Luria, S. M. Weldon, A. K. Kabcenell, R. H. Ingraham, D. Matera, H. Jiang, R. Gill, C. Morisseau, J. W. Newman and B. D. Hammock, *J. Biol. Chem.*, 2007, **282**, 2891–2898.

[44] I. Fleming, A. Rueben, R. Popp, B. Fisslthaler, S. Schrodt, A. Sander, J. Haendeler, J. R. Falck, C. Morisseau, B. D. Hammock and R. Busse, *Arterioscler. Thromb. Vasc. Biol.*, 2007, **27**, 2612–2618.

[45] J. D. Imig, *Physiol. Rev.*, 2012, **92**, 101–130.

[46] K. Node, Y. Huo, X. Ruan, B. Yang, M. Spiecker, K. Ley, D. C. Zeldin and J. K. Liao, *Science*, 1999, **285**, 1276–1276.

[47] F. A. Fitzpatrick, M. D. Ennis, M. E. Baze, M. A. Wynalda, J. E. McGee and W. F. Liggett, *J. Biol. Chem.*, 1986, **261**, 15334–15338.

[48] B. T. Larsen, W. B. Campbell and D. D. Gutterman, *Trends Pharmacol. Sci.*, 2007, **28**, 32–38.

[49] B. Lauterbach, E. Barbosa-Sicard, M.-H. Wang, H. Honeck, E. Kärgel, J. Theuer, M. L. Schwartzman, H. Haller, F. C. Luft, M. Gollasch and W.-H. Schunck, *Hypertension*, 2002, **39**, 609–613.

[50] D. Ye, D. Zhang, C. Oltman, K. Dellsperger, H.-C. Lee and M. VanRollins, *J. Pharmacol. Exp. Ther.*, 2002, **303**, 768–776.

[51] M. VanRollins, *J. Pharmacol. Exp. Ther.*, 1995, **274**, 798–804.

[52] P. McLennan, P. Howe, M. Abeywardena, R. Muggli, D. Raederstorff, M. Mano, T. Rayner and R. Head, *Eur. J. Pharmacol.*, 1996, **300**, 83–89.

[53] A. Ulu, K. S. Stephen Lee, C. Miyabe, J. Yang, B. G. Hammock, H. Dong and B. D. Hammock, *J. Cardiovasc. Pharmacol.*, 2014, **64**, 87–99.

[54] C. Morisseau, B. Inceoglu, K. Schmelzer, H.-J. Tsai, S. L. Jinks, C. M. Hegedus and B. D. Hammock, *J. Lipid Res.*, 2010, **51**, 3481–3490.

[55] N. Chacos, J. Capdevila, J. R. Falck, S. Manna, C. Martin-Wixtrom, S. S. Gill, B. D. Hammock and R. W. Estabrook, *Arch. Biochem. Biophys.*, 1983, **223**, 639–648.

[56] G. M. Pacifici, A. Temellini, L. Giuliani, A. Rane, H. Thomas and F. Oesch, *Arch. Toxicol.*, 1988, **62**, 254–257.

[57] A. E. Enayetallah, R. A. French, M. S. Thibodeau and D. F. Grant, *J. Histochem. Cytochem.*, 2004, **52**, 447–454.

[58] J. W. Newman, C. Morisseau and B. D. Hammock, *Prog. Lipid Res.*, 2005, **44**, 1–51.

[59] C. B. McReynolds, I. Cortes-Puch, R. Ravindran, I. H. Khan, B. G. Hammock, P.-a. B. Shih, B. D. Hammock and J. Yang, *Front. Physiol.*, 2021, **12**, 663869.

[60] T. Frömel, Z. Naeem, L. Pirzeh and I. Fleming, *Pharmacol. Ther.*, 2022, **234**, 108049.

[61] D. A. Thompson and B. D. Hammock, *J. Biosci.*, 2007, **32**, 279–291.

[62] M. Fornage, E. Boerwinkle, P. A. Doris, D. Jacobs, K. Liu and N. D. Wong, *Circulation*, 2004, **109**, 335–339.

[63] C. L. Oltman, N. L. Weintraub, M. VanRollins and K. C. Dellsperger, *Circ. Res.*, 1998, **83**, 932–939.

[64] L. R. B. dos Santos and I. Fleming, *Prostaglandins Other Lipid Mediat.*, 2020, **148**, 106407.

[65] J. Hu, S.-I. Bibli, J. Wittig, S. Zukunft, J. Lin, H.-P. Hammes, R. Popp and I. Fleming, *J. Clin. Invest.*, 2019, **129**, 5204–5218.

[66] J. Hu, S. Dziumbla, J. Lin, S.-I. Bibli, S. Zukunft, J. de Mos, K. Awwad, T. Frömel, A. Jungmann, K. Devraj, Z. Cheng, L. Wang, S. Fauser, C. G. Eberhart, A. Sodhi, B. D. Hammock, S. Liebner, O. J. Müller, C. Glaubitz, H.-P. Hammes, R. Popp and I. Fleming, *Nature*, 2017, **552**, 248–252.

[67] J. W. Fetterman, Jr. and M. M. Zdanowicz, *Am. J. Health Syst. Pharm.*, 2009, **66**, 1169–1179.

[68] P. C. Calder, *Am. J. Clin. Nutr.*, 2006, **83**, 1505S–1519S.

[69] S. Endres, R. Ghorbani, V. E. Kelley, K. Georgilis, G. Lonnemann, J. W. M. van der Meer, J. G. Cannon, T. S. Rogers, M. S. Klempner, P. C. Weber, E. J. Schaefer, S. M. Wolff and C. A. Dinarello, *N. Engl. J. Med.*, 1989, **320**, 265–271.

[70] E. M. Balk, A. H. Lichtenstein, M. Chung, B. Kupelnick, P. Chew and J. Lau, *Atherosclerosis*, 2006, **189**, 19–30.

[71] I. Lauritzen, N. Blondeau, C. Heurteaux, C. Widmann, G. Romey and M. Lazdunski, *EMBO J.*, 2000, **19**, 1784–1793.

[72] M. Hashimoto and S. Hossain, *J. Pharmacol. Sci.*, 2011, **116**, 150–162.

[73] M. J. James and L. G. Cleland, *Semin. Arthritis. Rheum.*, 1997, **27**, 85–97.

[74] J. D. Imig and B. D. Hammock, *Nat. Rev. Drug Discov.*, 2009, **8**, 794–805.

[75] Y. Suresh and U. N. Das, *Nutrition*, 2003, **19**, 213–228.

[76] J. A. Nettleton and R. Katz, *J. Am. Diet. Assoc.*, 2005, **105**, 428–440.

[77] S. C. Larsson, M. Kumlin, M. Ingelman-Sundberg and A. Wolk, *Am. J. Clin. Nutr.*, 2004, **79**, 935–945.

[78] Pronova, *Summary of Product Characteristics for Omacor®*, https://www.accessdata.fda.gov/drugsatfda_docs/label/2004/21654lbl.pdf, 2020.

[79] HMPC, *Assessment Report on Vazkepa®*, https://www.ema.europa.eu/en/documents/assessment-report/vazkepa-epar-public-assessment-report_en.pdf, 2021.

[80] EMA, *EMA Confirms Omega-3 Fatty Acid Medicines Are Not Effective in Preventing Further Heart Problems after a Heart Attack*, https://www.ema.europa.eu/en/documents/press-release/ema-confirms-omega-3-fatty-acid-medicines-are-not-effective-preventing-further-heart-problems-after_en.pdf, 2019.

[81] FDA. CDER, *Approved Drug Products with Therapeutic Equivalence Evaluations*, Food and Drug Administration, Forty-third edn, 2023.

[82] M. Aursnes, J. E. Tungen, A. Vik, J. Dalli and T. V. Hansen, *Org. Biomol. Chem.*, 2014, **12**, 432–437.

[83] J. E. Tungen, M. Aursnes and T. V. Hansen, *Tetrahedron Lett.*, 2015, **56**, 1843–1846.

[84] J. I. Nesman, J. E. Tungen, A. Vik and T. V. Hansen, *Tetrahedron*, 2020, **76**, 130821.

[85] A. F. Reinertsen, K. G. Primdahl, A. E. Shay, C. N. Serhan, T. V. Hansen and M. Aursnes, *J. Org. Chem.*, 2021, **86**, 3535–3545.

[86] J. E. Tungen, L. Gerstmann, A. Vik, R. De Matteis, R. A. Colas, J. Dalli, N. Chiang, C. N. Serhan, M. Kalesse and T. V. Hansen, *Chem. Eur. J.*, 2019, **25**, 1476–1480.

[87] A. F. Reinertsen, K. G. Primdahl, R. De Matteis, J. Dalli and T. V. Hansen, *Chem. Eur. J.*, 2022, **28**, e202103857.

[88] M. Aursnes, J. E. Tungen, A. Vik, R. Colas, C.-Y. C. Cheng, J. Dalli, C. N. Serhan and T. V. Hansen, *J. Nat. Prod.*, 2014, **77**, 910–916.

[89] J. Sønderskov, J. E. Tungen, F. Palmas, J. Dalli, C. N. Serhan, Y. Stenstrøm and T. Vidar Hansen, *Tetrahedron Lett.*, 2020, **61**, 151510.

[90] K. G. Primdahl, J. E. Tungen, P. R. S. De Souza, R. A. Colas, J. Dalli, T. V. Hansen and A. Vik, *Org. Biomol. Chem.*, 2017, **15**, 8606–8613.

[91] K. G. Primdahl, J. E. Tungen, M. Aursnes, T. V. Hansen and A. Vik, *Org. Biomol. Chem.*, 2015, **13**, 5412–5417.

[92] K. G. Primdahl, Y. Stenstrøm, T. V. Hansen and A. Vik, *Chem. Phys. Lipids*, 2016, **196**, 1–4.

[93] K. G. Primdahl, M. Aursnes, M. E. Walker, R. A. Colas, C. N. Serhan, J. Dalli, T. V. Hansen and A. Vik, *J. Nat. Prod.*, 2016, **79**, 2693–2702.

[94] A. Vik, T. V. Hansen, A. K. Holmeide and L. Skattebøl, *Tetrahedron Lett.*, 2010, **51**, 2852–2854.

[95] E. J. Corey, H. Niwa and J. R. Falck, *J. Am. Chem. Soc.*, 1979, **101**, 1586–1587.

[96] J. M. J. Nolsøe and T. V. Hansen, *Eur. J. Org. Chem.*, 2014, **2014**, 3051–3065.

[97] J. E. Baldwin, *J. Chem. Soc., Chem. Commun.*, 1976, 734–736.

[98] A. M. Langseter, L. Skattebøl and Y. Stenstrøm, *Tetrahedron Lett.*, 2012, **53**, 940–941.

[99] J. K. Stille, *Angew. Chem., Int. Ed. Engl.*, 1986, **25**, 508–524.

[100] D. Milstein and J. K. Stille, *J. Am. Chem. Soc.*, 1978, **100**, 3636–3638.

[101] L. Del Valle, J. K. Stille and L. S. Hegedus, *J. Org. Chem.*, 1990, **55**, 3019–3023.

[102] P. Espinet and A. M. Echavarren, *Angew. Chem., Int. Ed.*, 2004, **43**, 4704–4734.

[103] H. J. Reich, *Chem. Rev.*, 2013, **113**, 7130–7178.

[104] V. H. Gessner, C. Däschlein and C. Strohmann, *Chem. Eur. J.*, 2009, **15**, 3320–3334.

[105] J. Clayden and S. A. Yasin, *New J. Chem.*, 2002, **26**, 191–192.

[106] G. G. Haraldsson, A. Halldorsson and E. Kuls, *J. Am. Oil Chem. Soc.*, 2000, **77**, 1139–1145.

[107] S. Gupta, P. Sureshbabu, A. K. Singh, S. Sabiah and J. Kandasamy, *Tetrahedron Lett.*, 2017, **58**, 909–913.

[108] A. K. Holmeide and L. Skattebøl, *J. Chem. Soc., Perkin Trans. 1*, 2000, 2271–2276.

[109] E. Corey, S. S. Kantner and P. T. Lansbury, *Tetrahedron Lett.*, 1983, **24**, 265–268.

[110] P. Strazzolini, A. G. Giumanini and S. Cauci, *Tetrahedron*, 1990, **46**, 1081–1118.

[111] S. Flock, M. Lundquist and L. Skattebøl, *Acta Chem. Scand.*, 1999, **53**, 436–445.

[112] G. Gjessing, L.-I. G. Johnsen, S. G. Antonsen, J. M. J. Nolsøe, Y. Stenstrøm and T. V. Hansen, *Molecules*, 2022, **27**, 2295.

[113] N. Aizdaicher, A. Imbs, N. Latyshev, D. Kuklev and V. Bezuglov, *Phytochemistry*, 1992, **31**, 2401–2403.

[114] H. Hori, S. Arai and A. Nishida, *Org. Biomol. Chem.*, 2019, **17**, 4783–4788.

[115] M. Tang, Y. Kong, B. Chu and D. Feng, *Adv. Synth. Catal.*, 2016, **358**, 926–939.

[116] Z.-c. Yang and W.-s. Zhou, *Tetrahedron*, 1995, **51**, 1429–1436.

[117] E. Pretsch, P. Bühlmann and M. Badertscher, *Structure Determination of Organic Compounds: Tables of Spectral Data*, Springer Berlin Heidelberg, Berlin, Heidelberg, 2009, p. 415.

[118] R. E. Ireland and L. Liu, *J. Org. Chem.*, 1993, **58**, 2899–2899.

[119] S. D. Meyer and S. L. Schreiber, *J. Org. Chem.*, 1994, **59**, 7549–7552.

[120] D. B. Dess and J. C. Martin, *J. Am. Chem. Soc.*, 1991, **113**, 7277–7287.

[121] E. J. Corey, R. K. Bakshi and S. Shibata, *J. Am. Chem. Soc.*, 1987, **109**, 5551–5553.

[122] Y. Ma and G. A. O'Doherty, *Org. Lett.*, 2015, **17**, 5280–5283.

[123] O. Achmatowicz Jr., P. Bukowski, B. Szechner, Z. Zwierzchowska and A. Zamojski, *Tetrahedron*, 1971, **27**, 1973–1996.

[124] K. L. Jackson, J. A. Henderson, J. C. Morris, H. Motoyoshi and A. J. Phillips, *Tetrahedron Lett.*, 2008, **49**, 2939–2941.

[125] R. Tyagi, B. Shimpukade, S. Blättermann, E. Kostenis and T. Ulven, *Med. Chem. Commun.*, 2012, **3**, 195–198.

[126] B. O. Lindgren and T. Nilsson, *Acta Chem. Scand.*, 1973, **27**, 888–890.

[127] T. Sæther, S. M. Paulsen, J. E. Tungen, A. Vik, M. Aursnes, T. Holen, T. V. Hansen and H. I. Nebb, *Eur. J. Med. Chem.*, 2018, **155**, 736–753.

[128] K. Omura and D. Swern, *Tetrahedron*, 1978, **34**, 1651–1660.

[129] J. M. Aurrecoechea, B. López, A. Fernández, A. Arrieta and F. P. Cossío, *J. Org. Chem.*, 1997, **62**, 1125–1135.

[130] D. B. Dess and J. C. Martin, *J. Org. Chem.*, 1983, **48**, 4155–4156.

7 Spectral data

7.1 DHA (9)

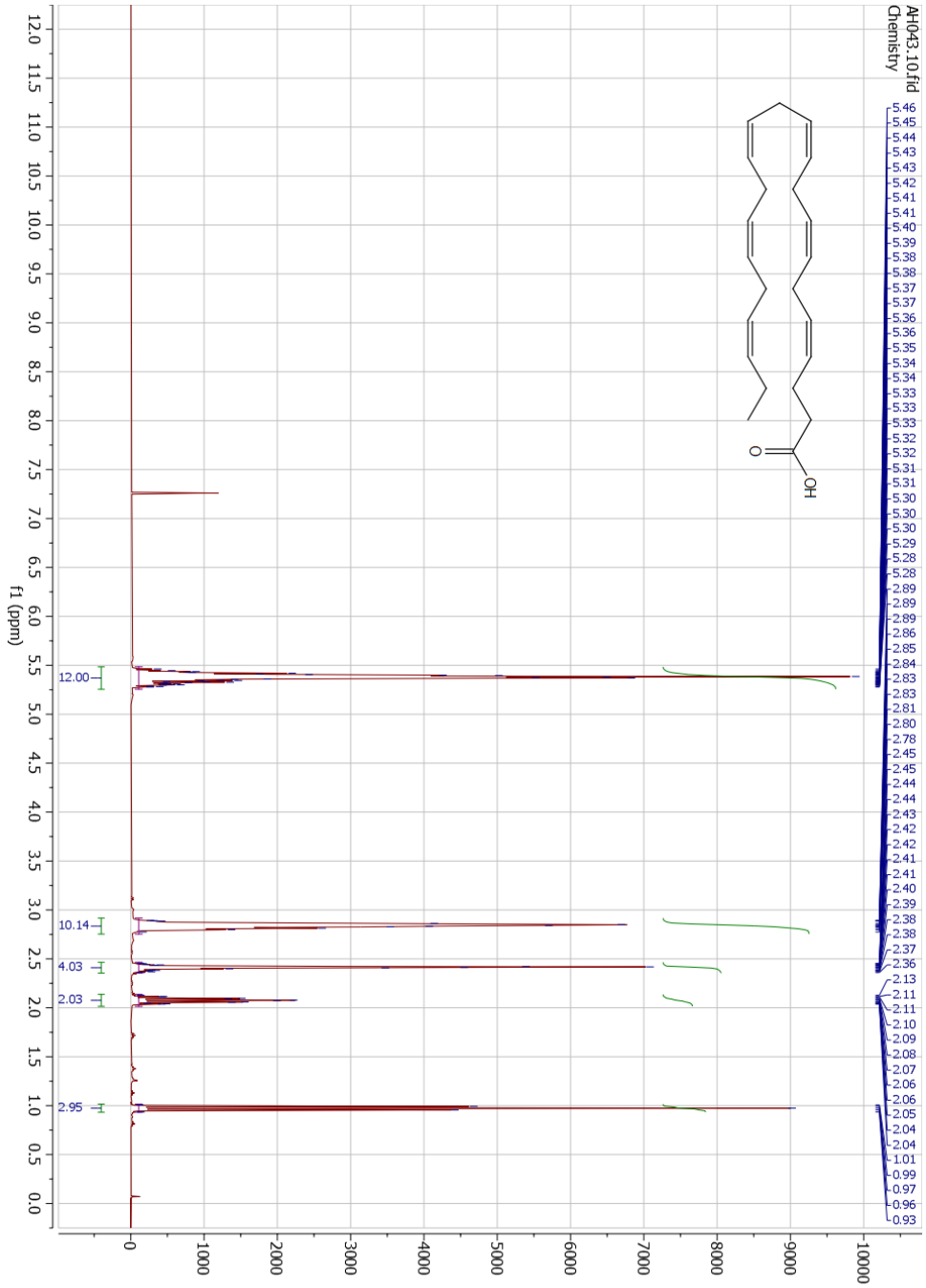

Fig. 7.1 ^{1}H NMR spectrum of DHA (**9**).

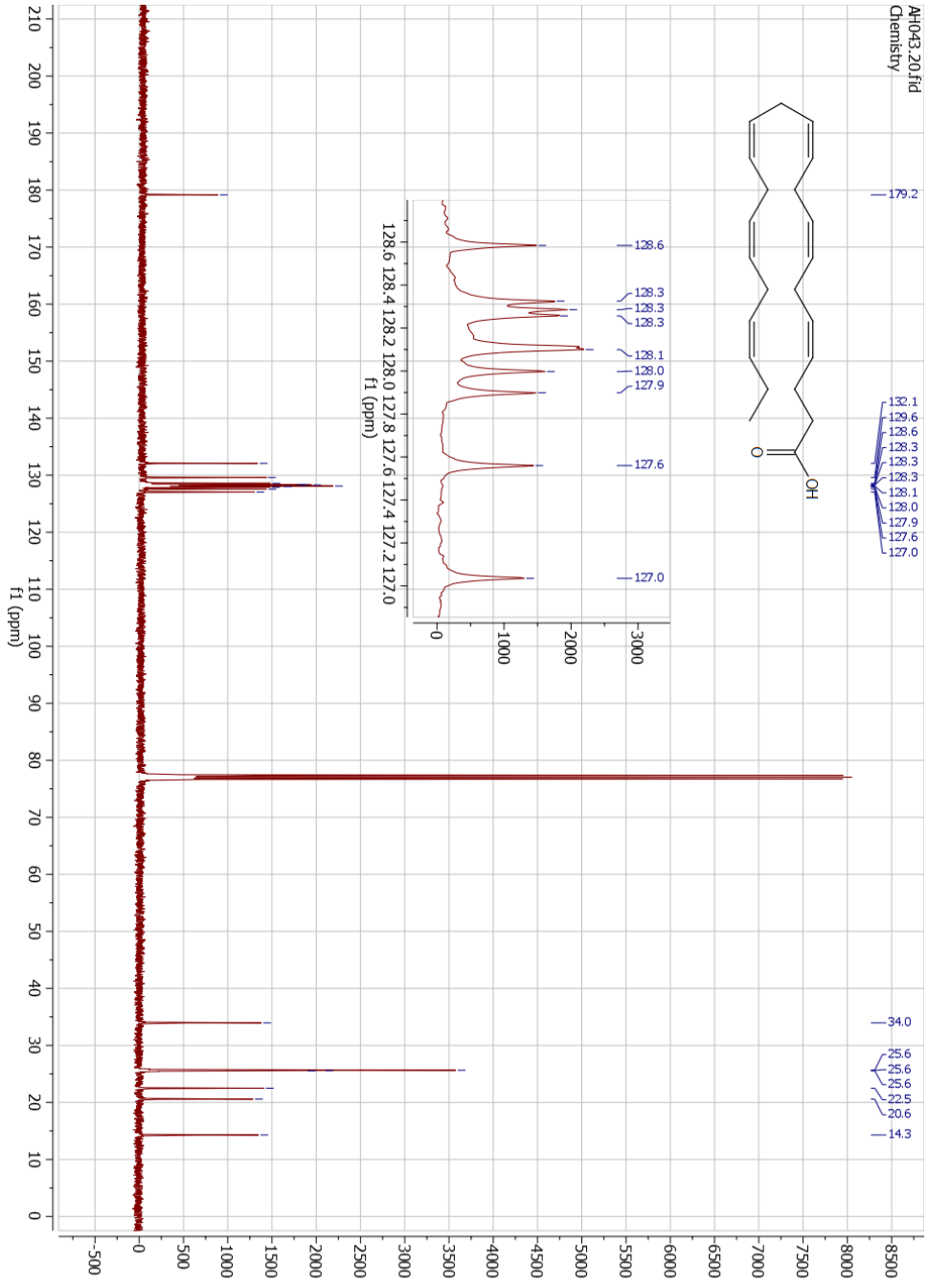

Fig. 7.2 ^{13}C NMR spectrum of DHA (**9**).

7.2 Iodolactone 29

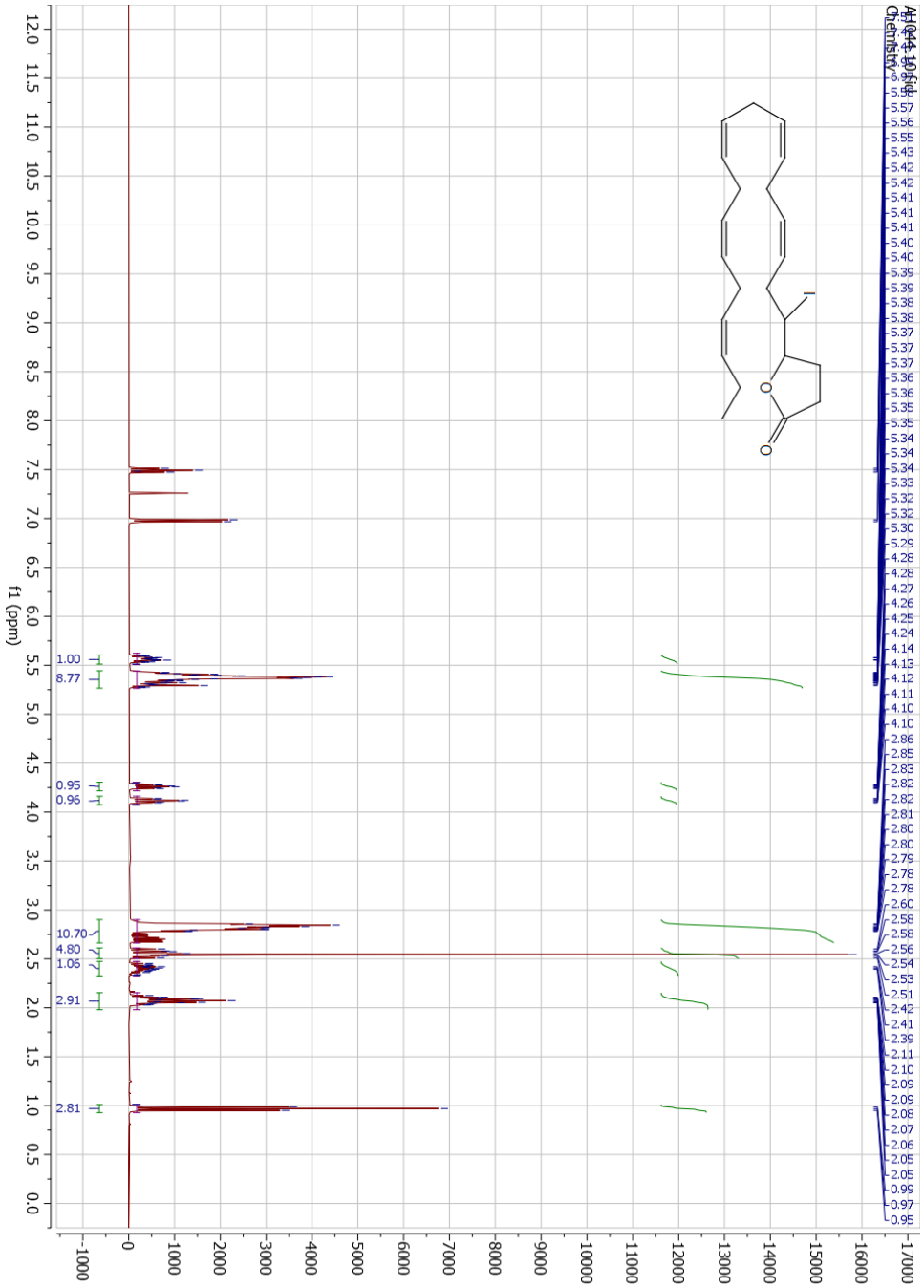

Fig. 7.3 ^{1}H NMR spectrum of crude mixture containing iodolactone **29**. Extra shifts correspond to 2,6-lutidine.[107]

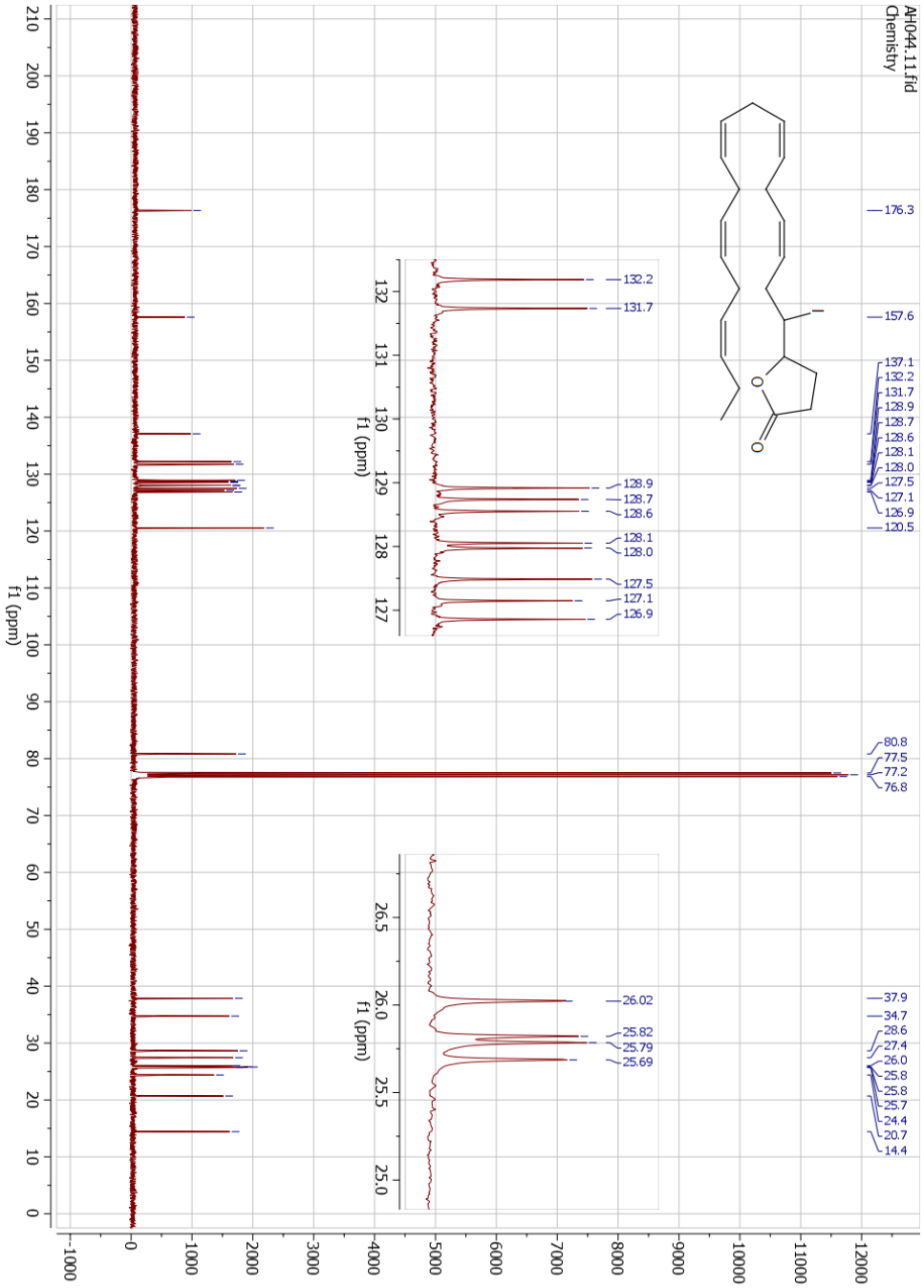

Fig. 7.4 ^{13}C NMR spectrum of crude mixture containing iodolactone **29**. Extra shifts correspond to 2,6-lutidine.[107]

7.3 Epoxide 5

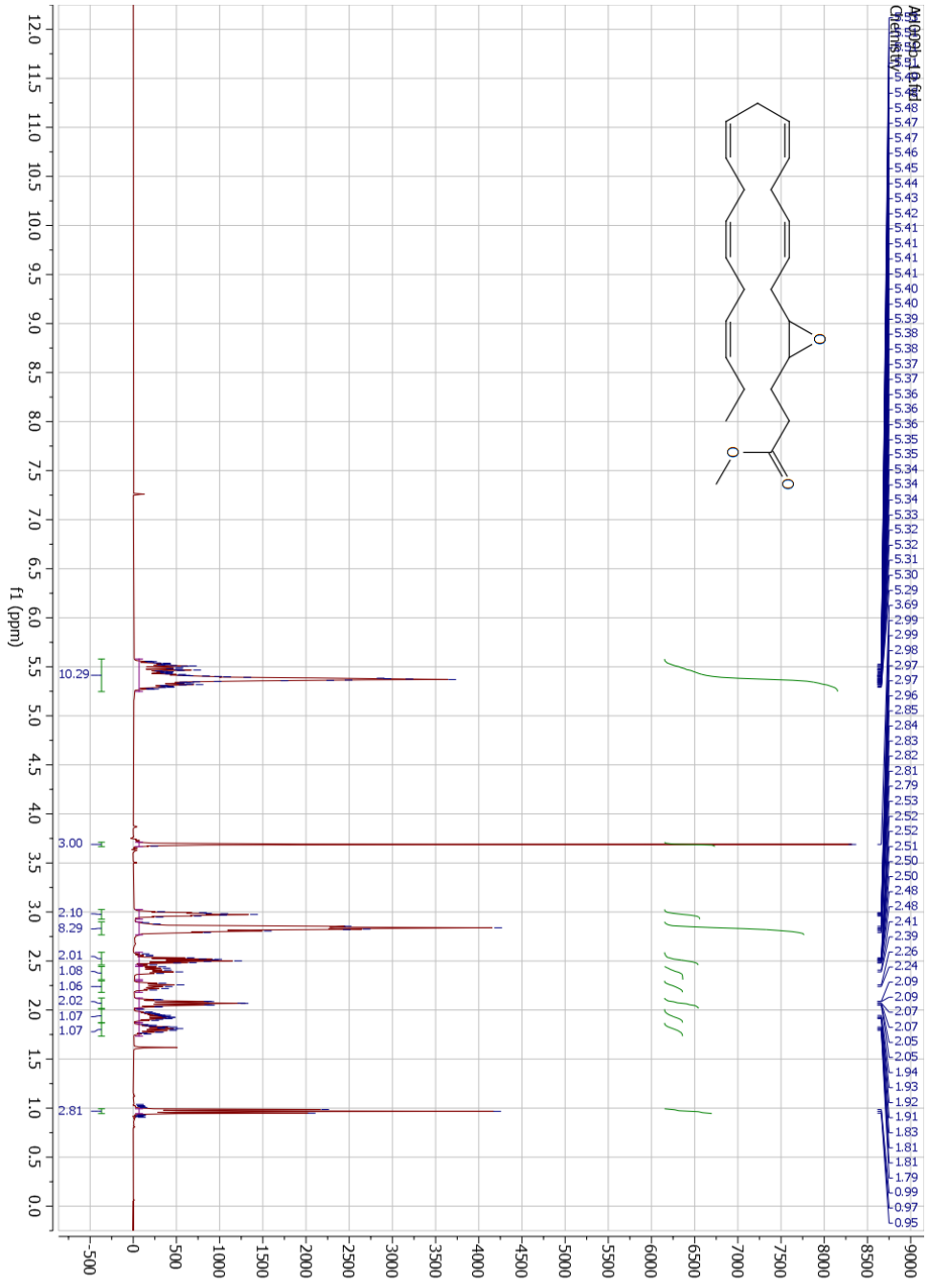

Fig. 7.5 ^{1}H NMR spectrum of epoxide **5**.

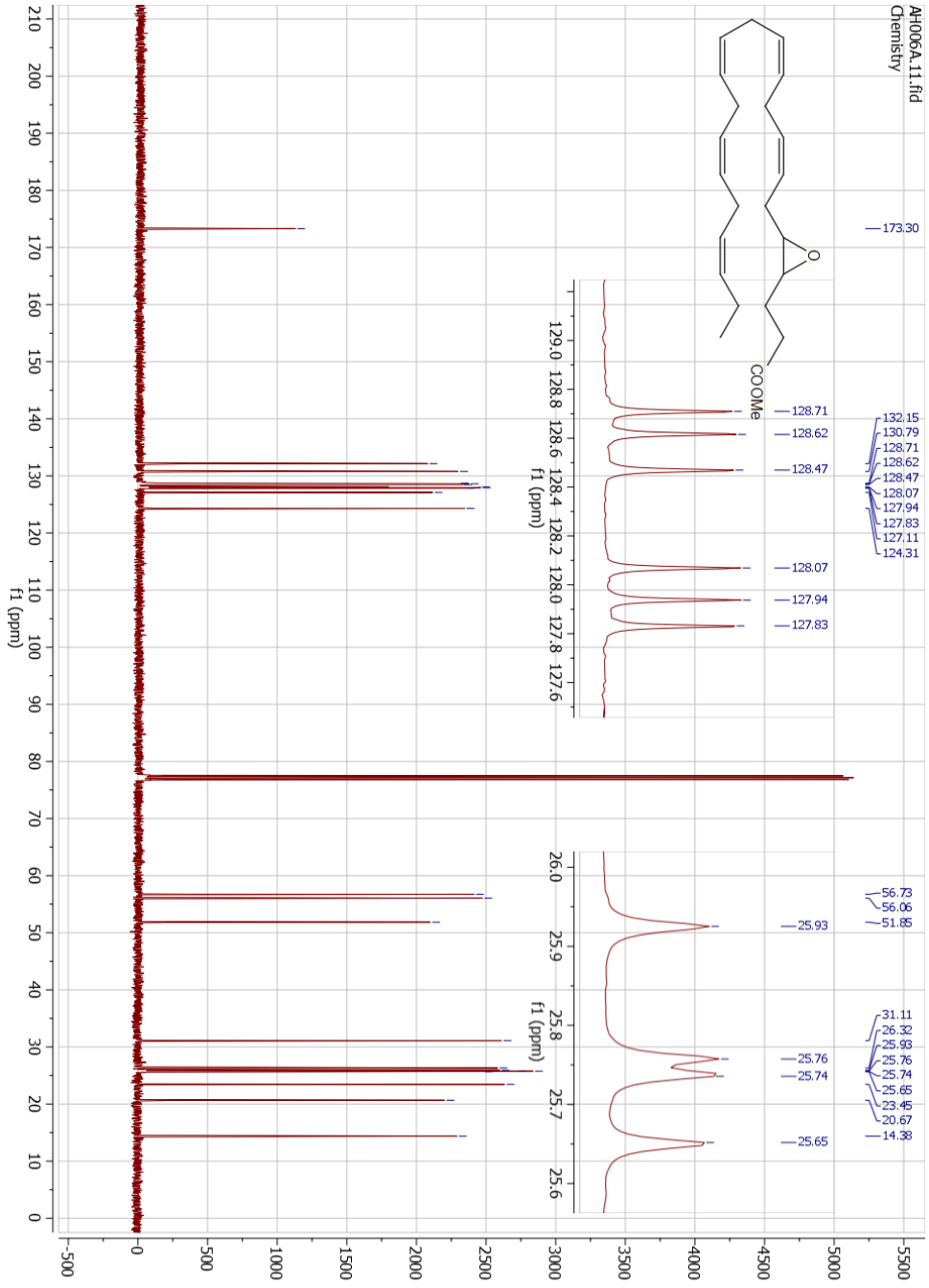

Fig. 7.6 ^{13}C NMR spectrum of epoxide **5**.

7.4 Aldehyde 4

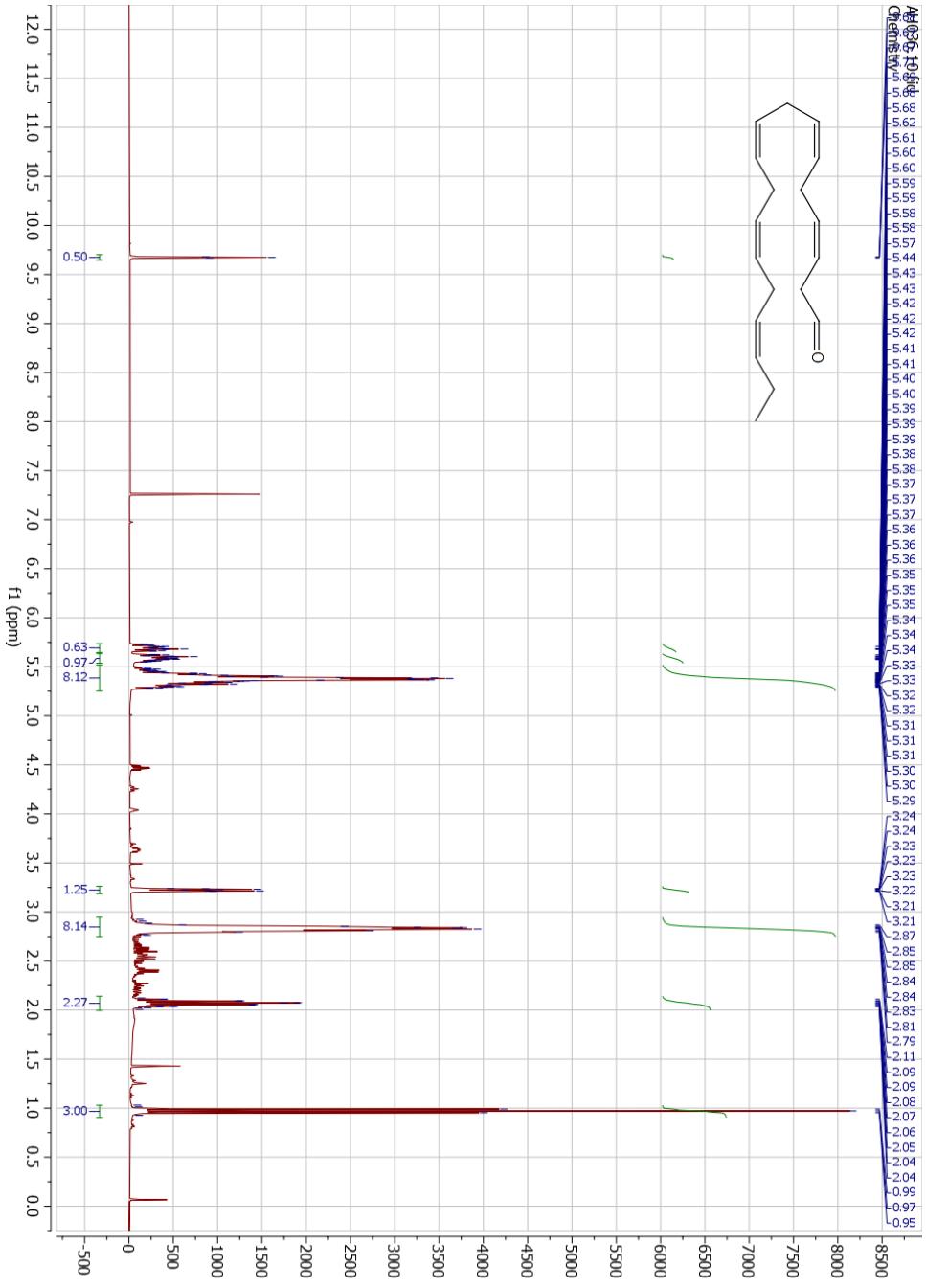

Fig. 7.7 ^{1}H NMR spectrum of crude mixture containing aldehyde **4**.

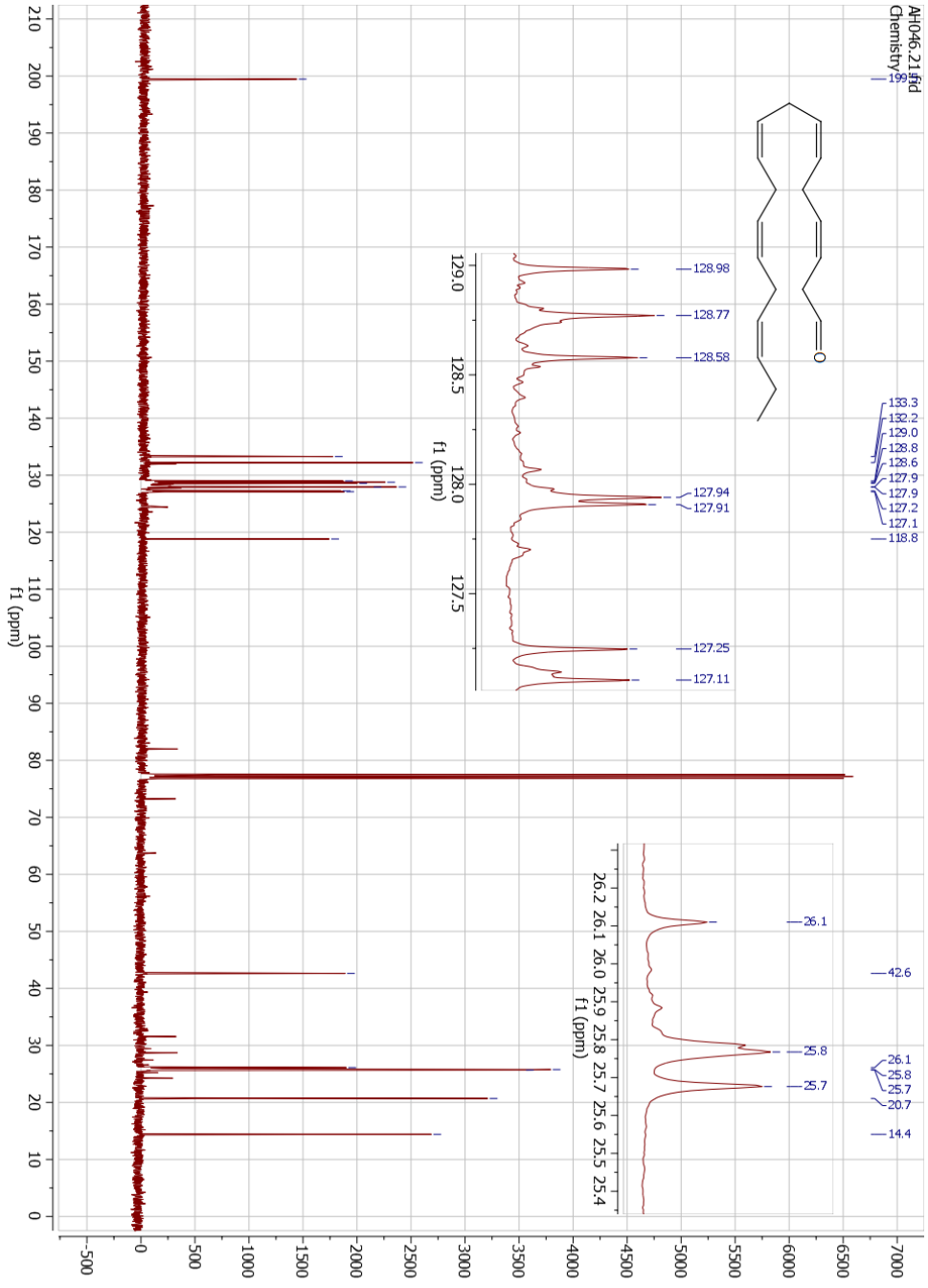

Fig. 7.8 ^{13}C NMR spectrum of crude mixture containing aldehyde **4**.

7.5 Acid 34

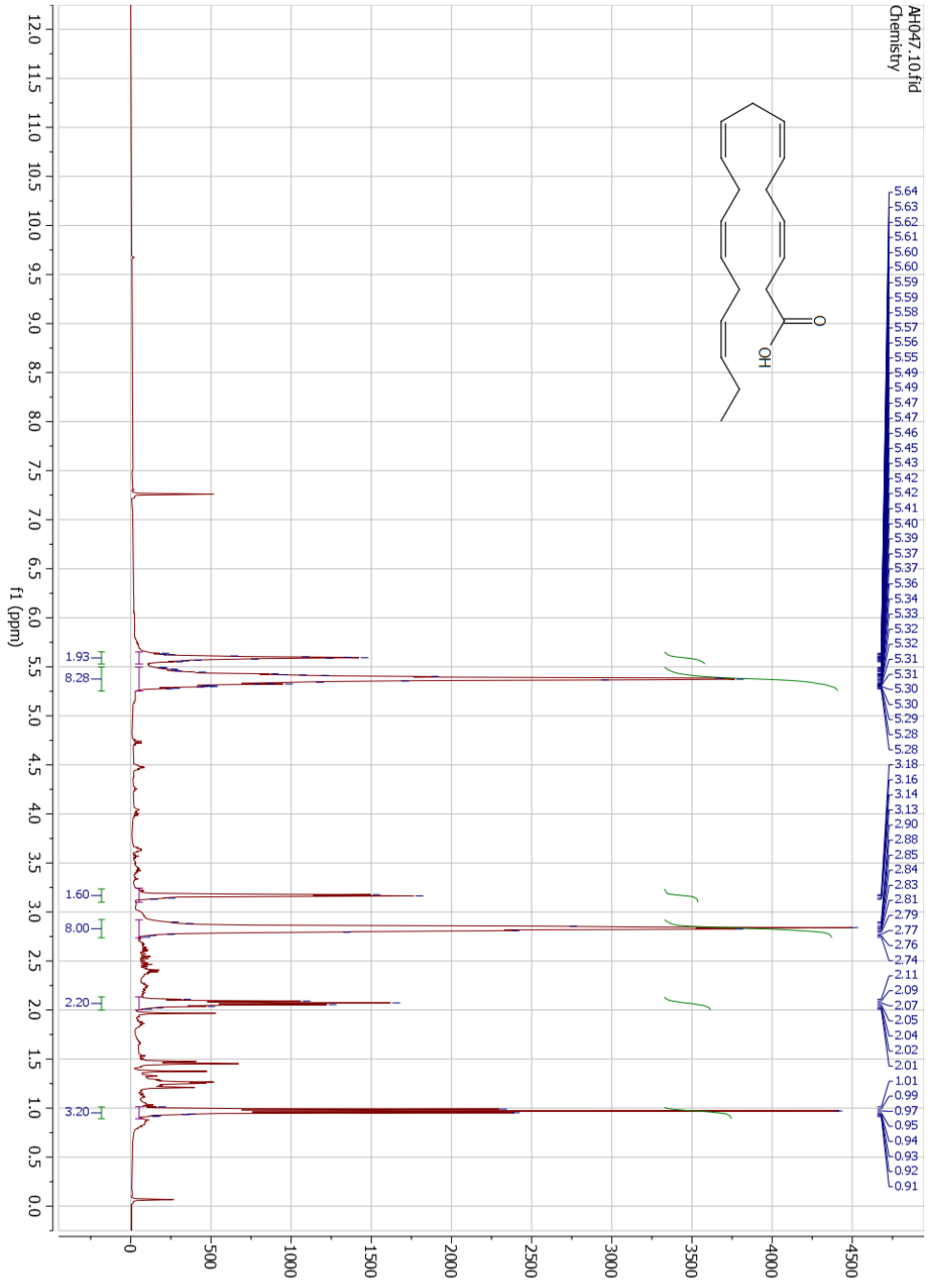

Fig. 7.9 ^{1}H NMR spectrum of crude mixture containing acid **34**.

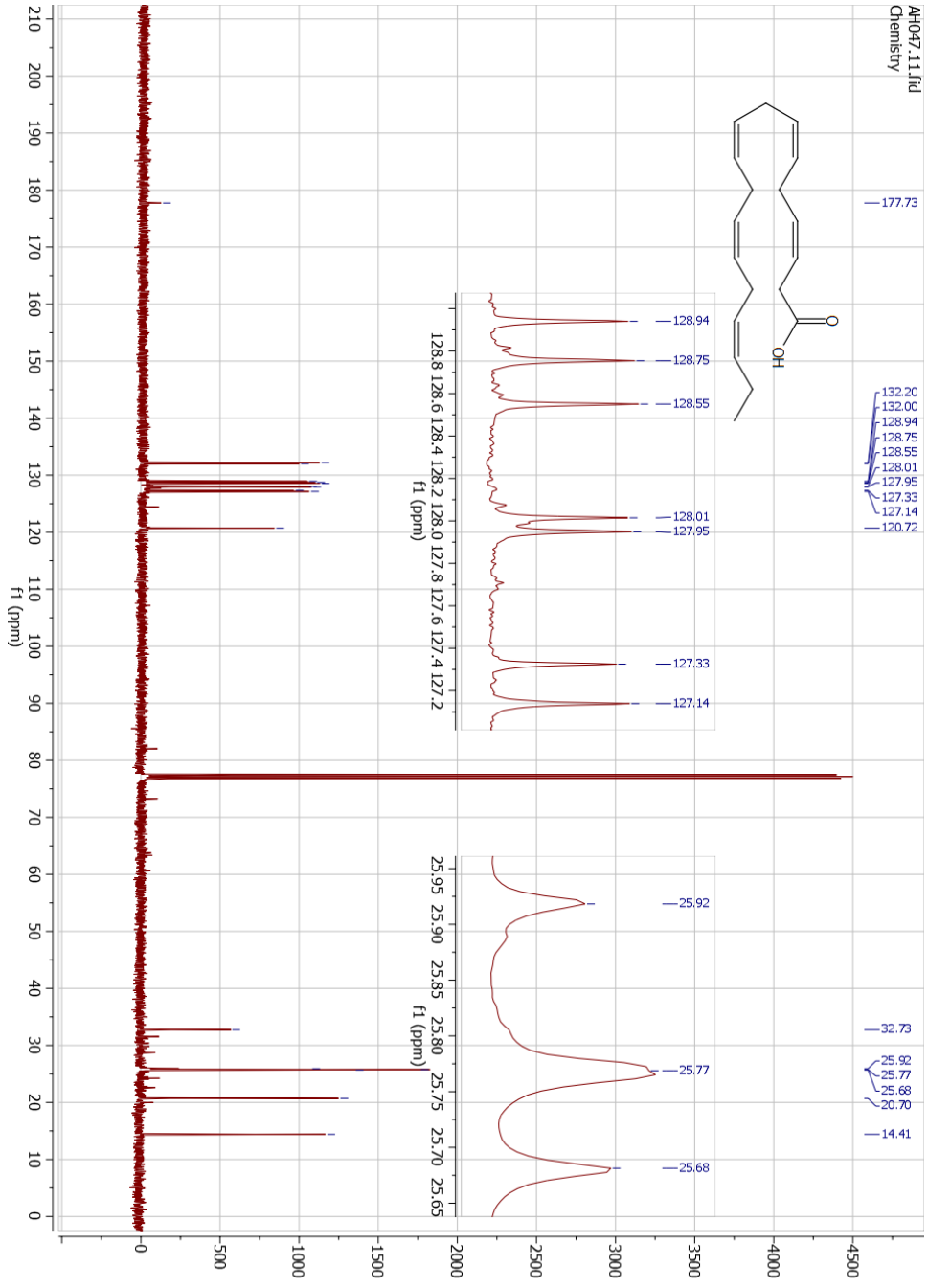

Fig. 7.10 ^{13}C NMR spectrum of crude mixture containing acid **34**.

7.6 Alcohol 36

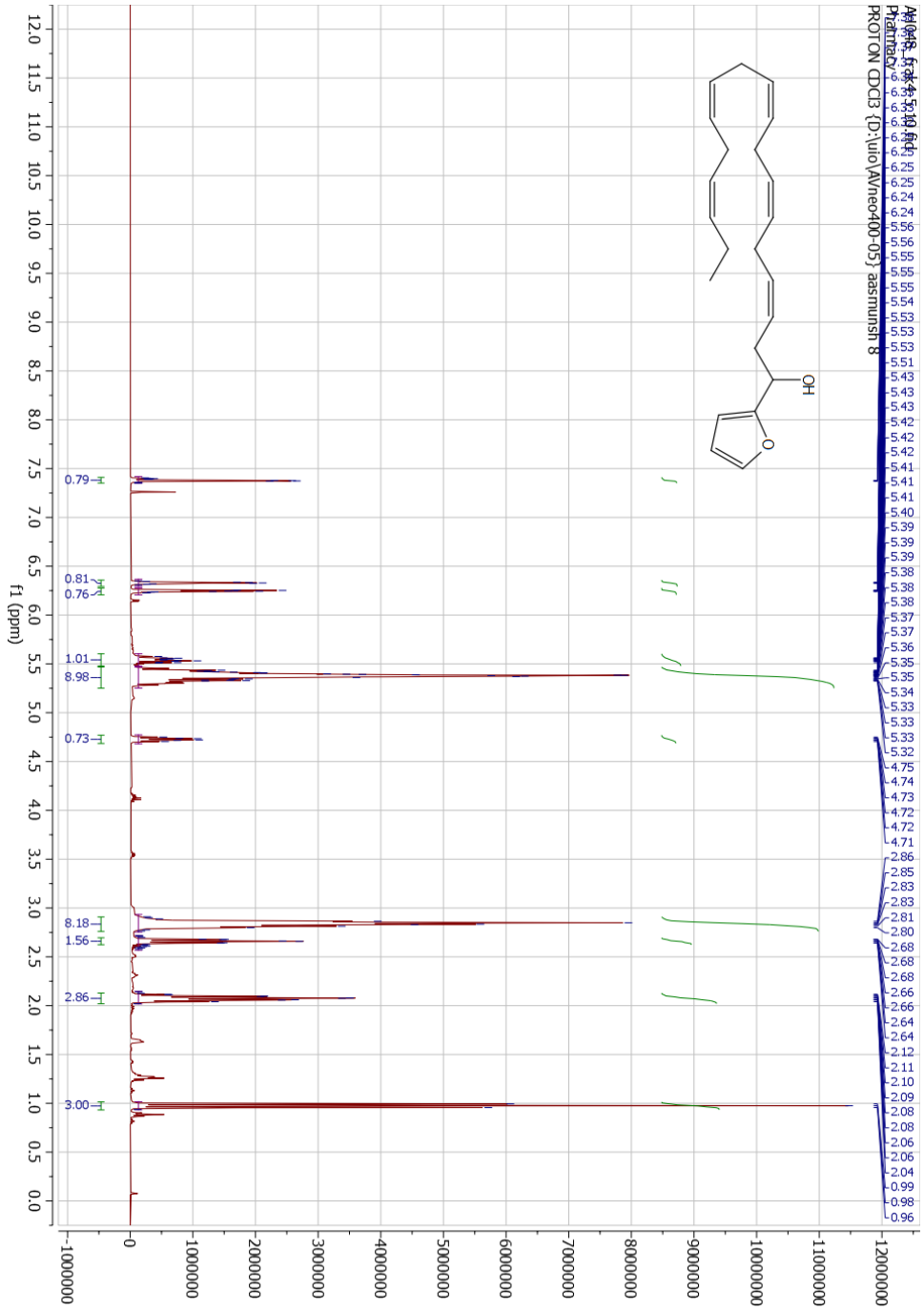

Fig. 7.11 ^{1}H NMR spectrum of alcohol **36**.

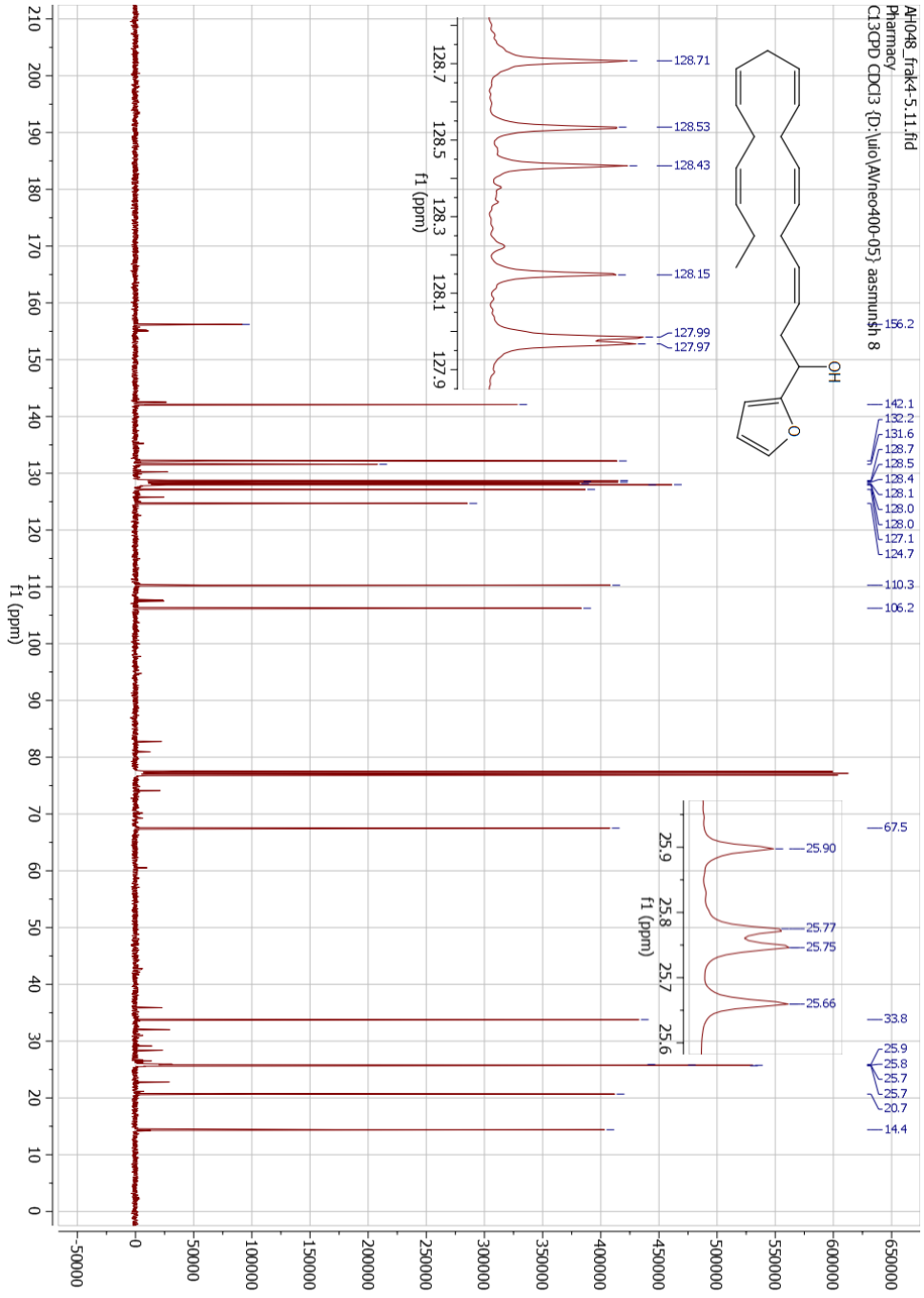

Fig. 7.12 ^{13}C NMR spectrum of alcohol **36**.

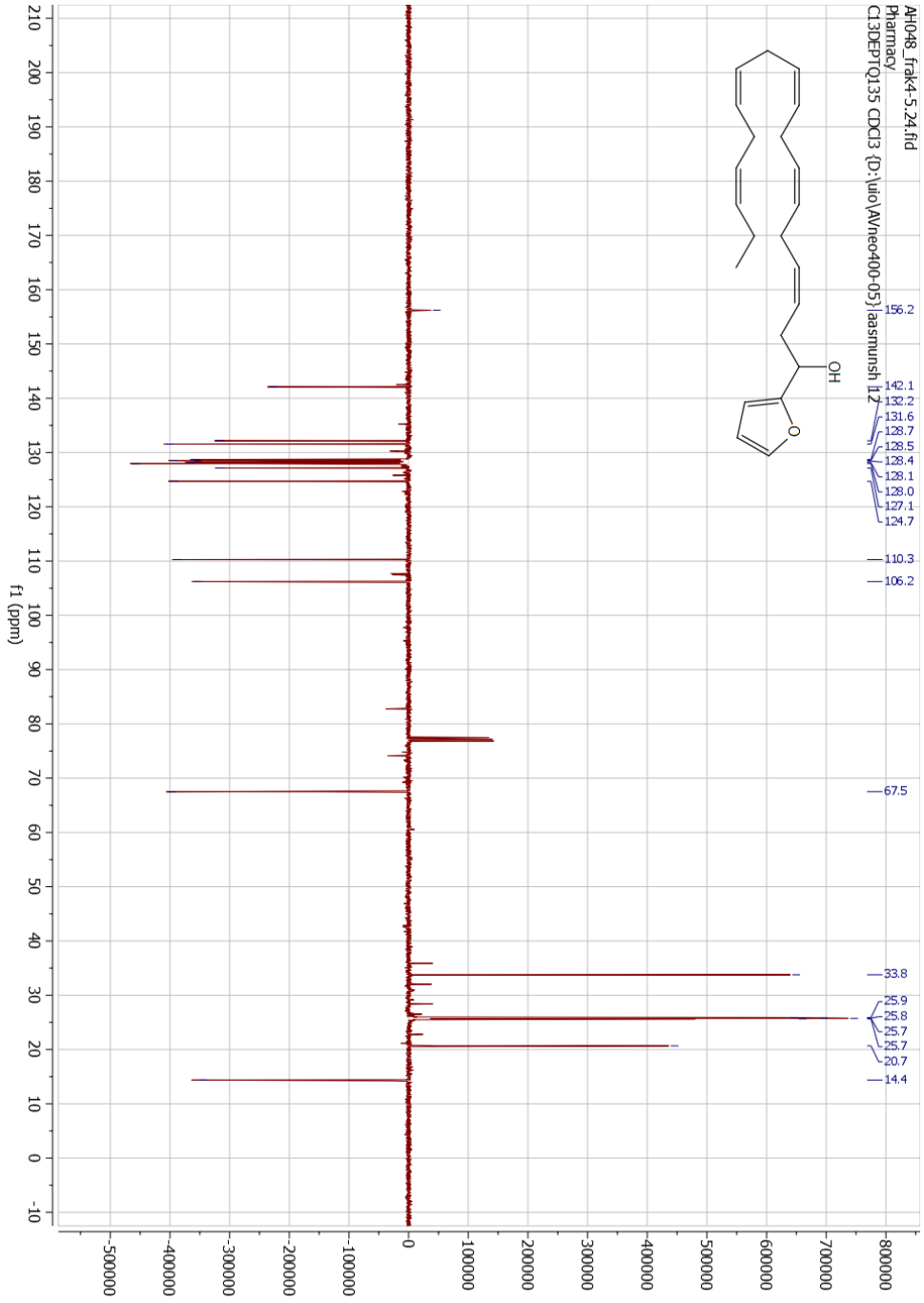

Fig. 7.13 DEPT-135 spectrum of alcohol **36**.

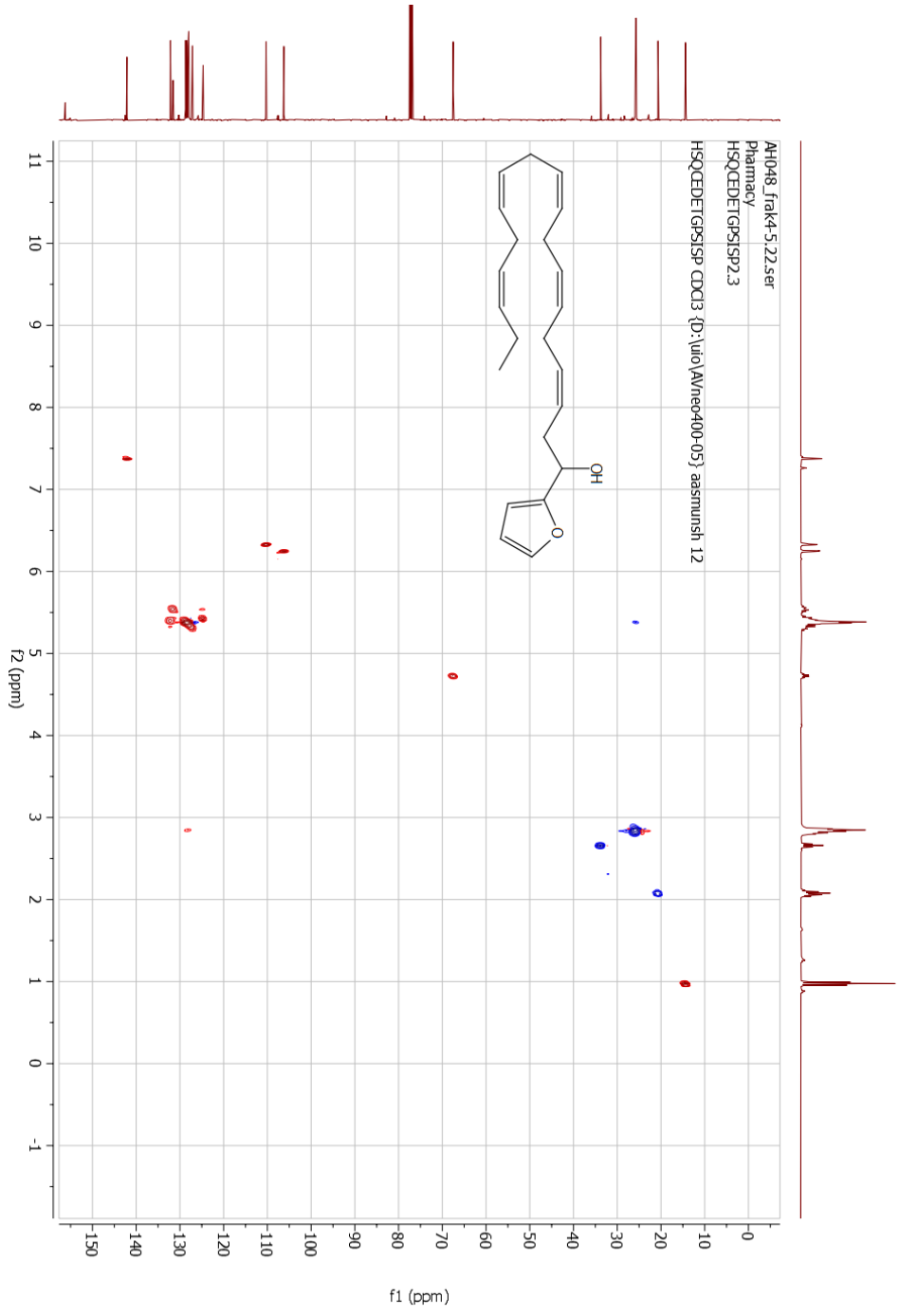

Fig. 7.14 HSQC spectrum of alcohol **36**.

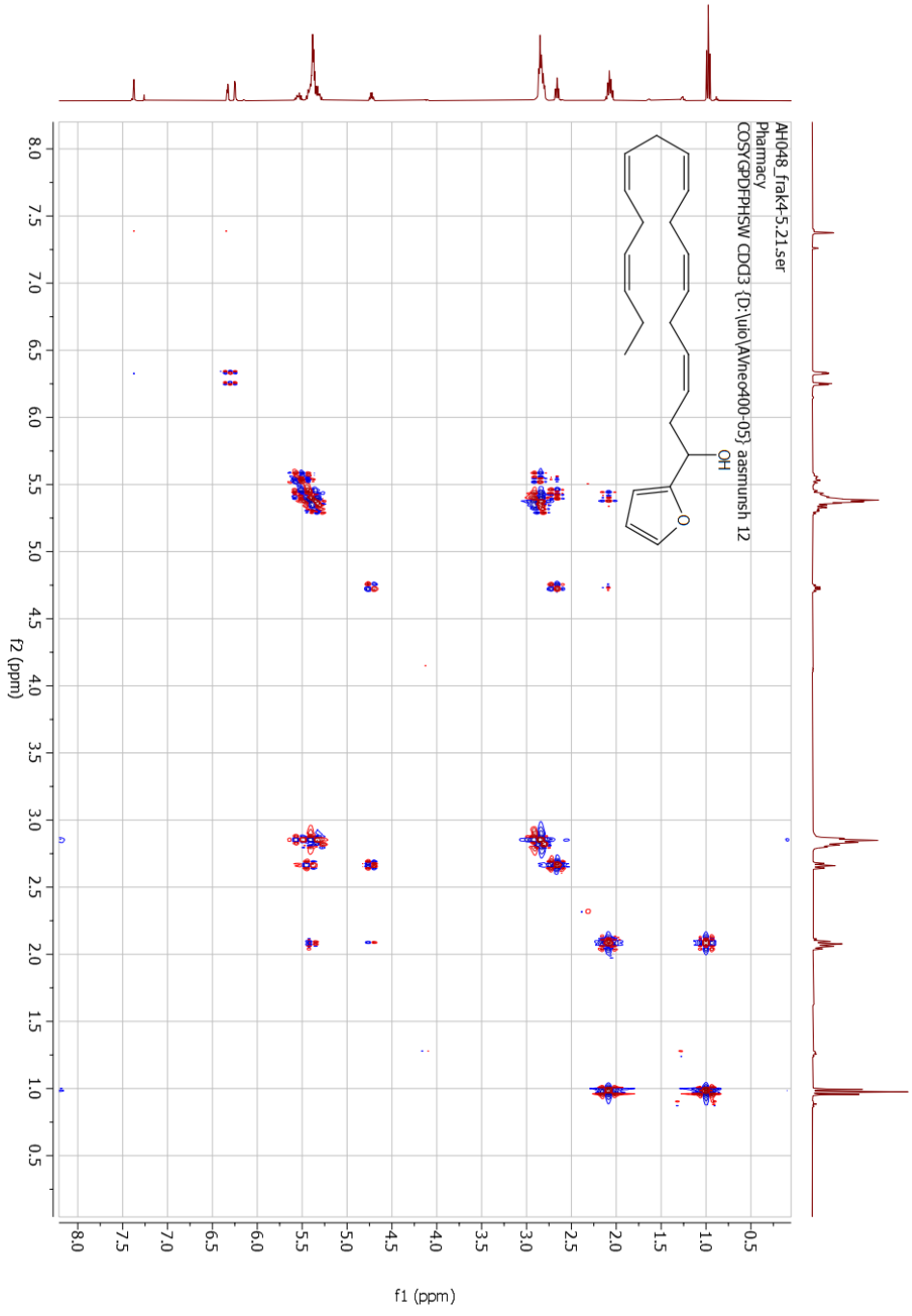

Fig. 7.15 COSY spectrum of alcohol **36**.

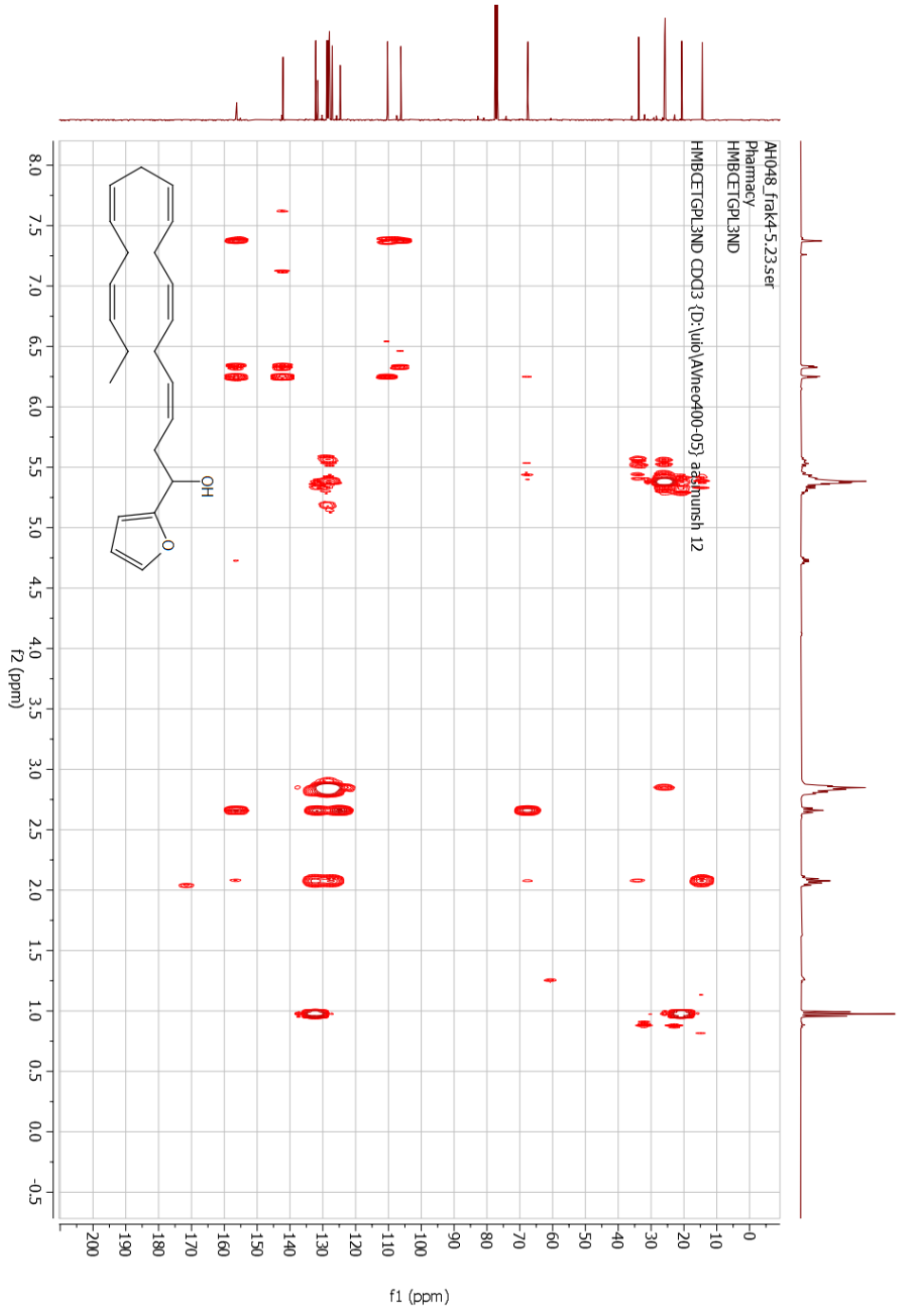

Fig. 7.16 HMBC spectrum of alcohol **36**.

Mass Spectrum List Report

Analysis Info

Analysis Name	D:\Data\maxis2023\19360.d	Acquisition Date	08-Mar-23 10:09:16 AM
Method	ESI_pos_50_1500_os.m	Operator	Erlend
Sample Name	AH048	Instrument	maXis II ETD 1823391.22318
Comment			

Acquisition Parameter

Source Type	ESI	Set Capillary	3500 V	Set Nebulizer	0.5 Bar
Focus	Not active	Set End Plate Offset	-500 V	Set Dry Heater	200 °C
Scan Begin	50 m/z	Set Charging Voltage	2000 V	Set Dry Gas	4.0 l/min
Scan End	1500 m/z	Set Corona	0 nA	Set Divert Valve	Waste
				Set APCI Heater	0 °C

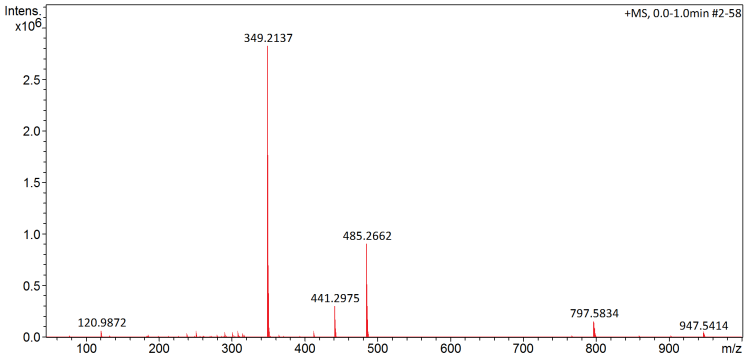

#	m/z	Res.	S/N	I	I %	FWHM
1	120.9872	28656	3715.4	66996	2.4	0.0042
2	183.0990	33453	796.2	14210	0.5	0.0055
3	185.1147	33133	1007.8	17963	0.6	0.0056
4	239.1616	36322	1434.3	28374	1.0	0.0066
5	251.1616	36980	1951.5	39829	1.4	0.0068
6	273.1671	37675	622.4	14158	0.5	0.0073
7	280.2246	37738	924.2	22064	0.8	0.0074
8	290.2689	39091	1538.2	37437	1.3	0.0074
9	301.1409	39542	1441.9	37248	1.3	0.0076
10	309.1824	39715	599.3	16791	0.6	0.0078
11	309.2212	39401	1467.0	41100	1.5	0.0078
12	315.1929	38452	874.8	25933	0.9	0.0082
13	317.2814	39913	530.4	15957	0.6	0.0079
14	349.2137	39014	74103.9	2825383	100.0	0.0090
15	349.3257	68048	917.7	35030	1.2	0.0051
16	350.2171	40544	18182.3	697973	24.7	0.0086
17	351.2202	39330	2357.1	91103	3.2	0.0089
18	365.1055	40863	441.0	18252	0.6	0.0089
19	413.2662	42809	806.0	41404	1.5	0.0097
20	441.2975	42522	5265.9	302176	10.7	0.0104
21	442.3010	42143	1478.8	85323	3.0	0.0105
22	443.3041	40807	244.3	14163	0.5	0.0109
23	485.2662	42903	13665.0	908181	32.1	0.0113
24	486.2696	43253	4503.0	299802	10.6	0.0112
25	487.2728	42338	807.5	53853	1.9	0.0115
26	797.5834	47837	1690.3	155879	5.5	0.0167
27	798.5868	47955	1006.3	92723	3.3	0.0167
28	799.5902	47883	303.2	27898	1.0	0.0167
29	947.5414	49482	522.5	36440	1.3	0.0191
30	948.5449	48958	342.1	23790	0.8	0.0194

Fig. 7.17 HRMS spectrum of alcohol **36**.

Spectrum/Peak Report Date 3/8/2023 Time 08:39:42 Page 1 of 1

Method file : <method not saved>
Information : Default Method
Data File : <data not saved>

Overlaid Spectra:

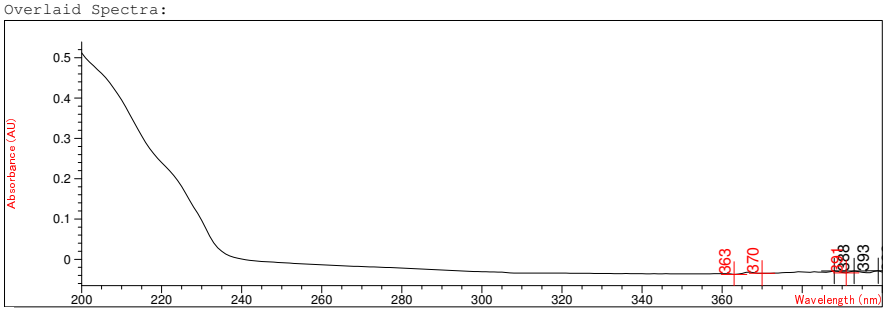

#	Name	Peaks(nm)	Abs(AU)	Valleys(nm)	Abs(AU)
1		399.0	-2.8248E-2	363.0	-3.7545E-2
1		393.0	-2.8673E-2	370.0	-3.4545E-2
1		388.0	-2.8911E-2	391.0	-3.3777E-2

Report generated by : Karoline Signature: .....

*** End Spectrum/Peak Report ***

Fig. 7.18 UV-Vis spectrum of alcohol **36**.

Agilent Technologies

Sample ID:2023-04-17T11-43-16

Method Name:C:\Users\Public\Documents\Agilent\MicroLab\Methods\Scan_4000-650.a2m

Sample Scans:16

User:admin

Background Scans:32

Date/Time:04.17.2023 11:43:16 a.m.

Resolution:4

Range:4000 - 650

System Status:Good

Apodization:Happ-Genzel

File Location:C:\Users\Public\Documents\Agilent\MicroLab\Results\\2023-04-17T11-43-16.a2r

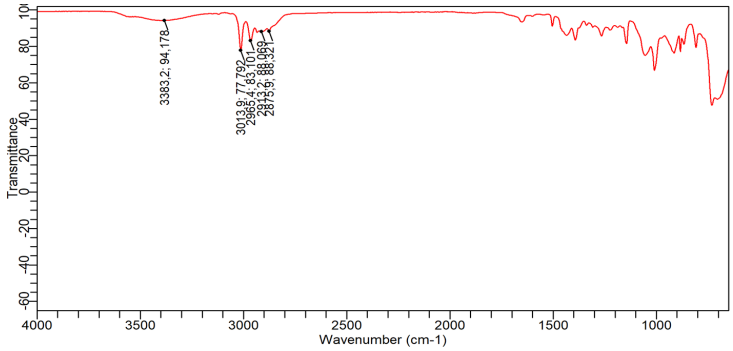

Peak Number	Wavenumber (cm^{-1})	Intensity
1	2875,9	88,321
2	2913,2	88,069
3	2965,4	83,101
4	3013,9	77,792
5	3383,2	94,178

4/17/2023 11:45:58 a.m. page 1 of 2

Fig. 7.19 IR spectrum of alcohol **36**.

7.7 Ketone 3

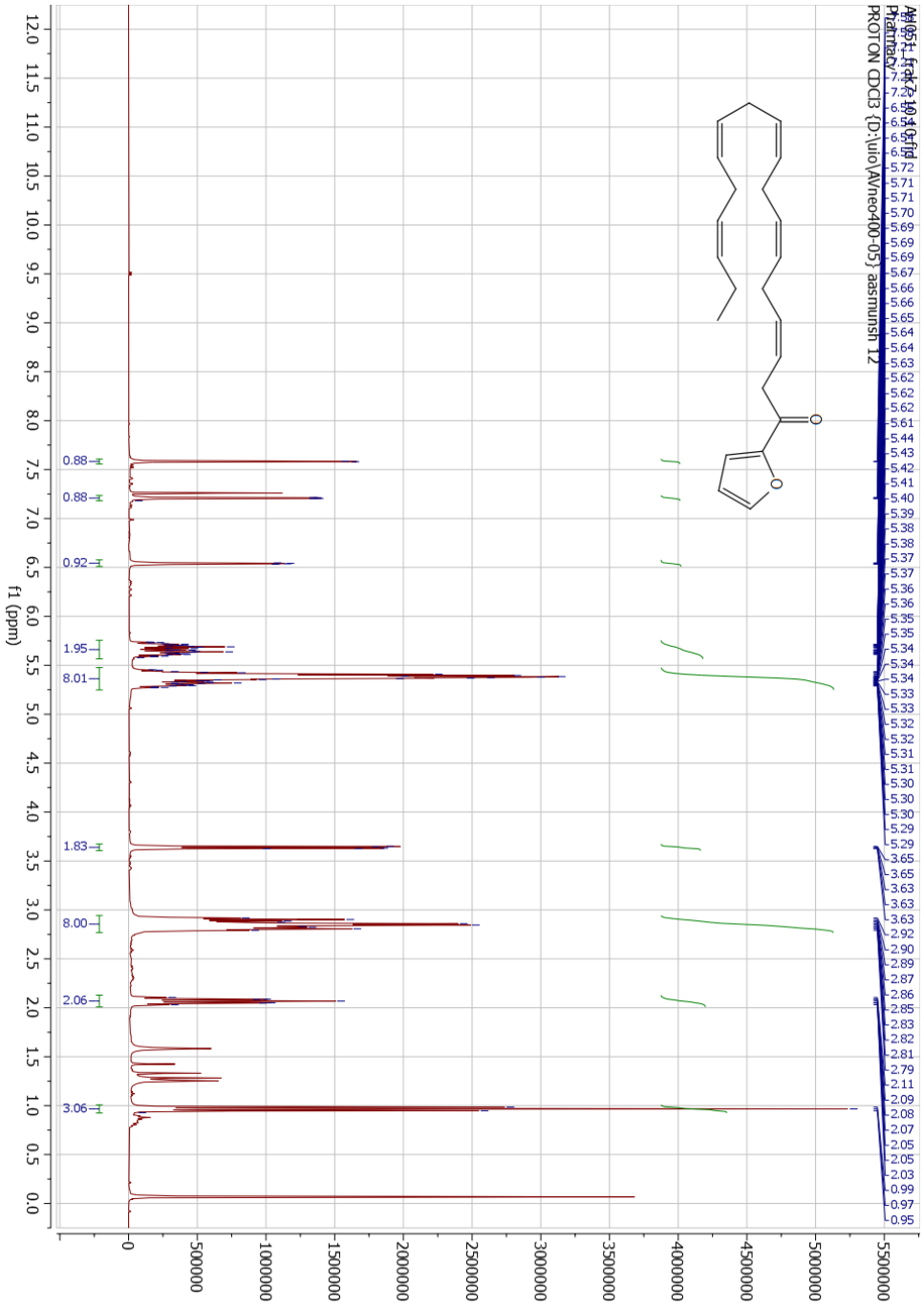

Fig. 7.20 ^{1}H NMR spectrum of ketone **3**.

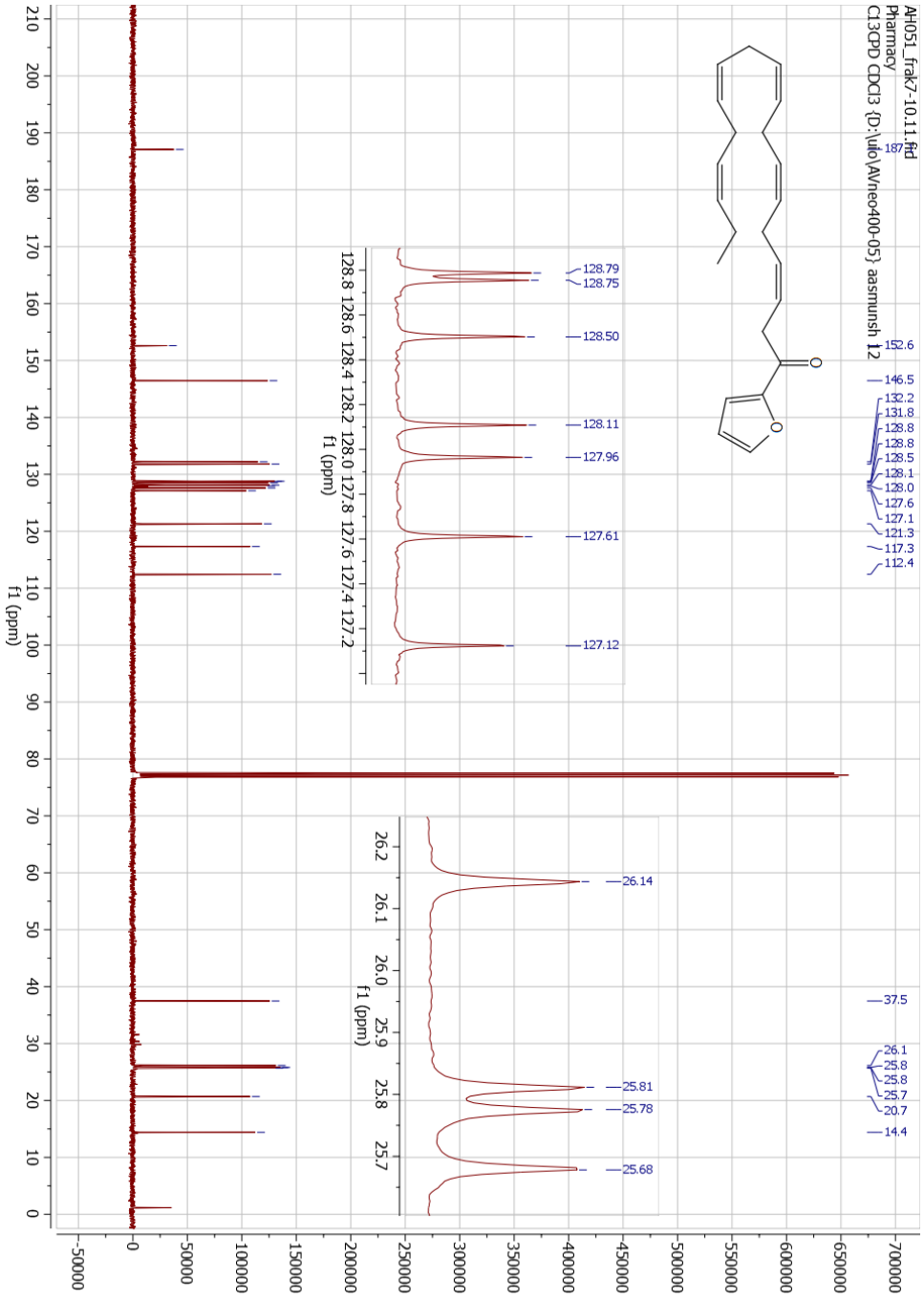

Fig. 7.21 ^{13}C NMR spectrum of ketone **3**.

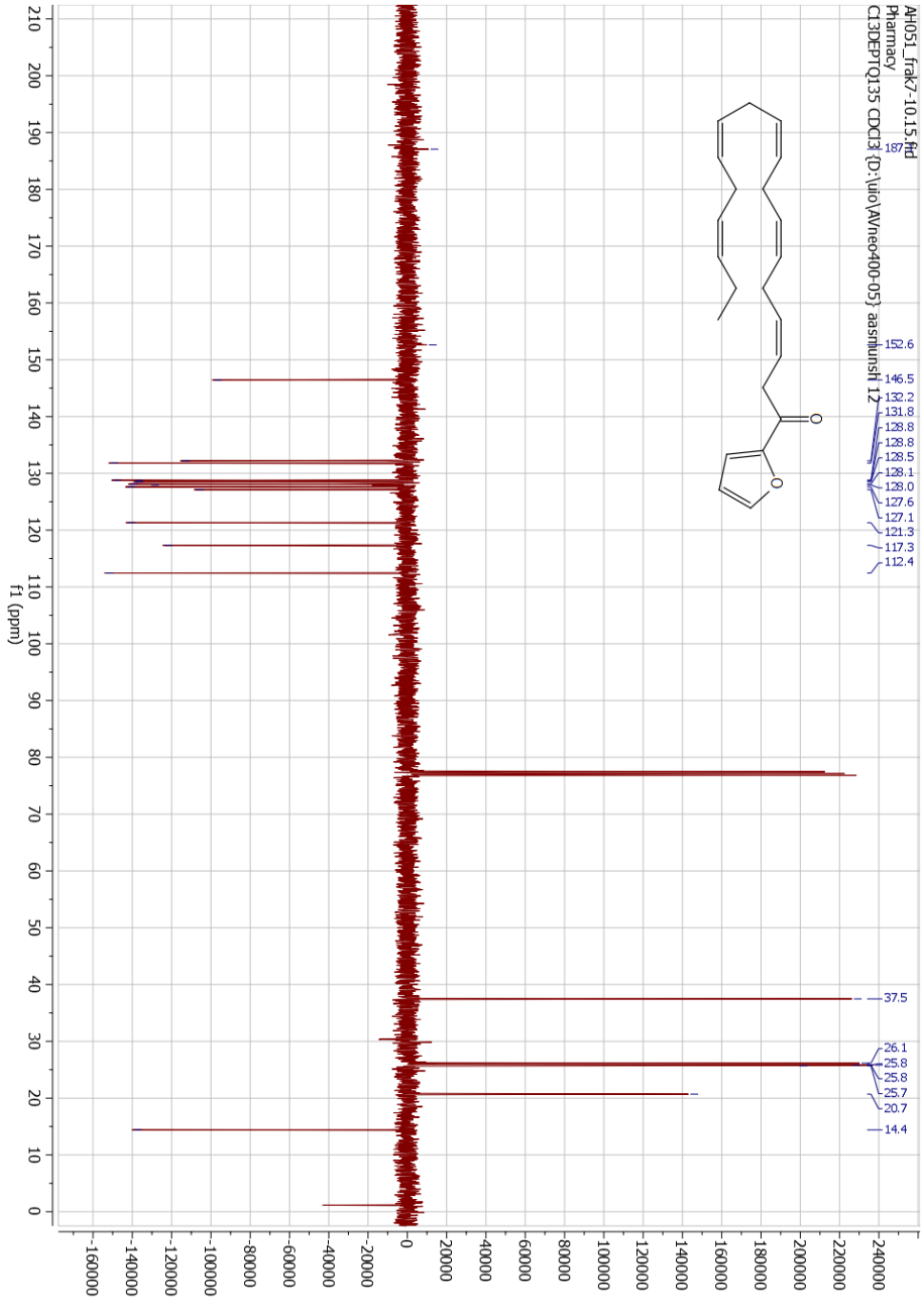

Fig. 7.22 DEPT-135 spectrum of ketone **3**.

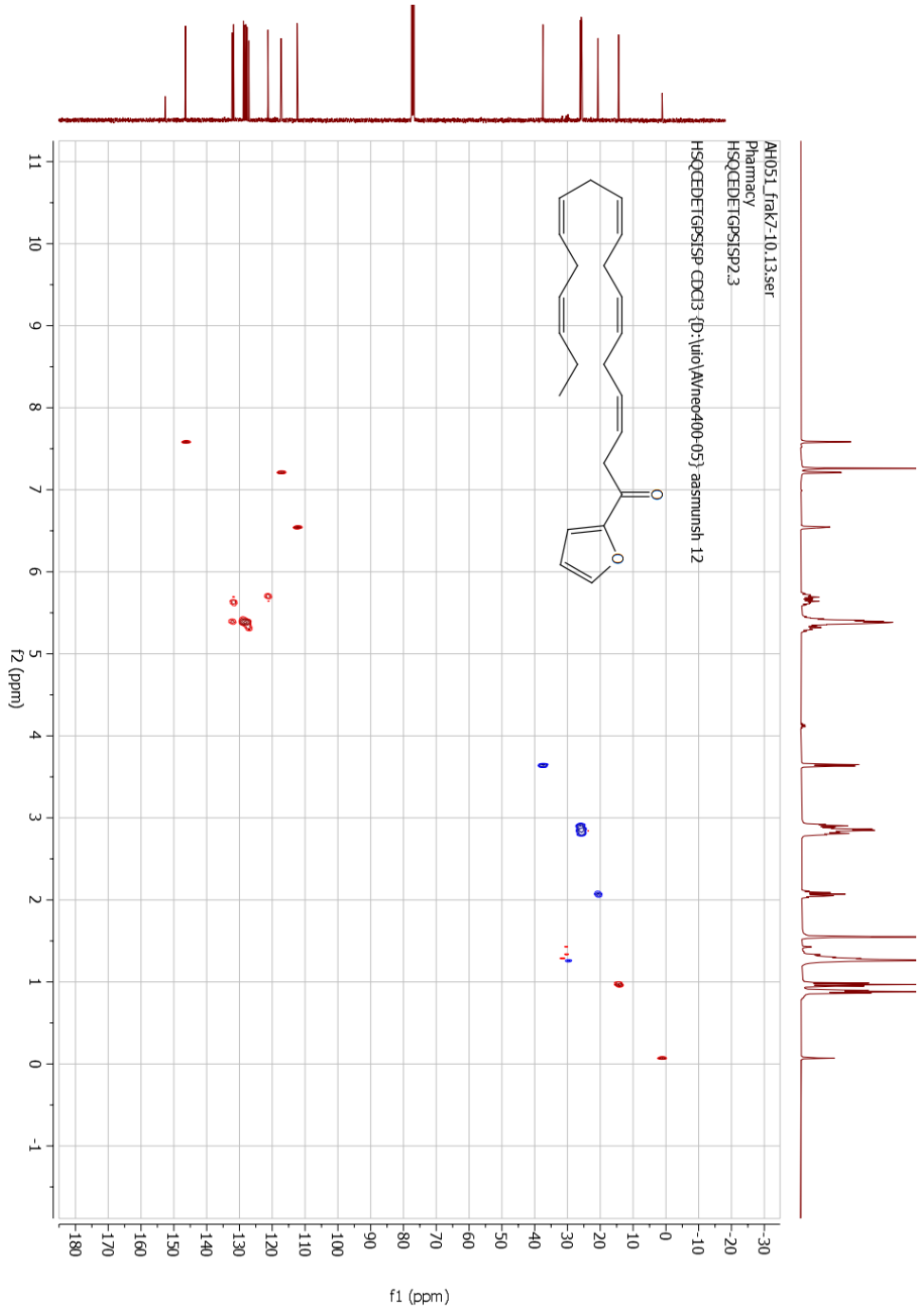

Fig. 7.23 HSQC spectrum of ketone **3**.

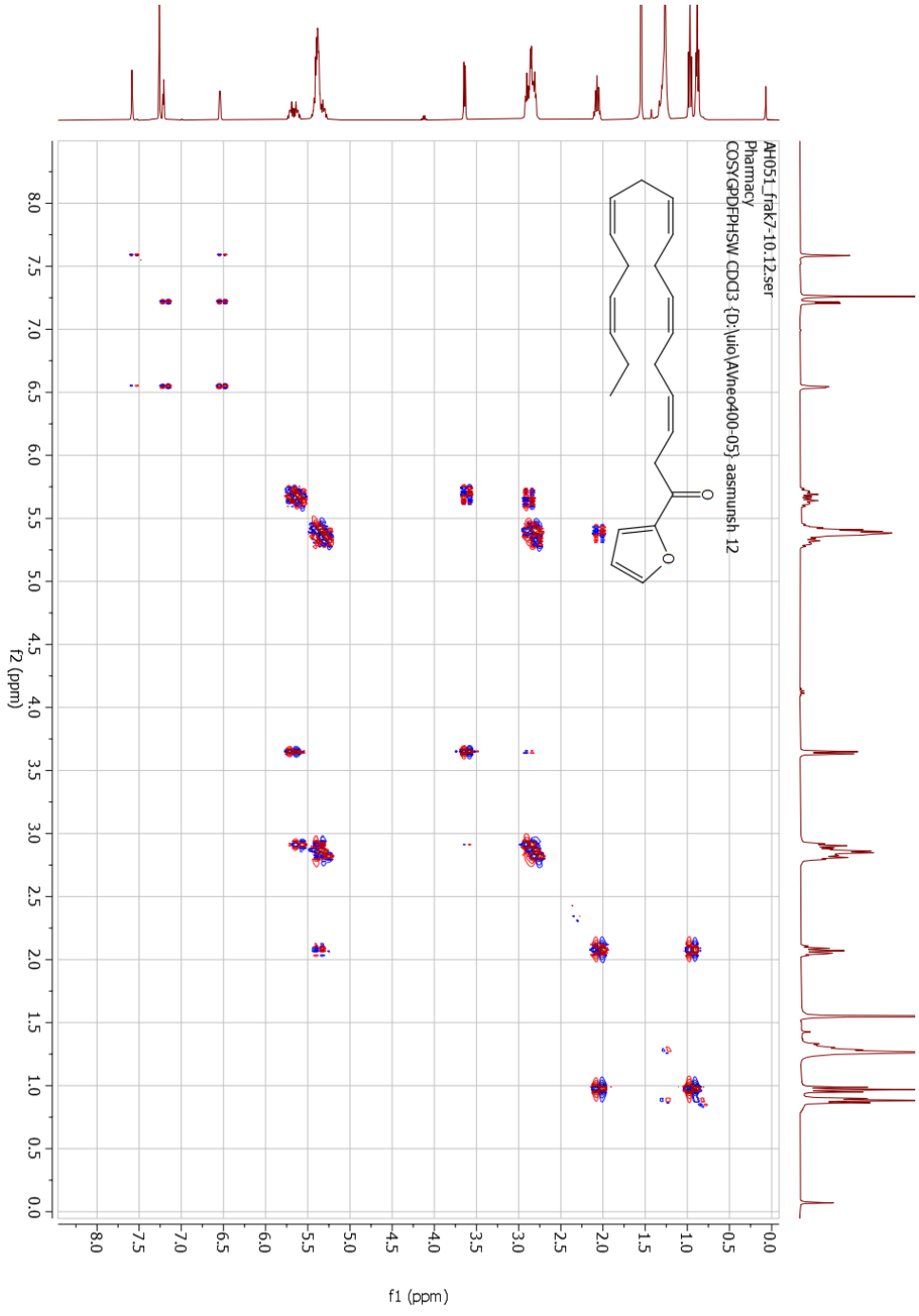

Fig. 7.24 COSY spectrum of ketone **3**.

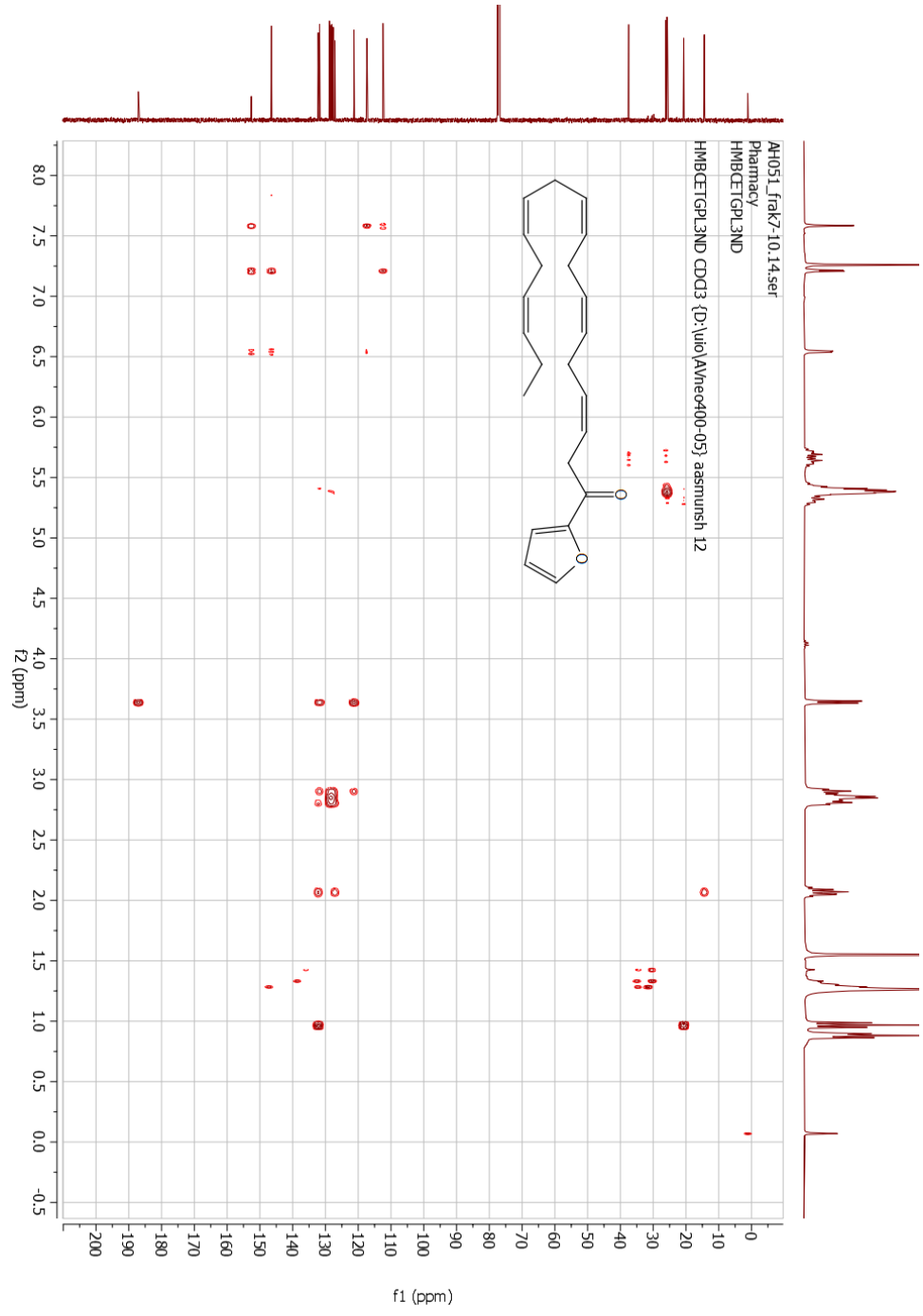

Fig. 7.25 HMBC spectrum of ketone **3**.

Mass Spectrum List Report

Analysis Info

Analysis Name	D:\Data\maxis2023\19462.d	Acquisition Date	11-Apr-23 11:48:16 AM
Method	ESI_pos_50_1500_os.m	Operator	Erlend
Sample Name	AH051	Instrument	maXis II ETD 1823391.22318
Comment			

Acquisition Parameter

Source Type	ESI	Set Capillary	3500 V	Set Nebulizer	0.5 Bar
Focus	Not active	Set End Plate Offset	-500 V	Set Dry Heater	200 °C
Scan Begin	50 m/z	Set Charging Voltage	2000 V	Set Dry Gas	4.0 l/min
Scan End	1500 m/z	Set Corona	0 nA	Set Divert Valve	Waste
				Set APCI Heater	0 °C

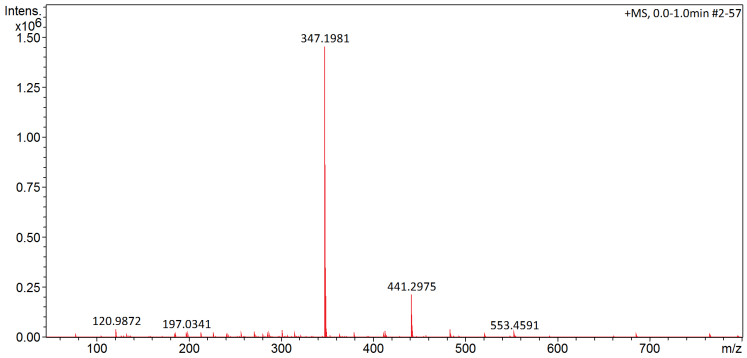

#	m/z	Res.	S/N	I	I %	FWHM
1	76.9974	22706	676.0	15003	1.0	0.0034
2	120.9872	28623	1927.1	41469	2.9	0.0042
3	133.0025	29442	653.7	13954	1.0	0.0045
4	185.0137	32909	643.0	13480	0.9	0.0056
5	185.1148	32251	763.4	16004	1.1	0.0057
6	197.0341	34075	1232.3	25995	1.8	0.0058
7	198.9930	34284	1034.7	21855	1.5	0.0058
8	212.9722	34814	1097.5	23367	1.6	0.0061
9	213.0086	33924	733.3	15615	1.1	0.0063
10	226.9879	34291	1107.5	23719	1.6	0.0066
11	242.9827	36782	679.6	14865	1.0	0.0066
12	256.9620	36506	1025.0	23036	1.6	0.0070
13	270.9777	38313	1283.7	30273	2.1	0.0071
14	284.9933	38353	654.8	15913	1.1	0.0074
15	286.9726	38915	858.8	20916	1.4	0.0074
16	300.9883	37364	605.7	15312	1.1	0.0081
17	301.1410	37913	1496.3	37846	2.6	0.0079
18	315.1930	38754	810.4	22132	1.5	0.0081
19	347.1981	40250	43617.0	1453703	100.0	0.0086
20	348.2015	40307	10391.4	349011	24.0	0.0086
21	349.2046	38437	1339.4	45224	3.1	0.0091
22	379.1880	41539	602.9	23247	1.6	0.0091
23	411.1778	42680	380.6	17310	1.2	0.0096
24	413.2662	42057	721.0	33044	2.3	0.0098
25	441.2975	42739	4165.2	215382	14.8	0.0103
26	442.3010	41941	1162.9	60429	4.2	0.0105
27	483.2506	43439	677.0	40262	2.8	0.0111
28	484.2541	43936	221.7	13250	0.9	0.0110
29	553.4591	44543	289.2	20550	1.4	0.0124
30	765.5069	46850	145.3	14233	1.0	0.0163

19462.d

Bruker Compass DataAnalysis 4.3 printed: 11-Apr-23 11:52:13 AM by: Erlend Page 1 of 1

Fig. 7.26 HRMS spectrum of ketone **3**.

```
================================================================================
Fixed Wavelength Report                        Date 4/19/2023 Time 10:29:31  Page   1 of 1
================================================================================


Method file :         C:\Chem32\1\METHODS\HAMID INST MET.M (modified)
                      Last update: Date 4/19/2023  Time 10:12:35 AM
Information :         Default Method
Data File   :         <data not saved>

Overlaid Spectra:
```

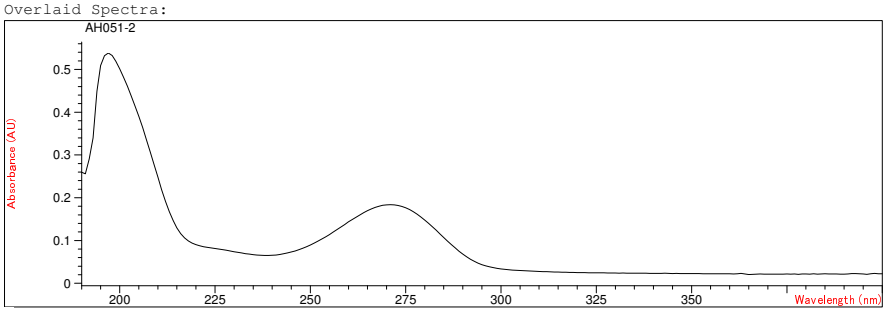

#	Name	Abs<205nm>	Abs<245nm>	Abs<273nm>
1	AH051-2	0.39024	7.3189E-2	0.18201

```
Report generated by : Karoline                              Signature: .................

--------------------------------------------------------------------------------
                        *** End Fixed Wavelength Report ***
--------------------------------------------------------------------------------
```

Fig. 7.27 UV-Vis spectrum of ketone **3**.

Agilent Technologies

Sample ID:2023-04-17T11-50-10
Method Name:C:\Users\Public\Documents\Agilent\MicroLab\Methods\Scan_4000-650.a2m
Sample Scans:16
User:admin
Background Scans:32
Date/Time:04.17.2023 11:50:10 a.m.
Resolution:4
Range:4000 - 650
System Status:Good
Apodization:Happ-Genzel
File Location:C:\Users\Public\Documents\Agilent\MicroLab\Results\\2023-04-17T11-50-10.a2r

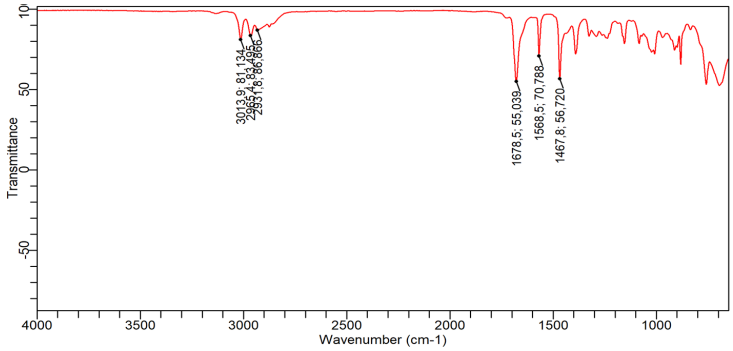

Peak Number	Wavenumber (cm^{-1})	Intensity
1	1467,8	56,720
2	1568,5	70,788
3	1678,5	55,039
4	2931,8	86,866
5	2965,4	83,495

4/17/2023 11:51:09 a.m. page 1 of 2

Fig. 7.28 IR spectrum of ketone **3**.